Climate, which is generally defined as “average weather,” is described in terms of the mean and variability of temperature, precipitation, and wind over a long period of time.

Warming of the climate is unequivocal, and the dominant effect of human activities in driving this change is clear (IPCC, 2021). Global surface temperatures during 2011-2020 were 0.95 to 1.20°C (1.71 to 2.16°F) warmer compared to 1850–1900 (IPCC, 2021). Each of the last four decades has been successively warmer than any preceding decade, with temperatures increasing at a faster rate since 1970 than in any other 50-year period over the past 2000 years.

Warming trends in the United States and California – including the acceleration of warming trends – are consistent with global changes. The average surface temperature for the contiguous 48 states has risen by about 0.16°F per decade since 1901; eight of the top ten warmest years on record have occurred since 1998, with 2012 and 2016 being the warmest (US EPA, 2021). Similarly, in California the past decade included eight of the warmest years; record high temperatures occurred in 2014 and 2015. As expected in a warming climate, temperatures at night – which generally correspond to minimum temperatures – increased faster than daytime temperatures. Warmer nights can impact public health, especially for certain sensitive groups, and can affect fruit and nut tree production in the state’s agricultural regions. Extreme heat events have become more frequent since 1950, especially in the last 30 years. These warming trends have been accompanied by an increase in “cooling degree days,” a temperature-based metric that indicates a greater need for energy to cool homes and buildings.

In California, precipitation has become more variable in recent decades, with very dry years interspersed with very wet years. This variability has been influenced by “atmospheric rivers,” long, narrow bands that transport most of the water vapor originating from the tropics to the poles (NOAA, 2017).

With warmer temperatures and lower precipitation volumes, drought conditions continue in the state. In fact, years 2000 to 2021 have been the driest 22-year period in the last millennium in California and the rest of the southwestern United States—part of what scientists are now calling an emerging “megadrought” era (Williams, et al., 2022).

Climate change is already making many weather and climate extremes such as heatwaves, heavy precipitation, and droughts even more extreme in every region across the globe (IPCC, 2022). In 2021, an unprecedented number of devastating extreme events occurred across the United States, costing an unprecedented $152.6 billion. In the past five years, such weather events are estimated to have cost more than

$14.2 billion/year in California – more expensive than in any other time period (NOAA, 2022).

INDICATORS: CHANGES IN CLIMATE

Air temperature *(updated)*
Extreme heat events *(updated)*
Winter chill *(updated)*
Cooling and heating degree days *(updated)*
Precipitation *(updated)*
Drought *(updated)*

References:

IPCC (2021). Summary for Policymakers. *In: Climate Change 2021: The Physical Science Basis. Contribution of Working Group I to the Sixth Assessment Report of the Intergovernmental Panel on Climate Change.* Masson-Delmotte V, Zhai P, Pirani A, Connors SL, Péan C, et al. (Eds.). Cambridge University Press, Cambridge, United Kingdom and New York, NY, USA.

IPCC (2022). *Climate Change 2022: Impacts, Adaptation, and Vulnerability. Contribution of Working Group II to the Sixth Assessment Report of the Intergovernmental Panel on Climate Change*. Pörtner H-O, Roberts DC, Tignor M, Poloczanska ES, Mintenbeck K, et al. (Eds.). Cambridge University Press.

NOAA (2017). National Oceanic and Atmospheric Administration: What Are Atmospheric Rivers? Retrieved August 2, 2021.

NOAA (2022). Billion-Dollar Weather and Climate Disasters. Retrieved June 09, 2022.

US EPA (2021). Climate Change Indicators in the United States. Retrieved June 23, 2022.

Williams AP, Cook BI and Smerdon JE (2022). Rapid intensification of the emerging southwestern North American megadrought in 2020–2021. *Nature Climate Change* **14**: 1-3.

AIR TEMPERATURE

Air temperatures have increased over the past century, driven mainly by changes in nighttime temperatures.

Figure 1. Statewide annual average temperatures

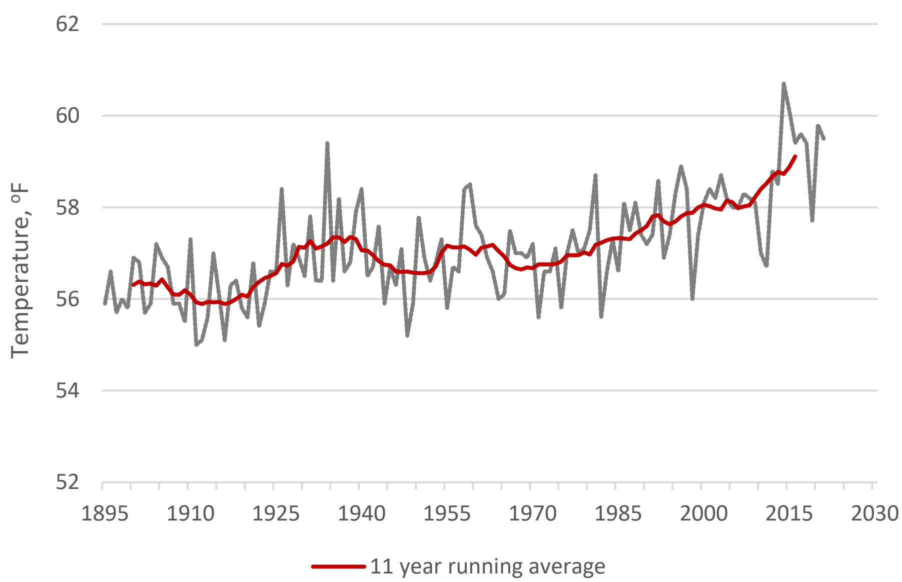

Source: WRCC, 2022

What does the indicator show?

Statewide air temperatures show a warming trend consistent with that found globally (IPCC, 2021; also see the globalwarmingindex). They have been recorded since 1895. Figure 1 presents annual average temperatures statewide. Annual average temperatures have increased by about 2.5 degrees Fahrenheit (˚F) (or about 2°F per century, which is a common way of measuring long-term temperature changes). Recent years were notably warm, with 2014 being the warmest on record, followed by 2015, 2020, 2017, 2016, and 2018. Some of these warmest years coincided with some of the driest years in the instrumental record and led to exacerbated drought conditions due to increased land surface temperatures, evapotranspiration, and evaporative demand.

Figure 2 depicts “departures” by decade from a long-term average (base period of 1901 to 2000) for minimum, mean, and maximum temperatures. Departures are the difference between each decade’s value and the long-term average. Before the 1930s, temperatures were cooler than the long-term average, then hovered around the average between the 1940s and the 1970s. The last four decades showed marked warming, as temperatures increased at a faster rate. Minimum, average, and maximum temperatures have increased overall. Minimum temperatures (which reflect overnight low temperatures) have increased the fastest.

Figure 2. Statewide Temperatures, Decadal Averages (relative to the 1901-2000 long-term average*)

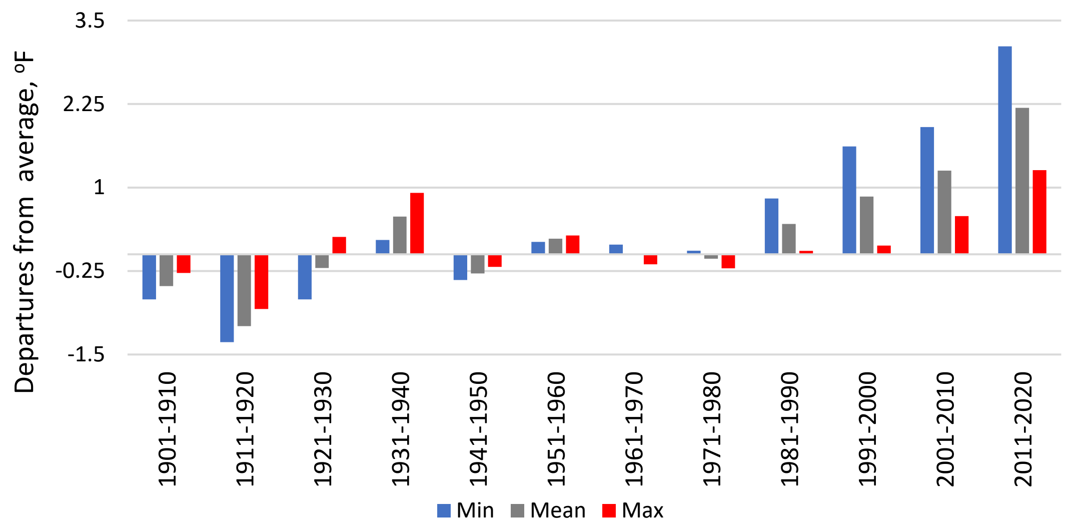

Source: WRCC, 2021

** Values shown for each decade are "departures" from the long-term average, 1901-2000—that is, the difference between the long-term average and the average for the decade.*

Figure 3. Regional and statewide temperature trends (1895 to 2020)

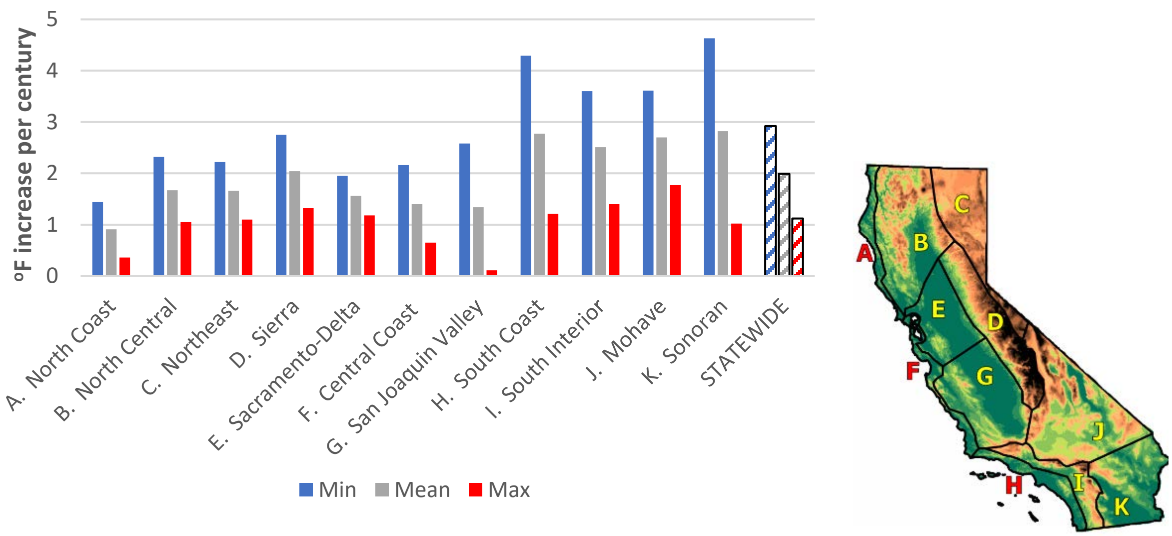

Source: WRCC, 2021

As shown in Figure 3, statewide minimum temperatures rose at a rate of 2.9°F per century. Maximum temperatures rose at 1.1°F per century. As minimum temperatures have increased the fastest, the increasing trend in the average California temperature is driven more by nighttime processes than by daytime processes.

All of California’s 11 climate regions have experienced warming trends over the last century, although at varying rates (Figure 3). The greatest increases are observed in the Sonoran Desert and South Coast regions. Minimum temperatures showed the greatest rate of increase in all the regions, consistent with statewide trends.

Why is this indicator important?

Temperature is a basic physical factor that affects many natural processes and human activities. Warmer air temperatures alter precipitation and runoff patterns, influencing the availability of freshwater supplies. Increased temperature leads to a wide range of impacts on ecosystems — including changes in species’ geographic distribution, in the timing of life cycle events, and in their abundance — as well as on human health and well-being. In addition, warming temperatures affect energy needed for cooling and heating, which in turn influences the types of energy generation, infrastructure, and management policies needed to meet these demands. Temperature changes can also increase the risk of severe weather events such as heatwaves and intense storms. Understanding observed temperature trends is important for refining future climate projections for climate-sensitive sectors and natural resources within the state (Cordero et al., 2011).

What factors influence this indicator?

Carbon dioxide and other greenhouse gas emissions into the atmosphere since the Industrial Revolution in the mid-1700s have driven unprecedented warming worldwide. (IPCC, 2021). Emissions of these greenhouse gases intensify the natural greenhouse effect, causing surface temperatures to rise. Greenhouse gases absorb heat radiated from the Earth’s surface and lower atmosphere and reflect much of the energy back toward the surface.

Temperatures are influenced by local topography, elevation, proximity to the ocean, and global and regional atmospheric and oceanic circulations. As previously mentioned, Figure 3 illustrates geographic differences in warming trends (WRCC, 2021). Regional information can be obtained from the California Climate Tracker. Climate patterns can vary widely from year to year and from decade to decade, in accordance with large-scale circulation changes around the Earth. The Pacific Ocean has a major effect on California temperatures all year along the coast, especially summer, and farther inland in winter. In addition to topography, local influences on temperature include changes in land surface and land use. For example, urbanization of rural areas is generally known to have a warming effect, due in large part to the heat-absorbing concrete and asphalt in building materials and roadways. Expansion of irrigation has been shown to have a cooling effect on summertime temperatures (Bonfils and Lobell, 2007).

Statewide seasonal temperature trends are shown in Figure 4. Across the seasons, minimum temperatures are increasing faster than maximum temperatures. Trends for the more recent time period (from 1971 to 2021, solid line in Figure 4) are greater than trends since 1895 (dotted line). The greatest increases in minimum temperatures occurred in the summer and fall over both time periods. For maximum temperatures, the greatest increases over the entire period of record occurred in the fall and winter; since 1971, the greatest increased occurred in the fall and summer.

Figure 4. Seasonal air temperature trends in California

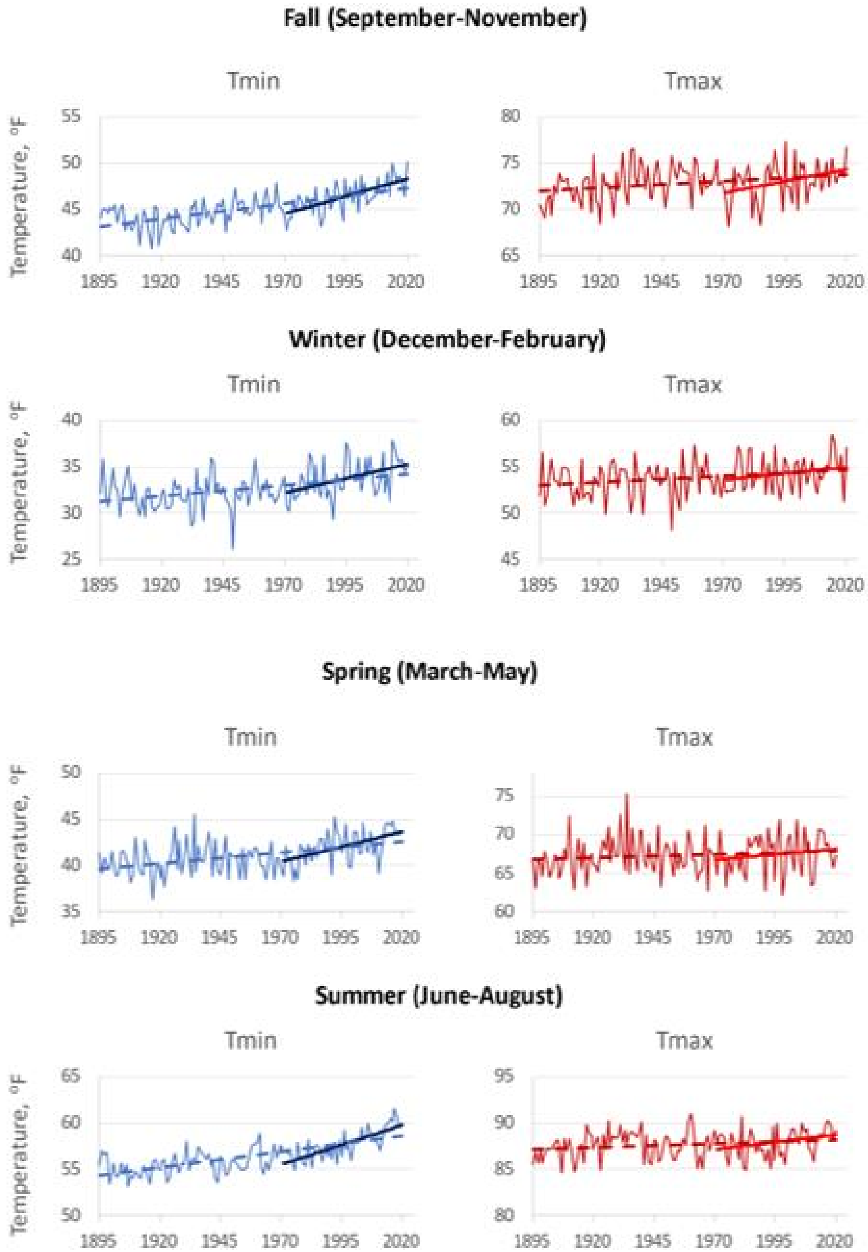

Source: WRCC, 2021

Average minimum temperature (Tmin) and average maximum temperature (Tmax) for each year are presented for each season. The linear trend for the entire period is shown as solid lines, and for 1971-2021 as dashed lines.

Technical considerations

Data characteristics

The Western Regional Climate Center (WRCC)'s California Climate Tracker provides monthly temperature values in California from 1895 to the present using the PRISM Climate Mapping Program from Oregon State University. PRISM is an analytical tool that generates fine scale grid-based estimates of monthly precipitation and temperature. The "About the California Climate Tracker" page provides more information. (WRCC has updated its methodology since the previous report for determining historical temperatures, so values in the current edition of this report slightly differ from the previous edition).

Strengths and limitations of the data

The datasets used are subjected to their own separate quality control procedures, to account for potentially incorrect data reported by the observer, missing data, and to remove inconsistencies such as station relocation or instrument change.

The PRISM dataset offers complete coverage across the state for every month of the record. Limitations include the bias of station data toward populated areas and the limited ability of quality control processes in remote or high terrain areas. The dataset is constantly updated to map climate in the most difficult situations, including high mountains, rain shadows, temperature inversions, coastal regions, and associated complex climate processes.

OEHHA acknowledges the expert contributions of the following to this report:

Dan McEvoy
Western Regional Climate Center
Division of Atmospheric Science
Desert Research Institute
(775) 674-7010
Daniel.McEvoy@dri.edu

Michael L. Anderson, Ph.D., P.E.
State Climatologist
California Department of Water Resources
(916) 574-2830
Michael.L.Anderson@water.ca.gov

References:

Bonfils C and Lobell D (2007). Empirical evidence for a recent slowdown in irrigation-induced cooling. *Proceedings of the National Academy of Sciences* **104**(34): 13582-13587.

Cordero E, Kessomkiat W, Abatzoglou JT and Mauget S (2011). The identification of distinct patterns in California temperature trends. *Climatic Change* **108**(1-2): 357-382.

IPCC (2021). *AR6 Climate Change 2021: The Physical Science Basis. Contribution of Working Group I to the Sixth Assessment Report of the Intergovernmental Panel on Climate Change*. Masson-Delmotte V, Zhai P,Pirani A, Connors SL, Péan C, S. Berger S, et al. (Eds.). Geneva, Switzerland: Intergovernmental Panel on Climate Change.

WRCC (2022). Western Regional Climate Center: California Climate Tracker. Retrieved March 4, 2022.

EXTREME HEAT EVENTS

Extreme heat has become more frequent in California since 1950, especially at night. Across most locations studied here, the number and magnitude of extreme heat events have significantly increased. Heat waves – two or more consecutive heat events – vary from year to year, but have become more frequent in the past decade.

Figure 1. Magnitude and frequency of extreme heat events (trend per decade, 1950-2021)

A. Daytime extreme heat events **B. Nighttime extreme heat events**

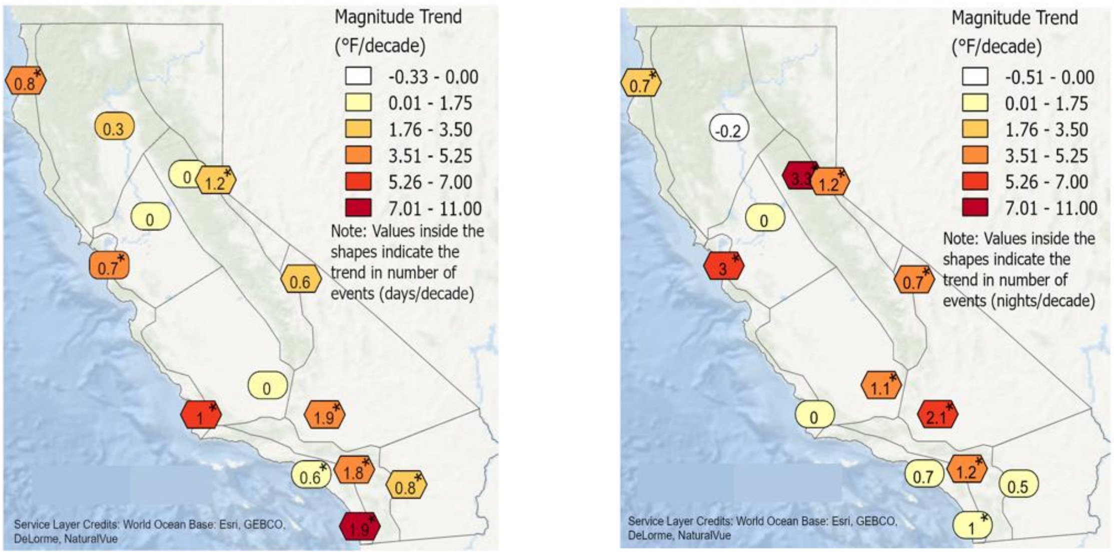

Source: Cal-Adapt, 2018, Dunn 2019, and RCC-ACIS, 2021

An extreme heat event occurs between April and October when the temperature is at or above a location-specific historical temperature threshold, set at the 95th percentile of daily maximum for daytime extreme events (Figure 1A), or of daily minimum temperatures for nighttime events (Figure 1B), during the 1960-1990 reference period.

*The rate of change (per decade) in **frequency,** the total number of extreme heat events each year, is the value in each shape (hexagon or oval); an asterisk indicates a statistically significant trend ($p \leq 0.05$). The rate of change (per decade) in **magnitude**, the annual sum of daily exceedances above the historical temperature threshold, in degrees Fahrenheit (°F), is presented using the fill colors (see legend); a hexagon denotes a trend that is statistically significant ($p \leq 0.05$), while an oval is not significant. The outlines on the map show the boundaries of the eleven climate regions, as defined by the Western Regional Climate Center.*

What does the indicator show?

Since 1950, nighttime extreme heat events have increased in magnitude and frequency more than daytime heat events, as shown in Figure 1. The maps show decadal trends in the magnitude and frequency of daytime and nighttime extreme heat events during the warm months between April and October at selected locations (see Figure 2 map of weather stations).

For a given location, a daytime extreme heat event occurs when the historical threshold for daily maximum temperature is exceeded, and a nighttime extreme heat event, when the historical threshold for daily minimum temperature is exceeded. There is no standard temperature for defining an extreme heat event. Researchers often apply a threshold between the 85th and 98th percentile of historical values. Here, the threshold is set at the location-specific 95th percentile of either the daily maximum temperatures (for daytime events) or the daily minimum temperatures (for nighttime events) from April to October during the 1960-1990 reference period.

Figure 2. Selected weather stations*

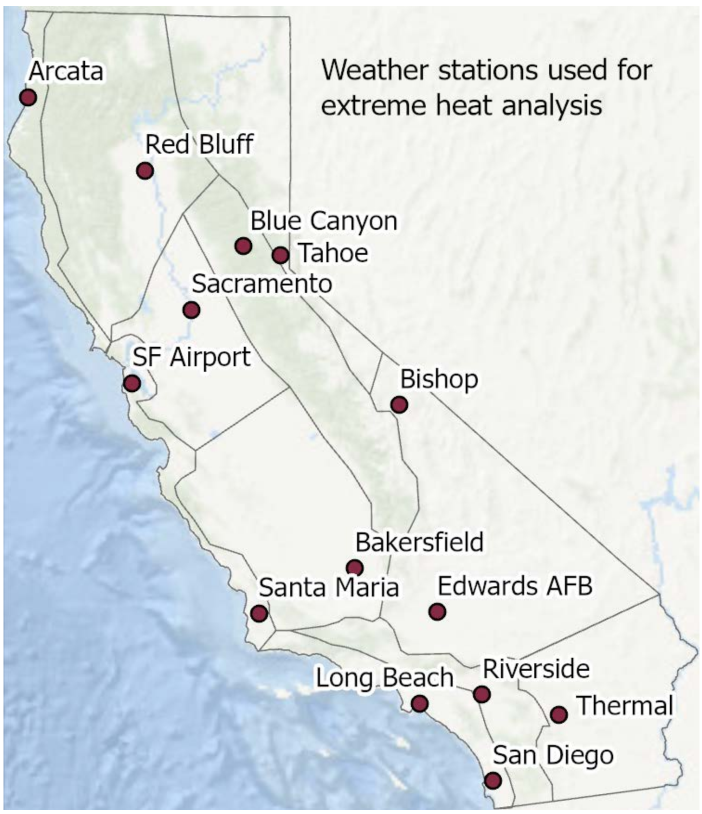

**At least one weather station is from each of California's eleven climate regions (outlined in gray; refer to map, Figure 8). Data sources are discussed in "Technical considerations."*

From 1950 to 2021, the magnitude of extreme heat events increased by at least 1.76 degrees Fahrenheit (°F) per decade during the day at 10 of the 14 stations and at night at 8 stations (stations with orange to dark red fill in Figure 1A and B, respectively). During the same period, the frequency of heat events increased by at least 1 event per decade at 5 stations for daytime events, and at 7 stations for nighttime events (values inside shapes in Figure 1A and 1B, respectively). Out of the stations analyzed, the number of daytime heat events increased the fastest in Edwards AFB and San Diego, with the latter also showing the fastest increase in magnitude (Figure 1A). Blue Canyon experienced the greatest increase in the number of nighttime heat events (with San Francisco Airport a close second) and magnitude (Figure 1B).

The magnitude and frequency of daytime and nighttime extreme heat events each year at the selection locations are presented in Figures 3 and 4, respectively. The magnitude shown is the sum of daily or nightly exceedances above the historic threshold in a given year at that location.

Figure 3. Annual daytime extreme heat events at the selected locations (1950-2021)

A. Daytime Extreme Heat Events: Magnitude (°F)

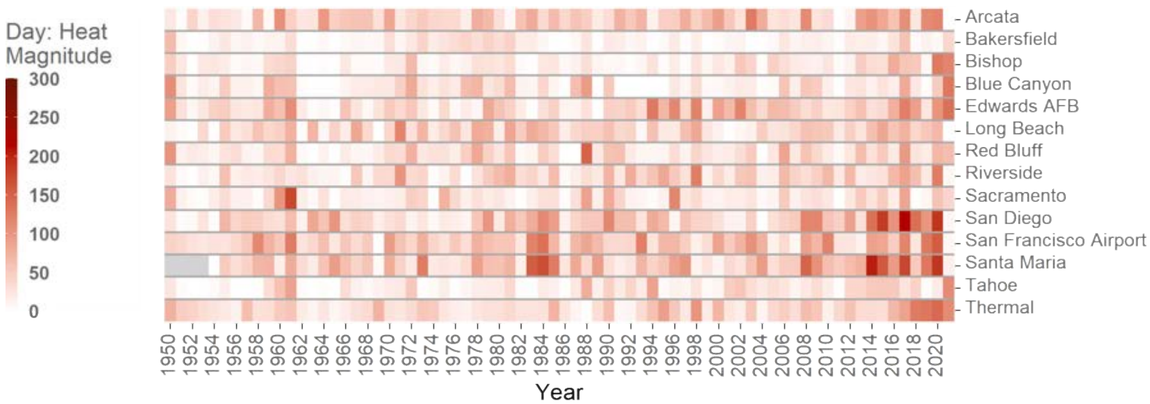

B. Daytime Heat Events: Frequency (days)

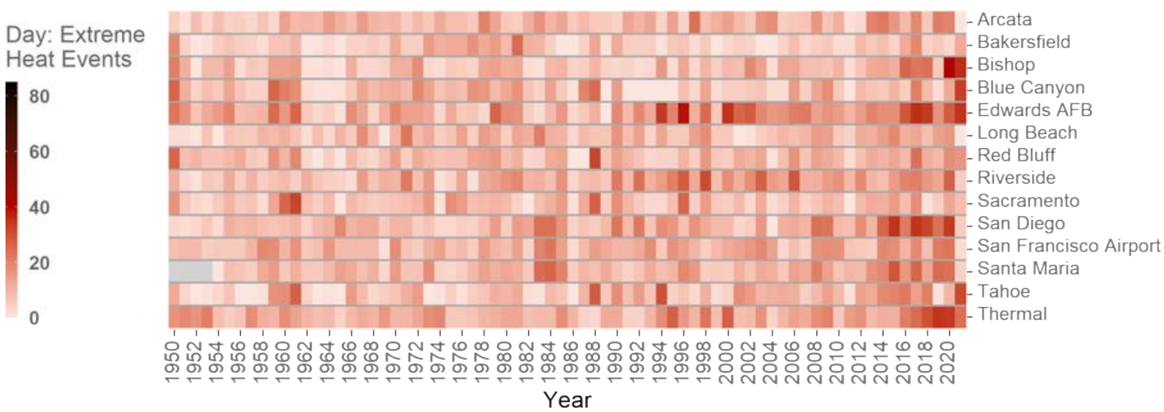

Source: Cal-Adapt, 2018, Dunn 2019, and RCC-ACIS, 2021

Annual values for magnitude and frequency are presented for each location. Greyed out areas mean no data are available for that timeframe. A location-specific threshold of the 95th percentile was used to determine extreme heat events.

At Edwards AFB, San Diego, San Francisco Airport, and Santa Maria, the magnitude of daytime extreme heat in the last decade is especially notable with at least one year having reached at least 150°F (Figure 3A); note that this is the annual sum of the daily exceedance above the 95th percentile. Similarly, daytime heat events have become more frequent in the last decade, notably at Bishop, Edwards AFB, San Diego, and Thermal, where at least one year having reached 35 or more events (Figure 3B).

Compared to daytime heat events, nighttime events have seen greater increases in magnitude and frequency (Figure 4). Blue Canyon, Edwards AFB, Long Beach,

Figure 4. Annual nighttime extreme heat events at the selected locations (1950-2021)

A. Nighttime Heat Events: Magnitude (°F)

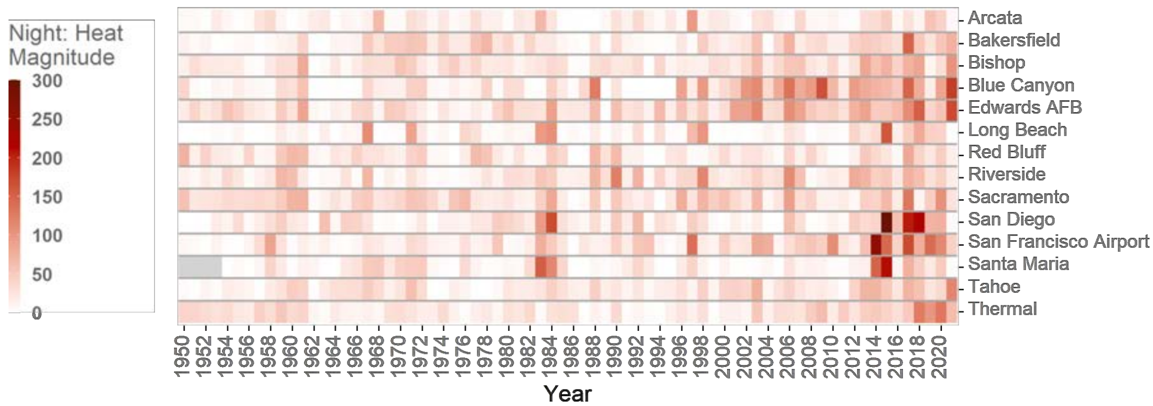

B. Nighttime Heat Events: Frequency (days)

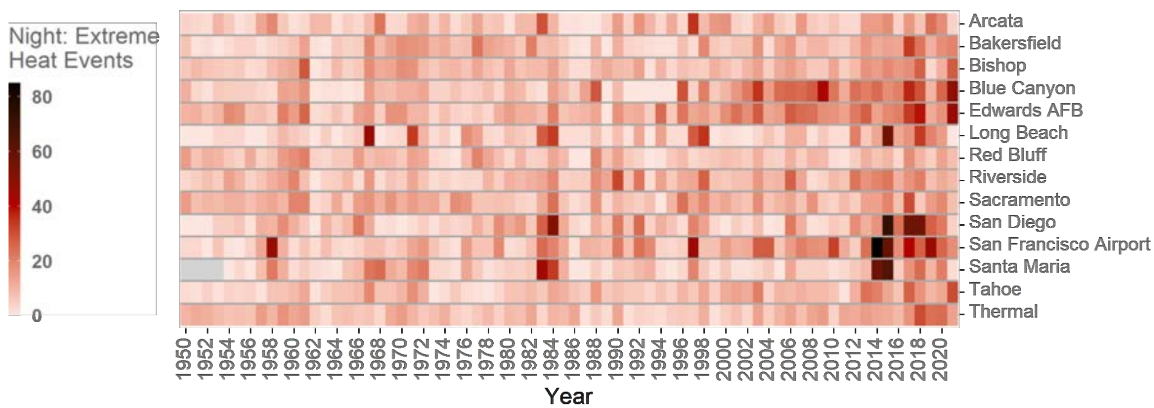

Source: Cal-Adapt, 2018, Dunn 2019, and RCC-ACIS, 2021

Annual values for magnitude and frequency are presented for each location. Greyed out areas mean no data are available for that timeframe. A location-specific threshold of the 95th percentile was used to determine extreme heat events.

San Diego, San Francisco Airport and Santa Maria had at least one year when the magnitude of nighttime heat events reached at least above150°F; San Diego and San Francisco Airport experienced one and three year(s) above 200°F, respectively, during this period (Figure 4A). The last decade also saw the same locations reaching over 35 nighttime heat events on at least one year, with San Diego, San Francisco Airport and Santa Maria recording over 50 nighttime heat events (Figure 4B).

There is no set definition for how many consecutive events make up a heatwave. For purposes of this indicator, a heat wave consists of two or more consecutive daytime or nighttime heat events. Figures 5 and 6 present location-specific averages by decade for daytime and nighttime heatwaves, respectively; values presented for the last decade ("2020") are for 2020 and 2021 only. For comparison, the frequency and magnitude of extreme heat events are also presented.

Figure 5. Daytime heat wave and extreme heat by decade at the selected locations

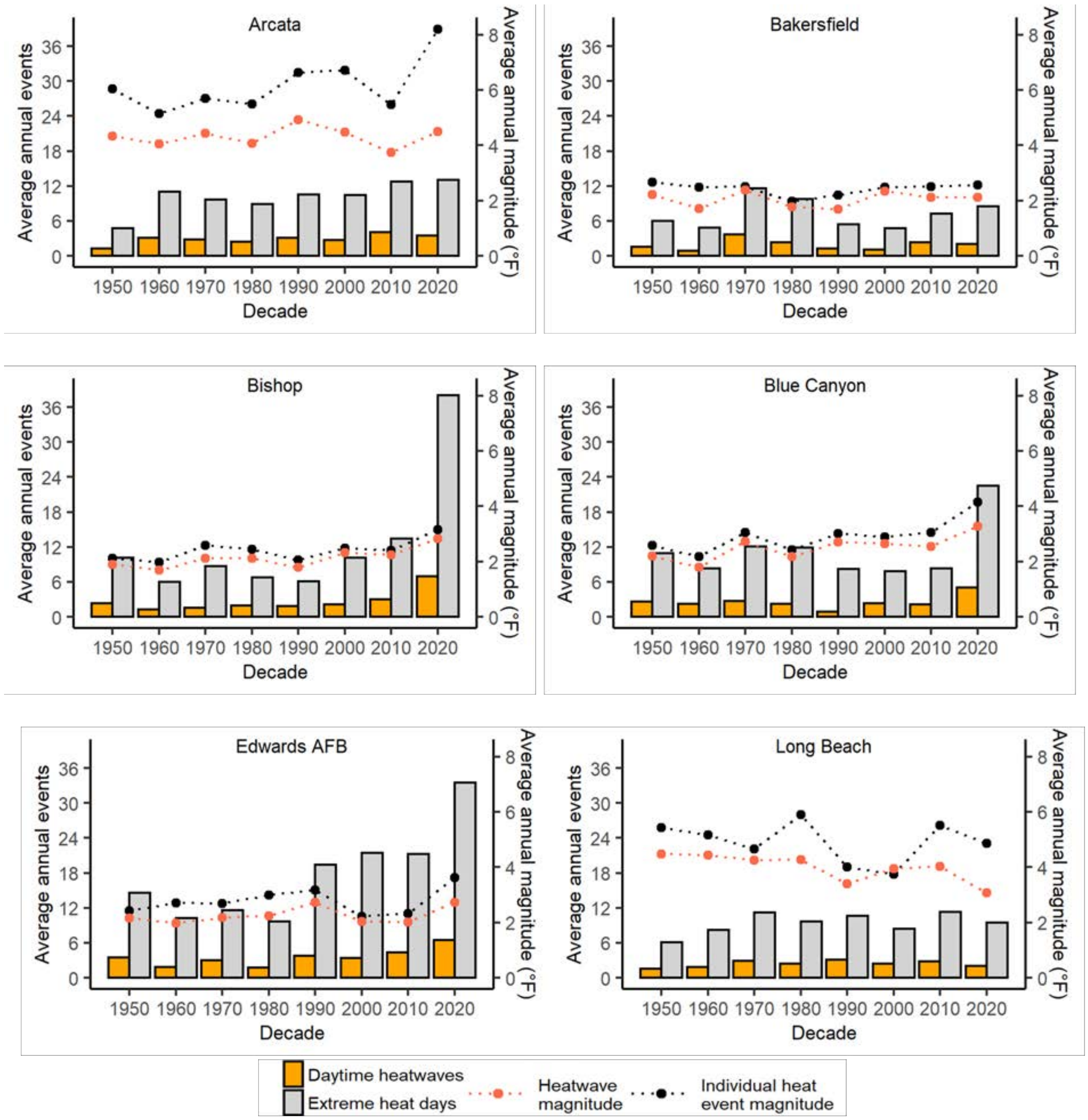

The average annual values by decade for the number of daytime heatwaves and extreme heat events (bars) and their magnitude (the sum of daily exceedances above the historical threshold, in degrees Fahrenheit (°F)) (dots and lines) are presented for each station. A daytime heatwave is defined as two or more consecutive extreme heat days at a given location. Note: Values for the "2020 decade" include data from 2020 and 2021.

Figure 5, continued

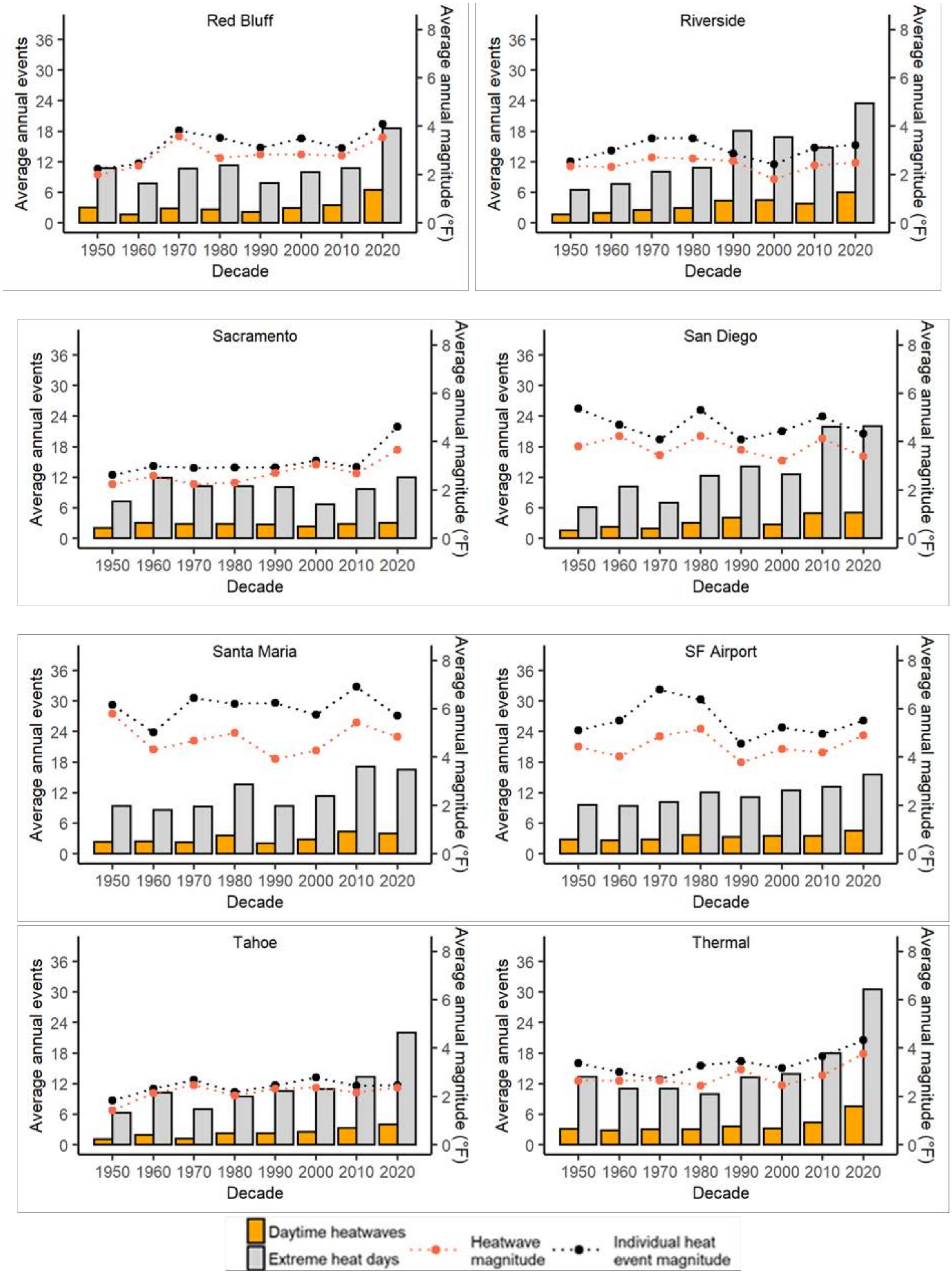

Figure 6. Nighttime extreme heat wave and extreme heat by decade at the selected locations

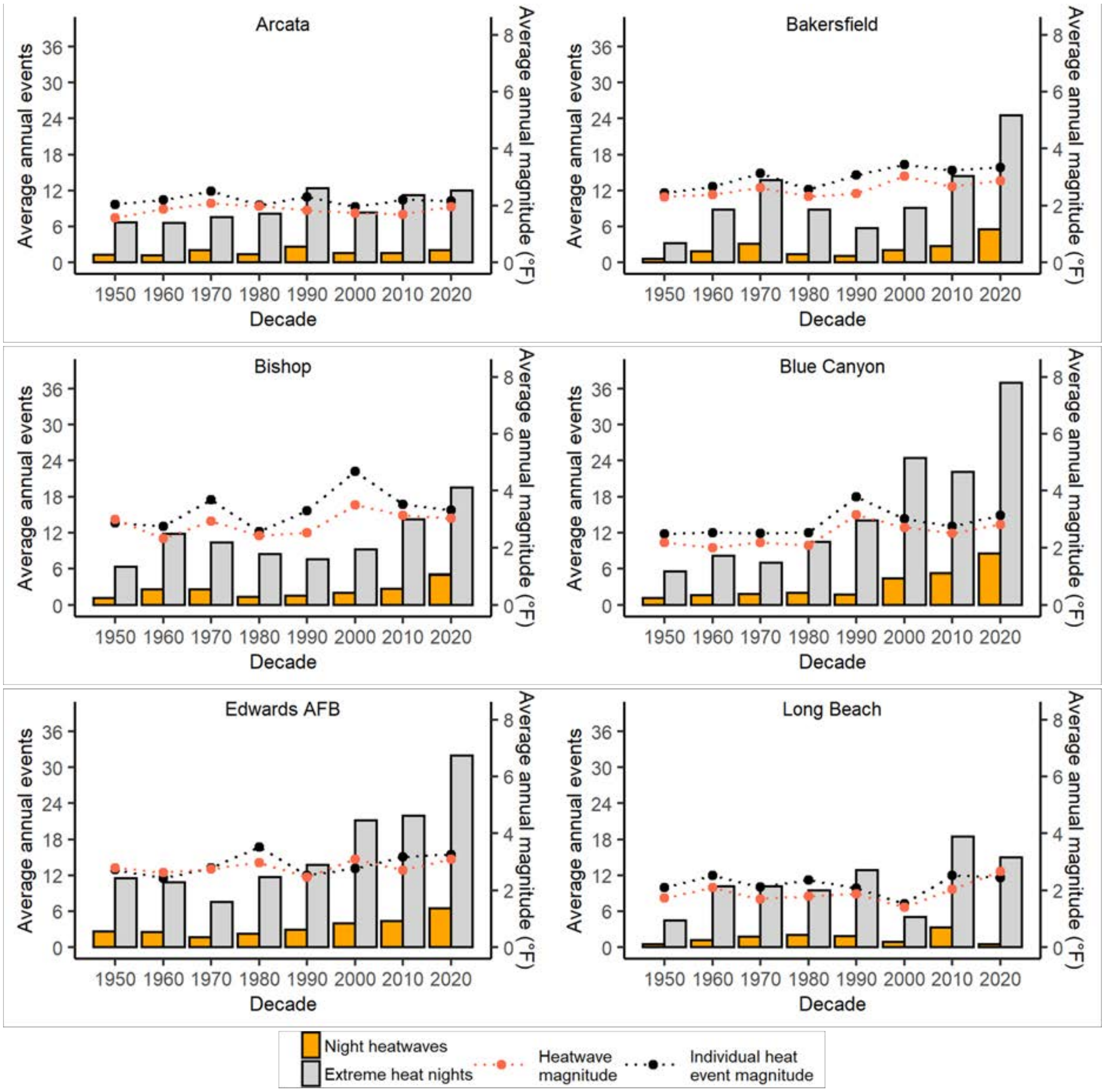

The average annual values for the number of nighttime heatwaves and extreme heat events (bars) and their magnitude (the sum of nightly exceedances above the historical threshold, in degrees Fahrenheit (°F)) (dots and lines) are presented for each station by decade. A nighttime heatwave is defined as two or more consecutive extreme heat nights at a given location. Note: Values for the "2020 decade" include data from 2020 and 2021.

Figure 6, continued

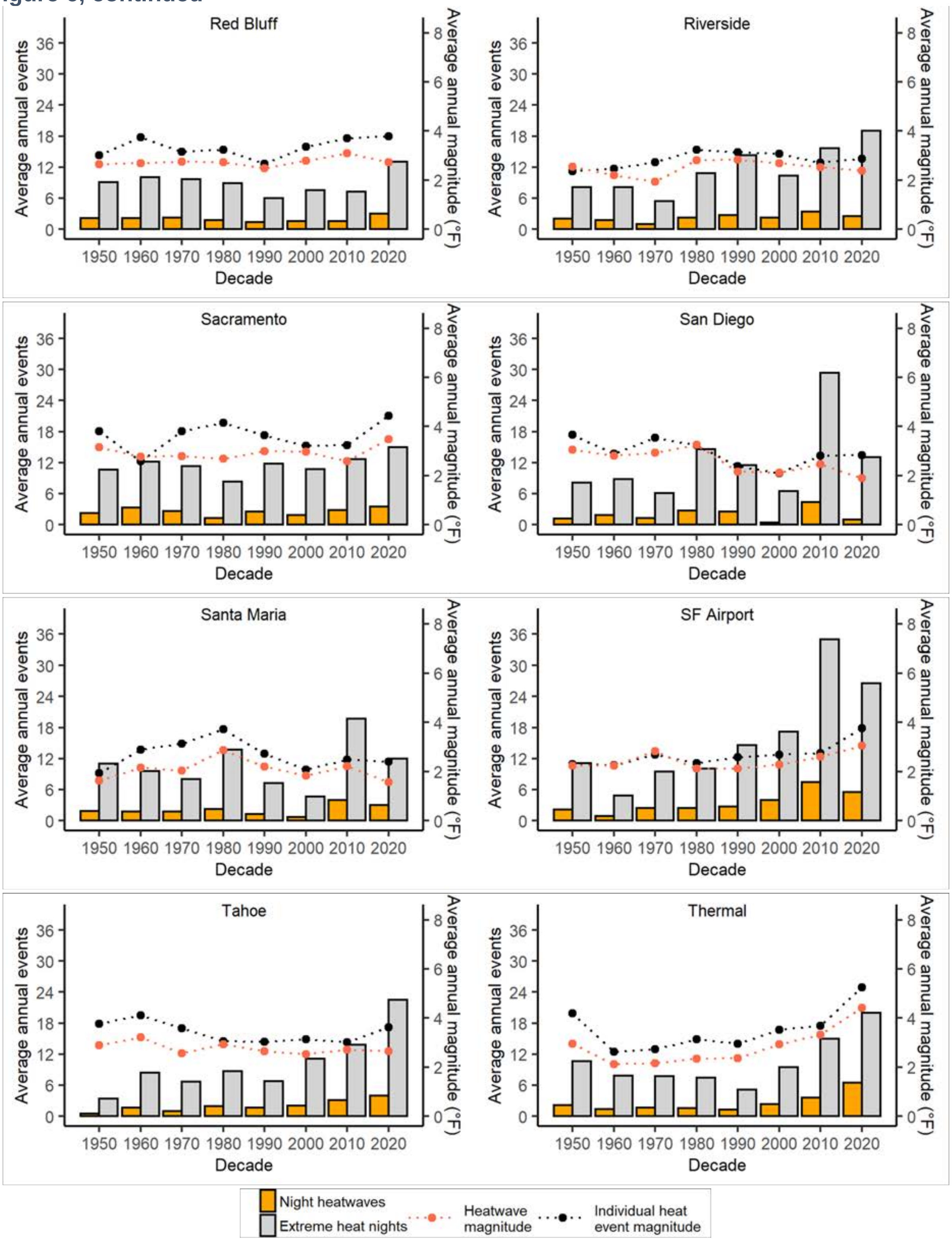

Since 1950, the average number of daytime heatwaves per decade at each station has been relatively constant, ranging between 1 and 3 at most stations, however certain stations have experienced more frequent daytime heatwaves in the 2010s and in 2020/2021: Bishop, Blue Canyon, Edwards AFB, Red Bluff, and Thermal (Figure 5).

The magnitude of daytime heat waves shows no clear trends, although several stations experienced more intense heatwaves in 2020/2021 (Arcata, Bishop, Blue Canyon, Edwards Air Force Base, Red Bluff, Sacramento, San Francisco Airport, and Thermal). Several stations have recorded more frequent nighttime heat waves in the 2010s and in 2020/2021, including Bakersfield, Bishop, Blue Canyon, Edwards AFB, San Francisco Airport, Thermal, and Tahoe (Figure 6). Nighttime heatwave and extreme heat event magnitude are variable but appear to be increasing at San Francisco Airport and Thermal. In general, the magnitude of heat events and heatwaves are higher during the day than at night, but there are more nighttime extreme heat events and heat waves. For most of the stations, the magnitude and frequency of extreme heat events and of heatwaves are higher in the second half of the time series for both nighttime and daytime events.

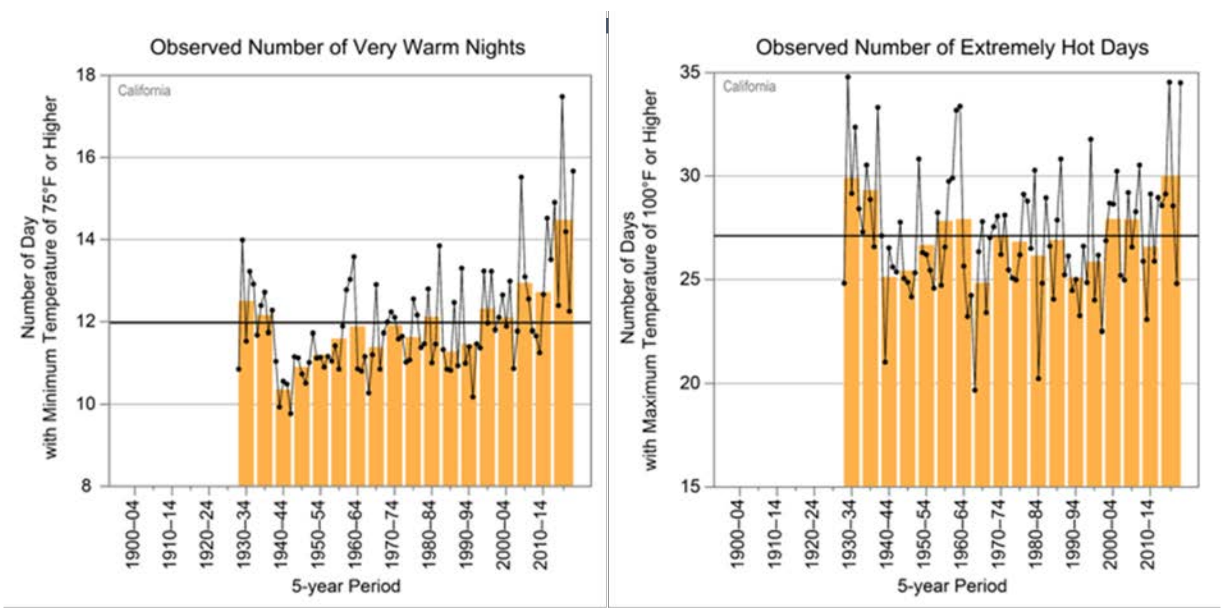

Source: Figures 2a and 3 from Frankson et al., 2022

Left: Observed annual number of extremely hot days (maximum temperature of 100°F or higher) 1930 to 2020. Right: Observed annual number of very warm nights (minimum temperature of 75°F or higher). Dots show annual values. Bars show averages over 5-year periods (last bar is a 6-year average). The horizontal black lines show the long-term (entire period) averages: 27 days and 12 nights, respectively.

Statewide, the number of extremely hot days (Figure 7, right) – defined as days on which the maximum temperature was at or above 100°F – has been variable since

1930, both in terms of annual and five-year averages; the greatest number of hot days were observed during the 2015-2020 period, followed by 1930-1934. A more pronounced increase is evident in the number of very warm nights (Figure 7, left), when minimum temperatures were at or above 75°F. As with extremely hot days, the 2015-2020 period had the greatest number of very warm nights; numbers have exceeded the long-term average on all five-year periods since 1995-1999. Figure 7 is based on statewide analyses conducted by the National Oceanic and Atmospheric Administration's National Centers for Environmental Information (Frankson et al., 2022).

Why is this indicator important?

Periods of extremely high temperatures have significant public health, ecological and economic impacts. Heat causes the most weather-related deaths in the United States (NOAA, 2021). Heat waves accompanied by high humidity are especially dangerous to human health. Humidity prevents surfaces from cooling down at night, leading to higher nighttime temperatures (Gershunov et al., 2009). People, animals (including household pets) and plants adapted to California's traditionally dry daytime heat and nighttime cooling are unable to recover from extreme heat, especially when humidity is high at night. Heat can accelerate the formation of ground-level ozone, and trap ozone, particulate matter and other harmful air pollutants (Peel et al., 2013). Temperature specifically is frequently the leading metrological driver to ozone formation (Nolte et al., 2018). Air pollution may also work in synergy with extremely high temperatures to increase adverse cardiovascular, respiratory and other health effects (Anenberg et al., 2020; see *Heat related mortality and morbidity* indicator).

Although warmer temperatures are likely to impact a range of individuals and populations, certain subgroups are at greatest risk of health impacts from extreme heat due to intrinsic factors (such as age and health status), greater likelihood of exposures, or less capacity for adaptive measures (such as access to air conditioning). These include the elderly, children, those with lower socioeconomic status, those who are socially, linguistically, or geographically isolated, or those who work in agriculture, construction, landscaping or other outdoor occupations (see *Heat related mortality and morbidity* and *Occupational heat-related illness* indicators).

Extreme heat impacts infrastructure and economies (LCI, 2021). Urban infrastructure is especially threatened by cascading effects of extreme heat stress on interdependent water, power, and transportation systems. High heat can deteriorate pavement, buckle railway tracks, and restrict aircraft operations. During hot weather, increased use of air conditioning and refrigeration increases electricity usage, thus straining the electrical grid (see *Cooling and heating degree days* indicator). Further, the increase in electricity generation to meet the demand for air conditioning during extreme heat events leads to increased emissions of nitrogen oxides (NO_x) (Abel et al., 2017; Peel et al., 2013). NO_x has been associated with decreased lung function, lung inflammation, asthma symptoms, and decreased immune response. It is also a precursor for ozone formation.

Water resources are strained during heat events due to increased domestic, industrial and agricultural demand. Extreme heat conditions can also influence tourism, such as in California's Coachella Valley, where it is projected that hotter temperatures will deter visitors and pose a major financial impact to the local economy (Yanez et al., 2020).

Agricultural systems across California and globally are experiencing the impacts of heat stress and decreased water supplies (Parker et al., 2020). Extreme heat exposure stresses plants and stunts development of agricultural crops, resulting in reduced quality and lower yields. Scientists fear that current heat adaptation practices such as enhanced irrigation and crop breeding may not be sustainable under future climate conditions. Heat stress also affects livestock by reducing weight gain or milk and egg production; in extreme cases, heat stress can lead to animal mortality (Walsh et al., 2020).

Climate scientists report that the Western United States has experienced a larger frequency of simultaneously occurring dry and hot years in recent decades (see *Drought* indicator). Multiple extreme events can amplify ecological and societal damages, as shown by the exceptionally dangerous wildfire seasons in recent years. For example, the Thomas fire in December 2017 and the Woolsey fire in November 2018, which caused tremendous devastation in four southern California counties, were both preceded by record-breaking heatwaves and extraordinarily dry autumn conditions (Hulley et al., 2020). A warming climate promotes concurrence of weather extremes, a higher risk of environmental disasters and greater reliance on emergency management and relief resources.

Heat events are projected to become more intense, more frequent, and longer lasting (IPCC, 2021). Taking action to mitigate and adapt to the impacts of extreme heat in California is critical, particularly given the largely preventable adverse effects on public health (LCI, 2021). Recognizing the need for a comprehensive, statewide approach to extreme heat, California is developing a strategic framework of state actions to adapt and build resilience to extreme heat (CNRA, 2021).

What factors influence the indicator?

The increased frequency and intensity of temperature extremes since pre-Industrial times is attributable to human-induced greenhouse gas emissions (IPCC, 2021). Some recent hot extreme events would have been extremely unlikely without human influence on the climate system. Regional patterns are influenced by feedback processes involving land-atmosphere interactions (for example, between soil moisture and evapotranspiration), local land use and land cover changes, aerosol concentrations, and El Niño-Southern Oscillation events and other large-scale modes of climate variability.

Air temperature varies according to the time of day, the season of the year, and geographic location. Urbanization can amplify the effects of global warming in cities, especially at night (the urban heat island effect). However, rural locations see comparable increases in extreme heat days and nights and all regions of California are affected by regional climate change (see *Annual Air Temperature* indicator). The asymmetric increase in nighttime California heat wave activity and extreme heat nights compared to daytime heat extremes is consistent with impacts expected under global climate change.

As air temperatures rise due to anthropogenic emissions of other greenhouse gases, the water vapor content of the atmosphere increases. Water vapor absorbs outgoing longwave terrestrial radiation and re-radiates energy back to the surface, thus impeding radiative cooling. Therefore, there is less nighttime respite from heat when specific humidity is high. Moreover, humid heat waves tend to last longer due to the stronger coupling of maximum and minimum temperatures during humid heat waves (Gershunov et al., 2009).

Technical considerations

Data characteristics

This indicator uses station data from [Hadley Integrated Surface Dataset](#) (HadISD) global record, hosted by CalAdapt, and station data from the National Oceanic and Atmospheric Administration's (NOAA) Regional Climate Centers (RCCs) cooperative observation network acquired from the [Applied Climate Information System](#) (ACIS). The stations using the RCC-ACIS data include: Blue Canyon, Bishop, Tahoe, and Thermal, all the other data used here are from the CalAdapt dataset. Both the RCC-ACIS and HadISD datasets have gone through quality control checks.

At least one station from each of California's climate regions, preferably those located in large urban centers, was selected for the analysis. The climate regions are shown in Figure 8. Only stations with NOAA complete records were used in the analysis. All stations have data starting from at least 1950, except for Santa Maria where data are available starting in 1954. Trends were calculated using the Mann-Kendall analysis.

Figure 8. California's Climate Regions

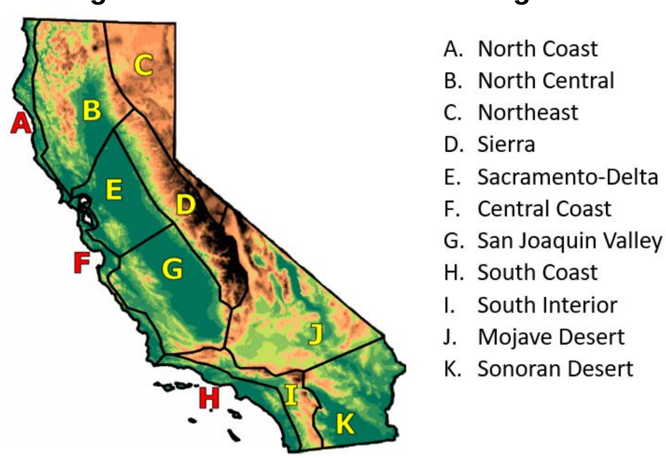

Source: WRCC, 2017

Strengths and limitations of the data

The datasets hosted on CalAdapt consist of hourly observed historical station datasets with at least 30 years of observations from the HadISD global record. The HadISD dataset is compiled from NOAA's Integrated Surface Database, which is a collection of highly quality-controlled weather data from various data sources. The RCC-ACIS (or SCENIC) dataset is comprised of station data containing minimum and maximum daily temperature. RCC-ACIS station data pulls weather information from various networks such as the Cooperative Observer Program (COOP) and the Weather-Bureau-Army-Navy (WBAN). The vast majority of the COOP observers are trained volunteers, and the network also includes the National Weather Service (NWS) principal climatological stations. The observing equipment used at all the stations, whether at volunteer sites or federal installations, are calibrated and maintained by NWS field representatives, Cooperative Program Managers, and Hydro-Meteorological Technicians.

The station data have received a high measure of quality control through computer and manual edits, and are subjected to internal consistency checks, compared against climatological limits, checked serially, and evaluated against surrounding stations. Station coverage is not uniformly distributed geographically, and a limited number of stations were analyzed. Recorded temperatures in urban areas can also be affected by the urban heat island effect due to land surface modification and other human activities. Since most of California's population resides in urban areas, heat impacts from urban-induced warming on health are significant. Quantification of the specific magnitudes of station-based urban heat contributions are beyond the scope of the present study but are the subject of ongoing research.

OEHHA acknowledges the expert contribution of the following to this report:

Western Regional Climate Center

Benjamin Hatchett, Ph.D.
Desert Research Institute
Western Regional Climate Center
Benjamin.Hatchett@dri.edu
(775) 674-7111

Michael L Anderson, Ph.D., P.E.
State Climatologist
California Department of Water Resources
michael.l.anderson@water.ca.gov
(916) 574-2830

References:

Abel D, Holloway T, Kladar RM, Meier P, Ahl D, et al. (2017). Response of Power Plant Emissions to Ambient Temperature in the Eastern United States. *Environmental Science & Technology* **51**(10): 5838-5846.

Alizadeh MR, Adamowski J, Nikoo MR, AghaKouchak A, Dennison P, et al. (2020). A century of observations reveals increasing likelihood of continental-scale compound dry-hot extremes. *Science Advances* **6**: eaaz4571.

Cal-Adapt (2018). Cal-Adapt website developed by University of California at Berkeley's Geospatial Innovation Facility under contract with the California Energy Commission. Data derived from the HadISD global record. Retrieved December 16, 2021.

CCSP (2008). *Analyses of the Effects of Global Change on Human Health and Welfare and Human Systems. Final Report, Synthesis and Assessment Product 4.6. A Report by the U.S. Climate Change Science Program and the Subcommittee on Global Change Research.* U.S. Climate Change Science Program.

CEDA (2020). Met Office Hadley Centre; National Centers for Environmental Information - NOAA (2020): HadISD: Global sub-daily, surface meteorological station data, 1931-2019, v3.1.0.2019f. Centre for Environmental Data Analysis. Retrieved August 31, 2021.

CNRA (2021). *2021 California Climate Adaptation Strategy, Extreme Heat Framework*. California Natural Resources Agency and the Governor's Office of Planning and Research.

Dunn RJH (2019). *HadISD version 3: monthly updates, Hadley Centre Technical Note.*

Forster P, Ramaswamy V, Artaxo P, Bernsten T, Betts R, et al. (2007). Changes in Atmospheric Constituents and in Radiative Forcing. In: *Climate Change 2007: The Physical Science Basis. Contribution of Working Group I to the Fourth Assessment Report of the Intergovernmental Panel on Climate Change.* Solomon S, Qin D, Manning M, Chen Z, Marquis M, et al. (Eds.). Cambridge University Press, Cambridge, United Kingdom and New York, NY, USA.

Frankson R, Stevens LE, Kunkel KE, Champion SM, Easterling DR, et al. (2022): *California State Climate Summary 2022. NOAA Technical Report NESDIS 150-CA.*

Gershunov A, Cayan DR and Iacobellis SF (2009). The Great 2006 Heat Wave over California and Nevada: Signal of an Increasing Trend. *Journal of Climate* **22**(23): 6181–6203.

Guirguis KJ and Avissar R (2008). A precipitation climatology and dataset intercomparison for the western United States. *Journal of Hydrometeorology* **9**(5): 825-841.

Hausfather, Z, Menne MJ, Williams CN, Masters T, Broberg R and Jones D (2013). Quantifying the effect of urbanization on U.S. Historical Climatology Network temperature records. *Journal of Geophysical Research: Atmospheres* **118**: 481-494.

Heinzerling A, Laws RL, Frederick M, Jackson R, Windham G, et al. (2021) Risk factors for occupational heat-related illness among California workers, 2000–2017. *American Journal of Industrial Medicine* **63**(12): 1145-1154.

Hulley GC, Dousset B, and Kahn BH (2020). Rising trends in heatwave metrics across Southern California. *Earth's Future.* **8**: e202 0EF001480.

IPCC (2021). Summary for Policymakers. In: *Climate Change 2021: The Physical Science Basis. Contribution of Working Group I to the Sixth Assessment Report of the Intergovernmental Panel on Climate Change*. Masson-Delmotte VP, Zhai A, Pirani SL, Connors C, Péan S, et al. (Eds.). Cambridge University Press. In Press.

LCI (2021). *Adapting to Extreme Heat in California: Assessing Gaps in State-Level Policies and Funding Opportunities.* UCLA Luskin Center for Innovation.

Maurer EP, Wood AW, Adam JC, Lettenmaier DP and Nijssen B (2002). A long-term hydrologically based dataset of land surface fluxes and states for the conterminous United States. *Journal of Climate* **15**(22): 3237-3251.data updated to 2010

NOAA (2021). National Oceanic and Atmospheric Administration, National Weather Service: Weather Related Fatality and Injury Statistics. Retrieved December 31, 2021.

Nolte CG, Dolwick PD, Fann N, Horowitz LW, Naik V, et al. (2018). Air Quality. *In Impacts, Risks, and Adaptation in the United States: Fourth National Climate Assessment, Volume II*. Reidmiller DR, Avery CW, Easterling DR, Kunkel KE, Lewis KLM, et al. (Eds.). U.S. Global Change Research Program, Washington, DC, USA, pp. 512–538.

Parker LE, McElronec AJ, Ostojaa SM and Forresteld EJ (2020). Extreme heat effects on perennial crops and strategies for sustaining future production. *Plant Science* **295:** 110397.

Peel JL, Haeuber R., Garcia V, Russell AG and Neas L (2013). Impact of nitrogen and climate change interactions on ambient air pollution and human health. *Biogeochemistry* **114**(1–3): 121–134.

RCC-ACIS (2021). Regional Climate Centers - Applied Climate Information System. "Applied Climate Information System." NOAA Regional Climate Centers, Retrieved December 16, 2021.

Richman MB and Lamb PJ (1985). Climatic Pattern Analysis of Three- and Seven-Day Summer Rainfall in the Central United States: Some Methodological Considerations and a Regionalization. *Journal of Climate and Applied Meteorology* **24**(12): 1325-1343.

USGCRP (2016). *Chapter 2: Temperature-Related Death and Illness. The Impacts of Climate Change on Human Health in the United States: A Scientific Assessment*. US Global Change Research Program.

Walsh MK, Backlund P, Buja L, DeGaetano A, and Melnick R (2020). *Climate Indicators for Agriculture.* USDA Technical Bulletin 1953. Washington, DC.

Yañez CC, Hopkins FM and Porter WC (2020). Projected impacts of climate change on tourism in the Coachella Valley, California. *Climatic Change* **162:** 707–721.

WINTER CHILL

Warming winter temperatures are reflected in declining trends in "winter chill," a measure of cold temperatures required for fruit and nut trees to produce flowers and fruits. Winter chill is tracked in two ways: "chill hours," a very sensitive and rudimentary metric used since the 1940s; and "chill portions," a biologically based metric that more closely approximates how California's agricultural trees experience winter chill. Both metrics show decreasing trends across the Central Valley over the past several decades.

Figure 1. Long-term trends in winter chill in California's Central Valley

A. Chill hours **B. Chill portions**

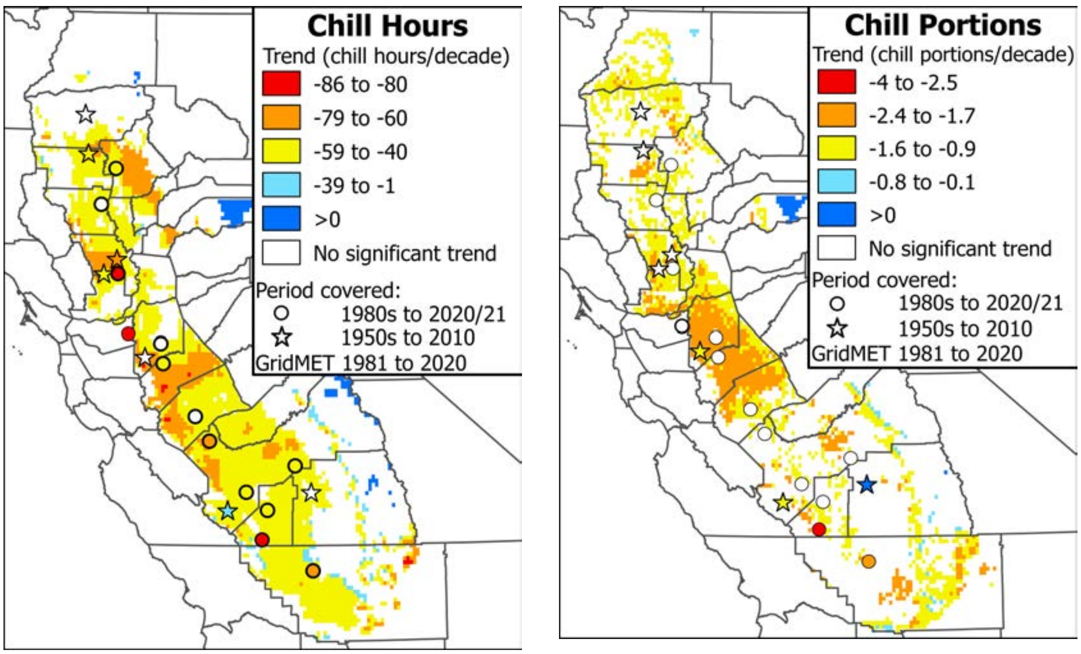

Source: GridMET analysis based on Zhang et al., 2021;
weather station analysis based on UC Davis, 2021

***A. Chill hours** represent the number of accumulated hours equal to or less than 45°F and above 32°F over the winter season. **B. Chill portions** accumulate most between 43° and 47°F, and progressively less at either side of this range, dropping to zero at 32°F and 54°F; periods of warm temperature can cancel this accumulation.*

Stars and circles represent trends at weather stations; coloring throughout the map represents trends derived from gridMET, a spatial data set, where white areas indicate non-significant trends (p<0.05). Trends for weather station sites use winter dates from November 1st to February 28th; gridMET-based trends use winter dates from November 1st to January 31st. (See Figure A-1 in the appendix for a map of weather station locations).

Figure 2. Location of weather stations analyzed for winter chill

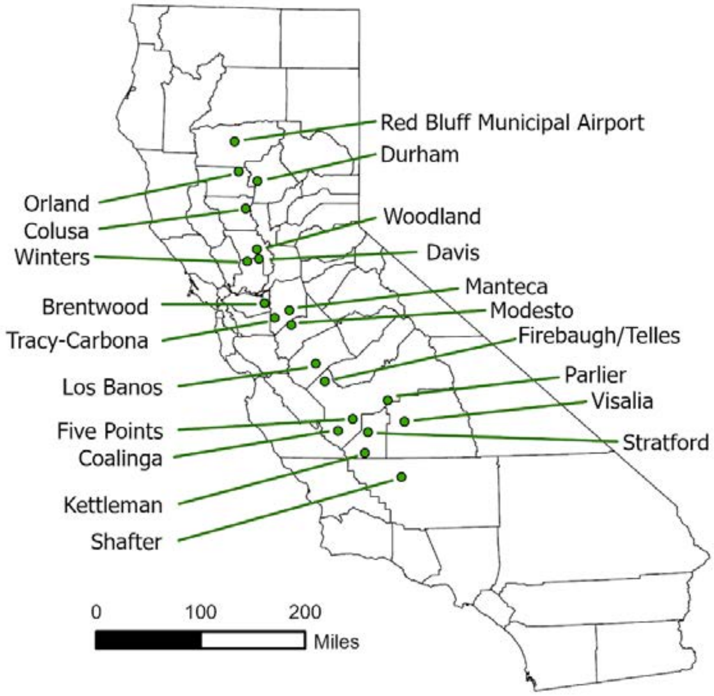

Table 1. Long-term decadal trends in winter chill at selected weather stations

Station	Years included	Chill hours trend (*p-value*)*	Chill portions trend (*p-value*)
Brentwood	1985-2019	-81.2 *(0.01)**	-2.4 *(0.17)*
Coalinga	1952-2010	-33.9 *(<0.01)**	-1.6 *(<0.01)**
Colusa	1983-2016	-70.7 (0.06)	0 (0.99)
Davis	1983-2021	-85.9 *(<0.01)**	-1.5 *(0.14)*
Durham	1983-2021	-46.8 *(0.03)**	-0.9 *(0.38)*
Firebaugh/Telles	1983-2020	-76.0 *(<0.01)**	-0.9 *(0.29)*
Five Points/WSFS USDA	1983-2020	-45.9 *(0.03)**	-0.8 *(0.38)*
Kettleman	1982-2016	-106.6 *(<0.01)**	-3.3 (0.02)*
Los Banos	1989-2020	-38.4 *(0.21)*	-1.5 *(0.23)*
Manteca	1988-2021	-30.1 *(0.29)*	-2.1 *(0.07)*
Modesto	1988-2021	-50.1 *(0.05)*	-2.0 *(0.05)*
Orland	1952-2010	-45.8 *(<0.01)**	-0.8 *(0.14)*
Parlier	1984-2021	-51.0 *(0.01)**	-1.1 *(0.32)*
Red Bluff Municipal Airport	1952-2010	-7.9 *(0.60)*	-0.1 *(0.84)*
Shafter/USDA	1983-2020	-69.6 *(<0.01)**	-1.9 *(0.03)**
Stratford	1983-2020	-43.6 *(0.04)**	-1.3 *(0.19)*
Tracy-Carbona	1952-2007	-19.7 *(0.23)*	-1.2 *(0.03)**
Visalia	1952-2010	-27.3 *(0.05)*	+1.2 *(0.02)**
Winters	1951-2010	-43.0 *(<0.01)**	-1.0 *(0.07)*
Woodland	1952-2010	-60.4 *(<0.01)**	-0.5 *(0.38)*

** Statistically significant trends (where p<0.05) are indicated with an asterisk.*

What does the indicator show?

Winter chill is a period of cold temperatures above freezing required for deciduous fruit and nut trees to produce flowers and fruits. Two commonly used winter chill metrics are presented in Figure 1. The first metric, chill hours (Figure 1A), represents the number of accumulated hours equal to or less than 45 degrees Fahrenheit (°F) and above 32°F over the winter season. Chill hours have been used since the 1940s. However, recent research favors the use of a more biologically based metric, chill portions (Figure 1B). Chill portions accumulate in a two-step process: (1) exposure to cold temperatures accumulate as a "chill intermediate"; this accumulation is negated by exposure to temperatures above 54°F; (2) a certain quantity of these intermediates make up a "chill portion," which cannot be reversed by high temperatures (Luedeling et al., 2009).

Figure 1 presents trends for chill hours and chill portions based on two sources: temperature observations from weather stations (stars and circles, refer to Figure 2 for locations), and modeled high-spatial resolution surface temperatures (gridMET) (colored or white areas on the map). Weather station data show that chill hours have declined at more than half of the weather stations studied (12 out of 20, $p<0.05$; at two other stations, $p=0.05$) (Figure 1A, Table 1). Chill portions show statistically significant declining trends at just four weather stations – Kettleman, Coalinga, Shafter, and Tracy-Carbona (at one other station, $p=0.05$) – and an increasing trend (also significant) at one station (Visalia; Figure 1B, Table 1). Graphs for each weather station presenting data for chill hours and chill portions are in Figure A-1.

Winter chill trends were calculated using gridMET for 19 counties within the Central Valley: Butte, Colusa, Glenn, Fresno, Kern, Kings, Madera, Merced, Placer, San Joaquin, Sacramento, Shasta, Solano, Stanislaus, Sutter, Tehama, Tulare, Yolo, and Yuba. These estimates show declining chill hours in much of the Central Valley (Figure 1A); chill portions are also declining, although at a smaller spatial extent (Figure 1B). The latter suggests that although temperatures have warmed in certain areas, they may not have warmed enough across the region to affect the accumulation of biologically based chill portions, which account for hours at a higher temperature threshold (54°F) than chill hours (32°F - 45°F).

The influence of temperature on the biological processes underlying the breaking of dormancy — and the processes themselves — are poorly understood. It is known, however, that not all "chill" is effective. The chill portion metric considers this by incorporating a more biologically based theoretical framework: temperatures above 54ºF —common during the winter months in California — cancel the effect of previous chill accumulation (Luedeling et al., 2009). Chill hours, which count the number of winter hours when temperatures are between the freezing point and 45ºF, do not account for this canceling effect. For California's Mediterranean climate and mild winters in California's fruit and nut-growing regions, chill portions are better suited for tracking winter chill than chill hours. (See *Technical considerations* for how these metrics are calculated.) The amount of chill that is required is dependent on the type of tree; for example, almonds require 250 to 350 chill hours or 22 to 32 chill portions; apples, 1200 to 1500 chill hours or 50 chill portions; and Bing cherries, 1000 to 1300 chill hours or 65 chill portions (Erez, 2020 and Ryugo, 1988).

Why is this indicator important?

An extended period of cold temperatures above freezing and below a threshold temperature is required for fruit and nut trees to become and remain dormant and then bear fruit. As noted above, this chill requirement can vary widely from one fruit or nut to another and even across varieties of the same fruit or nut. Fruit and nut trees need 200 to 1,500 hours of temperature between 32°F and 45°F during the winter (Baldocchi and Wong, 2006), or between 13 and 75 chill portions to produce flowers and fruits (Pope et al., 2014).

The warm winter of 1998 and 2013-2014 demonstrated the importance of winter chill (Figure 3). Above-normal temperatures in January and February of 1998 meant many fruit and nut trees did not receive sufficient chilling time necessary for dormancy; revenues from almonds and cherries dropped by about 40 and 50 percent, respectively, compared to the two prior years (USDA, 2022). During 2013-2014, the Central Valley's average chill portions dropped by 25 percent. As a result, orchards for many crops showed delayed and extended bloom, poor pollinizer overlap (when the pollen-producing flowers and the fruit-producing flowers do not open simultaneously), and weak leaf-out (when fewer leaves emerge). The low chill was likely responsible for much of the unusual tree behavior and low yields. Delayed bloom can extend later into spring, when conditions may be too warm for successful pollination. Extended bloom can result in changes in fruit or nut maturation timing, which could mean a more prolonged, costly harvest and an increased risk of pests eating crops (Pope, 2014).

Figure 3. Chill portions from 1981-2020

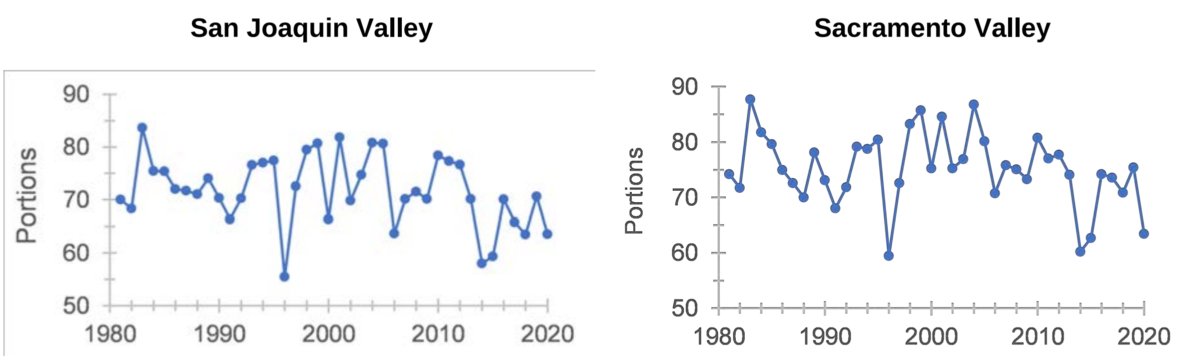

Source: Parker et al., 2022

Annual chill portions within two regions of the Central Valley (San Joaquin Valley and Sacramento Valley)

Prolonged periods of fog during the winter in the California Central Valley provide favorable conditions to meet dormancy requirements. In an analysis of weather data and satellite imagery for the Central Valley during the years 1981-2014, scientists found the number of winter fog events decreased by 46 percent, on average, with much year-to-year variability (Baldocchi and Waller, 2014). If prolonged periods of winter fog disappear in the future, the sun hitting buds in the Central Valley will increase the internal temperature in the buds, thus reducing the number of hours below the critical temperature. Agronomists are finding methods to adapt to this, such as by applying kaolin clay to reflect sunlight or calcium carbonate to modify incoming light (Beede, 2016).

Future trend projections show that continued warming will reduce the accumulated winter chill in the Central Valley (Luedeling et al., 2009). By the middle to the end of the 21st century, projections suggest that climatic conditions will no longer support current varieties of some of the main tree crops currently grown in California. Chill hours are projected to show greater declines than chill portions, and current varieties of major tree crops may tolerate a 20 percent decline in the winter chill. This decline would jeopardize the region's ability to sustain its production of high-value nuts and fruits like almonds, cherries, and apricots, resulting in serious economic, dietary, and social consequences. The tree crop industry will likely need to develop agricultural adaptation measures (e.g., using chill-compensating products or growing low-chill varieties) to cope with these projected changes.

What factors influence this indicator?

The indicator is derived from temperature data. As such, it is influenced by the same factors that influence air temperature; the increase in winter temperatures in the Central Valley (see *Air temperature* indicator) is reflected in the decrease in chill hours at most of the weather stations and throughout the region. In addition to regional influences such as topography and proximity to the ocean, local factors such as degree of urbanization and land use can affect temperature. Furthermore, "microclimates" exist within the same orchard, so temperature differences could occur at smaller spatial scales.

As discussed above, the choice of metric makes a difference in quantifying the magnitude of winter chill accumulation. The difference presented here between chill hours and chill portions is consistent with research that has modeled the potential impact of continued climate change. For example, one study using weather data and several greenhouse gas emissions scenarios throughout California's Central Valley projected chill portions to decrease by 14 to 21 percent and chill hours to decrease by 29 to 39 percent between 1950 and 2050 (Luedeling et al., 2009). Projected impacts appear far more dramatic when seen through the lens of chill hours, although the chill hours model appears to be more sensitive to changes in temperature than the trees themselves.

While both metrics quantify chill accumulation, factors such as proximity of the weather station or, as noted above, the presence of microclimates introduce uncertainties in whether the temperature measurements used in deriving them are representative of what trees are experiencing.

Technical considerations

Data characteristics

The indicator presents two metrics for winter chill: chill hours and the more mathematically complex chill portions. The primary differences in the calculations for these two metrics are:

- Chill hours equally count any hour when temperatures are between 32°F and 45°F. Chill portions accumulate when temperatures are between 32°F and 54°F, with the most accumulation occurring between 43°F and 47°F.
- Chill hours only count up to 45°F. Chill portions count up to 54°F, which better approximates effective chilling for trees grown in fairly mild climates.
- Chill hours are a sum of hours between the temperatures described above, without accounting for warm hours. Chill portions accumulate in a two-step process first reaching a “chill intermediate” that can be negated by exposure to high temperatures (above 54°F); a certain quantity of chill intermediates make up a “chill portion,” which cannot be reversed by high temperatures (Leudeling et al., 2009).

Weather station-based chill hours and chill portions were calculated using “chillR," a statistical model for phenology analysis (Leudeling, 2017). The model is an extension to a commonly used statistics software, R. Weather station data for Central Valley locations listed in Baldocchi and Wong (2008) were retrieved through the chillR downloading interface. Stations for which data were not retrievable from the University of California Statewide Integrated Pest Management Program (UCIPM) archive were omitted from the analysis.

The UCIPM archive includes data from the California Irrigation Management Information System (CIMIS) and the National Weather Service Cooperative Network (NWS COOP). Hourly temperature records, which are needed to calculate chill accumulation, are available from CIMIS. However, these stations only have data back to 1982. NWS COOP has records that date back decades earlier (the earliest records used in this indicator start in 1951), but only for daily maximum and minimum temperature; hourly temperatures were estimated using an algorithm based on diurnal temperature trends and reported maximum and minimum temperature (Leudeling, 2017).

To estimate chill hours and chill portions using gridMET, daily temperature time series were downscaled to hourly and fed into chillR (Zhang et al., 2021). GridMET trends were calculated for the 19 counties within the Central Valley: Butte, Colusa, Glenn, Fresno, Kern, Kings, Madera, Merced, Placer, San Joaquin, Sacramento, Shasta, Solano, Stanislaus, Sutter, Tehama, Tulare, Yolo and Yuba.

Strengths and limitations of the data

Summary statistics that are commonly used to track temperature (such as average, minimum and maximum) generally do not provide the resolution necessary to examine climate trends relevant to agriculture. Deriving chill accumulation from temperature data for the winter months yields a more meaningful measure for tracking a change in climate that would be more predictive of fruit production. Winter chill accumulation provides an indication of whether specific fruit and nut trees are experiencing sufficient periods of dormancy.

The hourly data from CIMIS provide direct inputs into the calculation of winter chill degree hours, unlike daily minimum and maximum temperature data from NWS, which require the use of an algorithm. CIMIS weather stations are designed to monitor agricultural climate conditions. Thus, they are almost exclusively in agricultural areas, with the monitoring equipment located in a well-irrigated pasture. NWS COOP weather stations are designed with a broader use in mind. As such, they are generally located in developed, paved areas – in towns and cities, or at airports. As a result, temperatures at the NWS COOP stations in the winter are likely higher than they would be in an open field a few miles away. While this means that the chill accumulation at each NWS COOP weather station may not be precisely representative of what an orchard in that area would experience, any trends of increased or decreased chill accumulation of years and decades would likely be similar.

Historical temperature records are rarely complete. Many different approaches are used to fill in gaps in temperature records to analyze long-term trends. In this report, hourly or daily station temperatures were interpolated following Luedeling (2017). If more than 50 percent of the winter record required interpolation, that winter was not included in the analysis.

GridMET provides a daily temperature product at a 4-km spatial resolution within the USA from 1979 to the present. This allows for analyses across the entire landscape, unlike weather station data which only shows weather at one location. Since gridMET is modeled product, it may not be as accurate as station-based data. However, like weather station data, the direction of the gridMET trends is accurate.

OEHHA acknowledges the expert contribution of the following to this report:

UCDAVIS
UNIVERSITY OF CALIFORNIA

Weather station data analysis:
Allan D. Hollander
University of California, Davis
Dept. of Environmental Science and Policy
adhollander@ucdavis.edu

gridMET analysis:
Ning Zhang, Ph.D.
University of California Merced
ninzhan@ucanr.edu

Lauren E. Parker
John Muir Institute of the Environment
University of California Davis
leparker@ucdavis.edu

Tapan B. Pathak
University of California Merced
tpathak@ucmerced.edu

References:

Baldocchi D and Waller E (2014). Winter fog is decreasing in the fruit growing region of the Central Valley of California. *Geophysical Research Letters* **41**(9).

Baldocchi D and Wong S (2006). *An Assessment of the Impacts of Future CO_2 and Climate on Californian Agriculture. #CEC-500-2005-187-SF* California Climate Change Center.

Baldocchi D and Wong S (2008). Accumulated winter chill is decreasing in the fruit growing regions of California. *Climatic Change* **87**(1): 153-166.

Beede B (2016). Sun Reflecting Products for Increased Winter Chill. Retrieved March 25, 2022.

Erez, A. (2000). *Temperate Fruit Crops in Warm Climates*. Springer Netherlands.

Luedeling E (2017). chillR: Statistical Methods for Phenology Analysis in Temperate Fruit Trees. R package version 0.66.

Luedeling E, Zhang M, Luedeling V, and Girvetz EH (2009). Sensitivity of winter chill models for fruit and nut trees to climatic changes expected in California's Central Valley. *Agriculture, Ecosystems & Environment* **133**(1–2): 23-31.

Luedeling, E., Brown, P.H., (2010) A global analysis of the comparability of winter chill models for fruit and nut trees. *Int. J. Biometeorol.* 55, 411–421.

Parker, L. E., Zhang, N., Abatzoglou, J. T., Ostoja, S. M., & Pathak, T. B. (2022). Observed Changes in Agroclimate Metrics Relevant for Specialty Crop Production in California. *Agronomy* ***12***(1), 205.

Pope KS (2014). Is Last Year's Warm Winter the New Normal? Retrieved February 12, 2022.

Pope KS, Brown PH, DeJong TM, and Da Silva D (2014). A biologically based approach to modeling spring phenology in temperate deciduous trees. *Agricultural and Forest Meteorology* **198**: 15-23.

Ryugo, K. (1988). *Fruit Culture: Its Science and Art*. Wiley.

UC Davis (2021). Chill hours and chill portions at selected Central Valley sites, estimated using chillR (Luedeling 2017), using data from UC IPM (Weather, Models, and Degree Days. University of California Statewide Integrated Pest Management System). November, 2021.

USDA (2022). California Agricultural Overview: 1998. U.S. Department of Agriculture, National Agricultural Statistics Service. Accessed May 12, 2022.

Zhang N, Pathak TB, Parker LE, & Ostoja SM (2021). Impacts of large-scale teleconnection indices on chill accumulation for specialty crops in California. *Science of The Total Environment 791*.

Appendix

Figure A-1. Long-term trends in chill hours and chill portions, by location.

Statistically significant trends ($p<0.05$) are shown as red lines; no trend line is shown for non-significant trends.

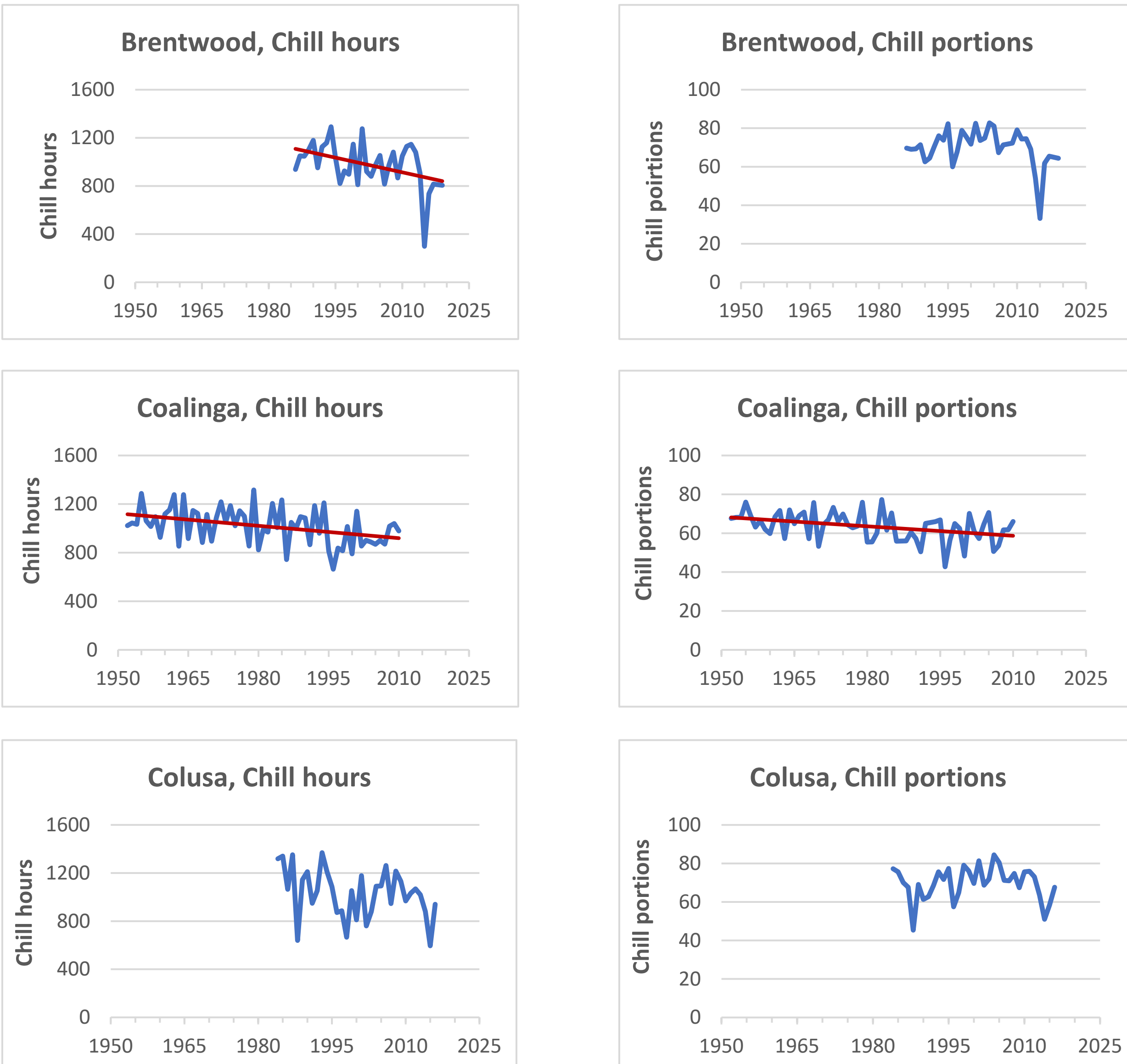

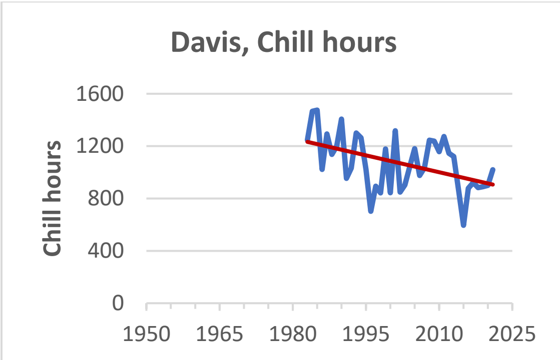
Davis, Chill hours
Chill hours
1600
1200
800
400
0
1950
1965
1980
1995
2010
2025

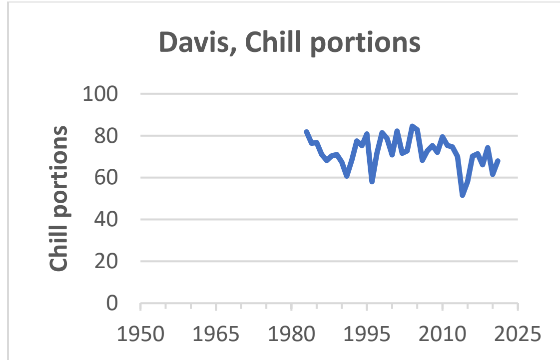
Davis, Chill portions
Chill portions
100
80
60
40
20
0
1950
1965
1980
1995
2010
2025

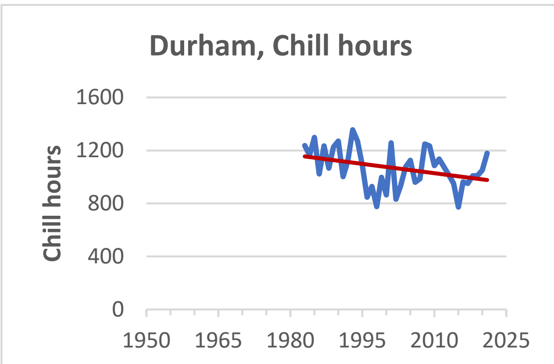
Durham, Chill hours
Chill hours
1600
1200
800
400
0
1950
1965
1980
1995
2010
2025

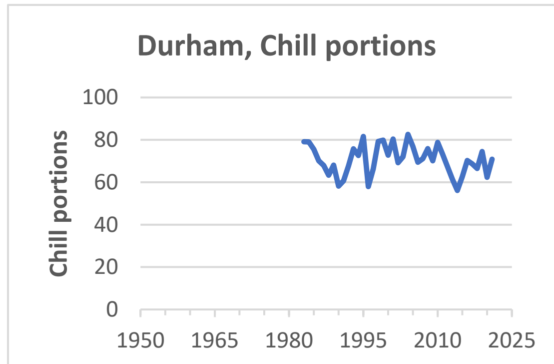
Durham, Chill portions
Chill portions
100
80
60
40
20
0
1950
1965
1980
1995
2010
2025

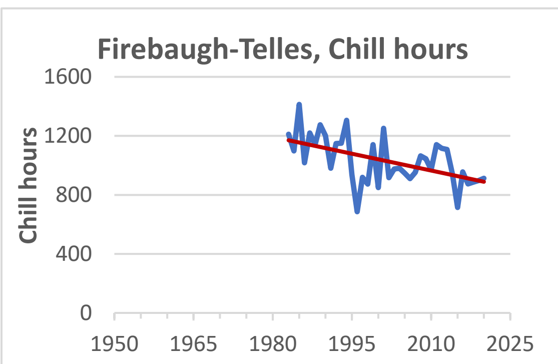
Firebaugh-Telles, Chill hours
Chill hours
1600
1200
800
400
0
1950
1965
1980
1995
2010
2025

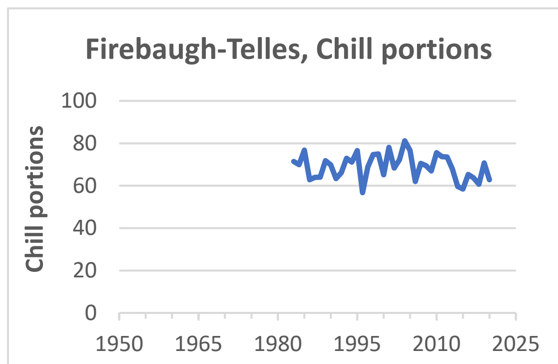
Firebaugh-Telles, Chill portions
Chill portions
100
80
60
40
20
0
1950
1965
1980
1995
2010
2025

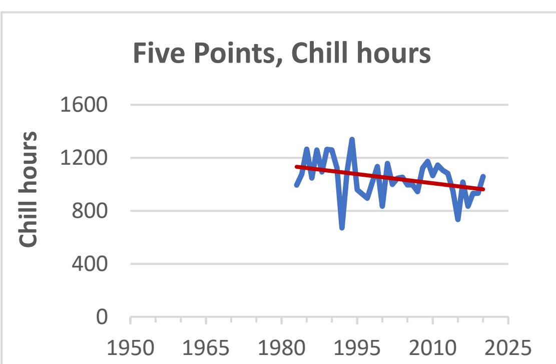
Five Points, Chill hours
Chill hours
1600
1200
800
400
0
1950
1965
1980
1995
2010
2025

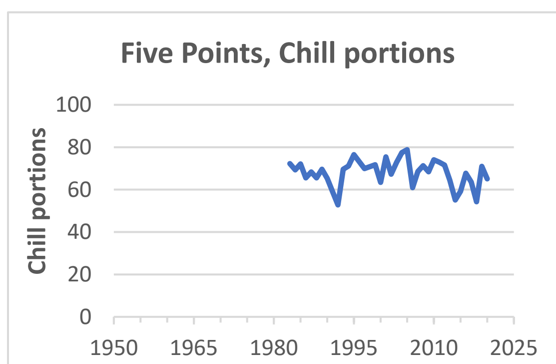
Five Points, Chill portions
Chill portions
100
80
60
40
20
0
1950
1965
1980
1995
2010
2025

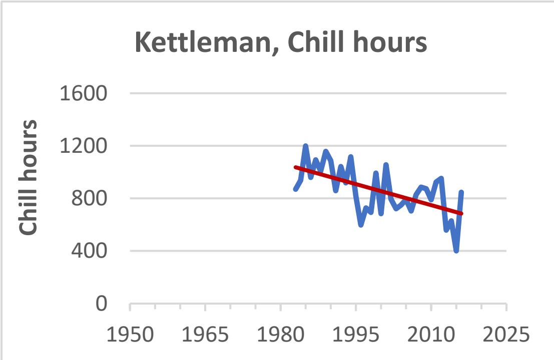
Kettleman, Chill hours
Chill hours
1600
1200
800
400
0
1950
1965
1980
1995
2010
2025

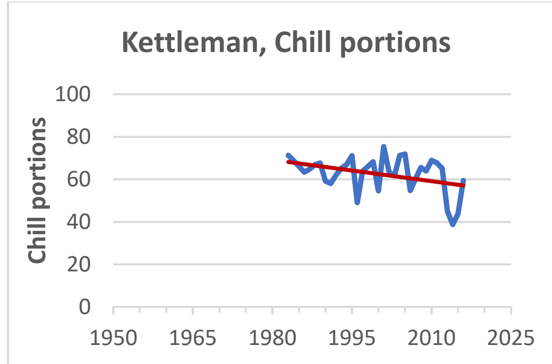
Kettleman, Chill portions
Chill portions
100
80
60
40
20
0
1950
1965
1980
1995
2010
2025

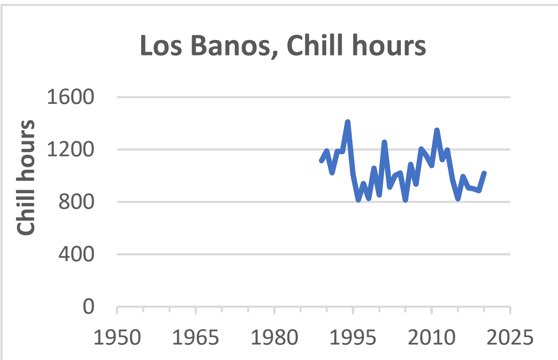
Los Banos, Chill hours
Chill hours
1600
1200
800
400
0
1950
1965
1980
1995
2010
2025

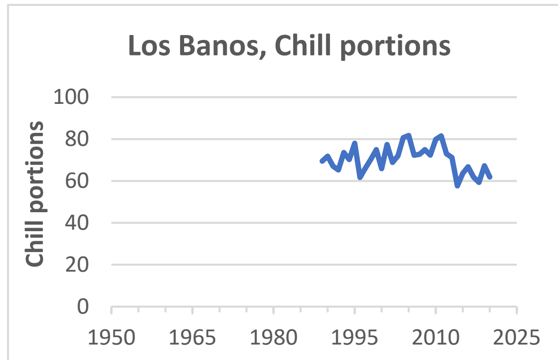
Los Banos, Chill portions
Chill portions
100
80
60
40
20
0
1950
1965
1980
1995
2010
2025

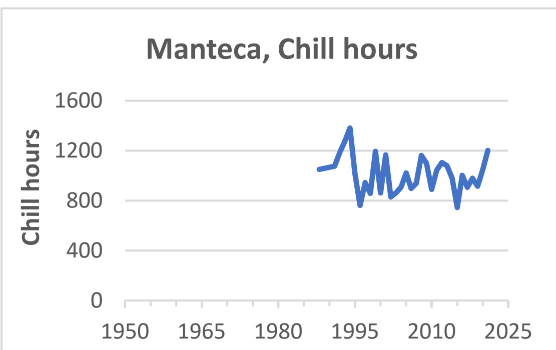
Manteca, Chill hours
Chill hours
1600
1200
800
400
0
1950
1965
1980
1995
2010
2025

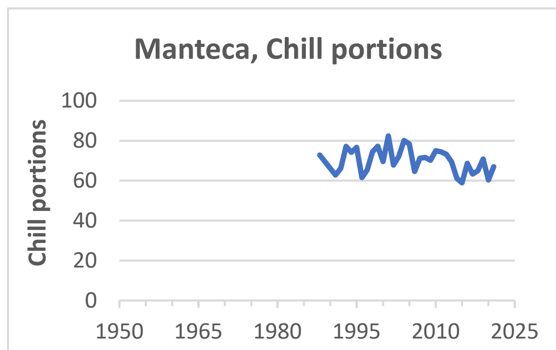
Manteca, Chill portions
Chill portions
100
80
60
40
20
0
1950
1965
1980
1995
2010
2025

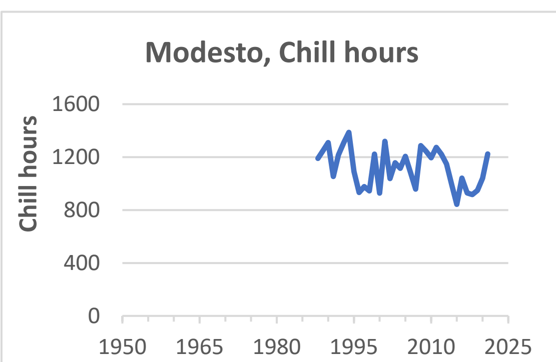
Modesto, Chill hours
Chill hours
1600
1200
800
400
0
1950
1965
1980
1995
2010
2025

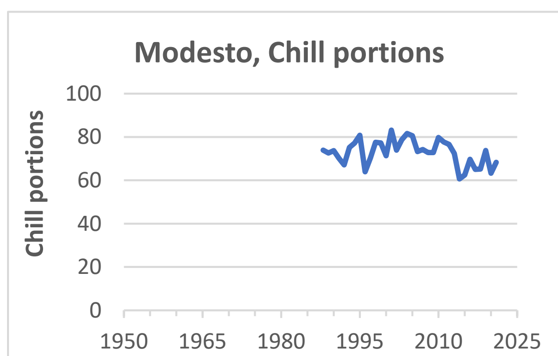
Modesto, Chill portions
Chill portions
100
80
60
40
20
0
1950
1965
1980
1995
2010
2025

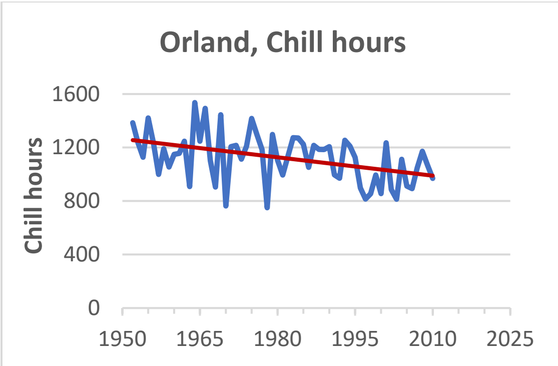
Orland, Chill hours
Chill hours
0
400
800
1200
1600
1950
1965
1980
1995
2010
2025

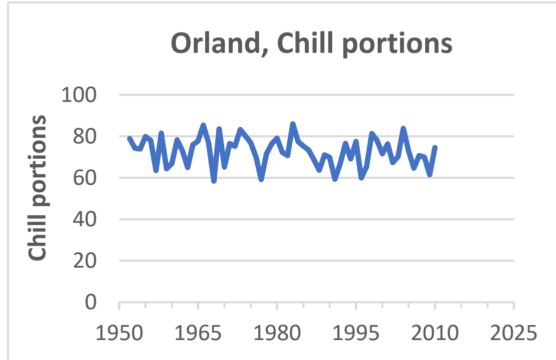
Orland, Chill portions
Chill portions
0
20
40
60
80
100
1950
1965
1980
1995
2010
2025

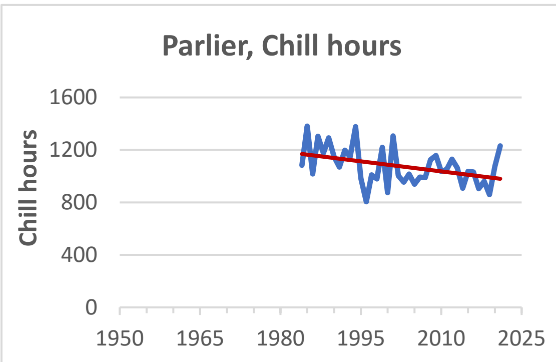
Parlier, Chill hours
Chill hours
0
400
800
1200
1600
1950
1965
1980
1995
2010
2025

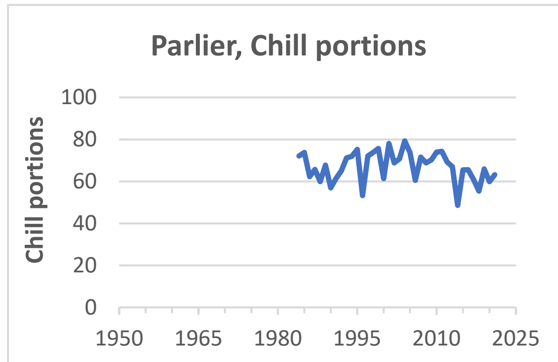
Parlier, Chill portions
Chill portions
0
20
40
60
80
100
1950
1965
1980
1995
2010
2025

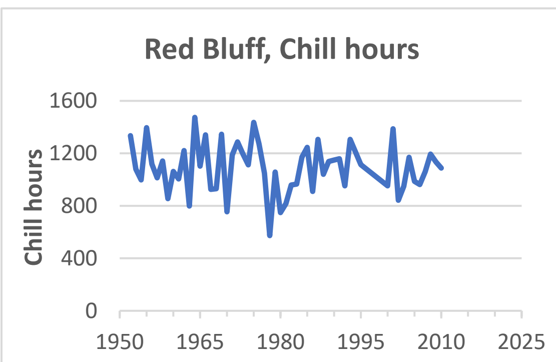
Red Bluff, Chill hours
Chill hours
0
400
800
1200
1600
1950
1965
1980
1995
2010
2025

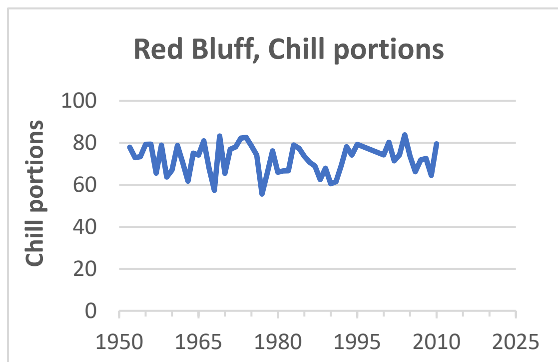
Red Bluff, Chill portions
Chill portions
0
20
40
60
80
100
1950
1965
1980
1995
2010
2025

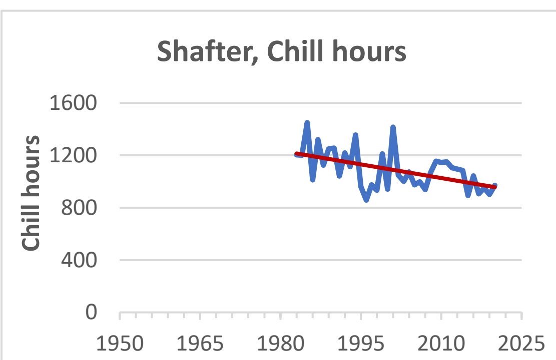
Shafter, Chill hours
Chill hours
0
400
800
1200
1600
1950
1965
1980
1995
2010
2025

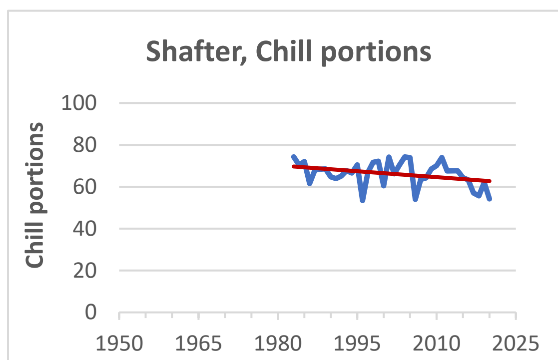
Shafter, Chill portions
Chill portions
0
20
40
60
80
100
1950
1965
1980
1995
2010
2025

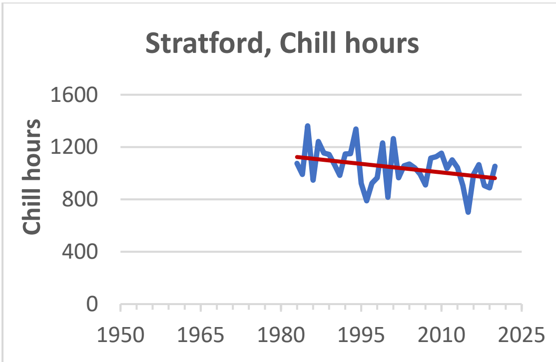
Stratford, Chill hours
Chill hours
1600
1200
800
400
0
1950
1965
1980
1995
2010
2025

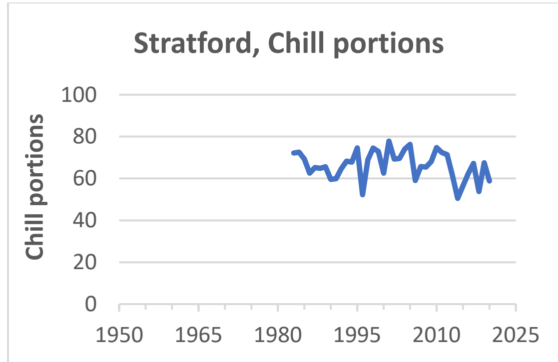
Stratford, Chill portions
Chill portions
100
80
60
40
20
0
1950
1965
1980
1995
2010
2025

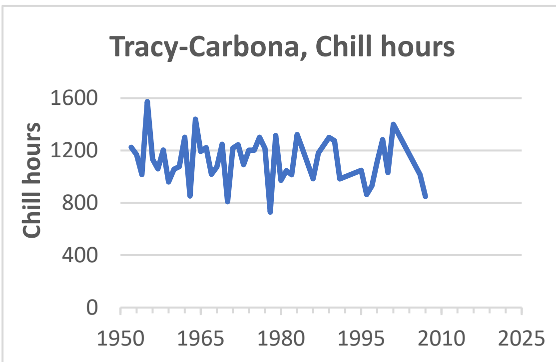
Tracy-Carbona, Chill hours
Chill hours
1600
1200
800
400
0
1950
1965
1980
1995
2010
2025

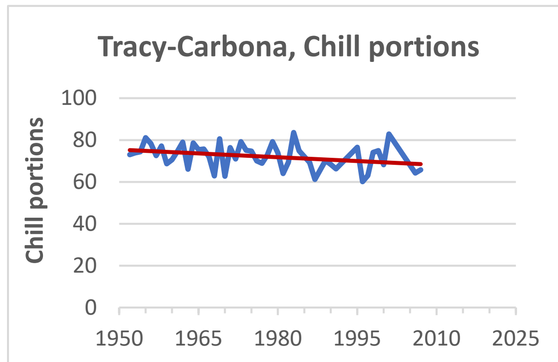
Tracy-Carbona, Chill portions
Chill portions
100
80
60
40
20
0
1950
1965
1980
1995
2010
2025

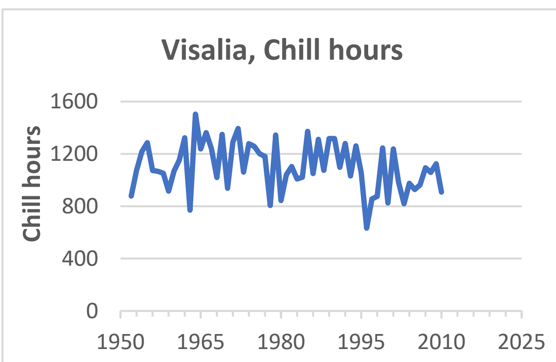
Visalia, Chill hours
Chill hours
1600
1200
800
400
0
1950
1965
1980
1995
2010
2025

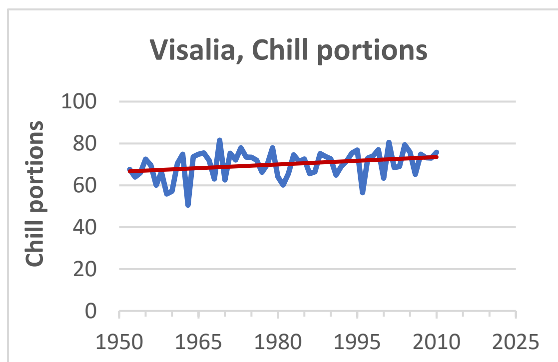
Visalia, Chill portions
Chill portions
100
80
60
40
20
0
1950
1965
1980
1995
2010
2025

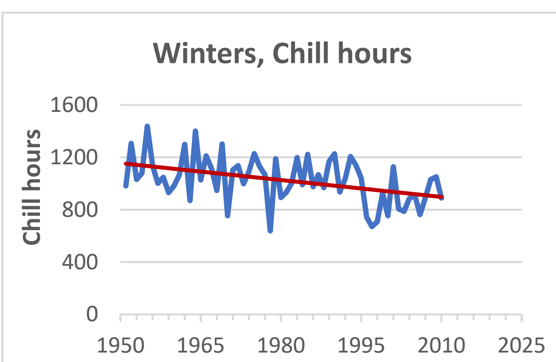
Winters, Chill hours
Chill hours
1600
1200
800
400
0
1950
1965
1980
1995
2010
2025

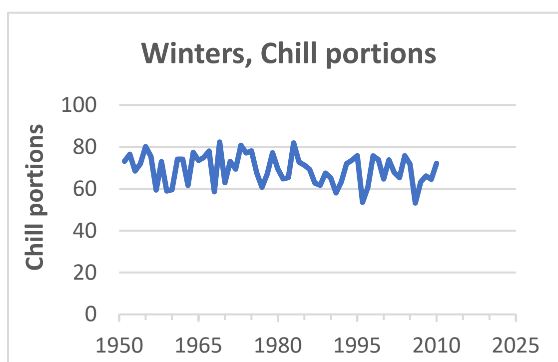
Winters, Chill portions
Chill portions
100
80
60
40
20
0
1950
1965
1980
1995
2010
2025

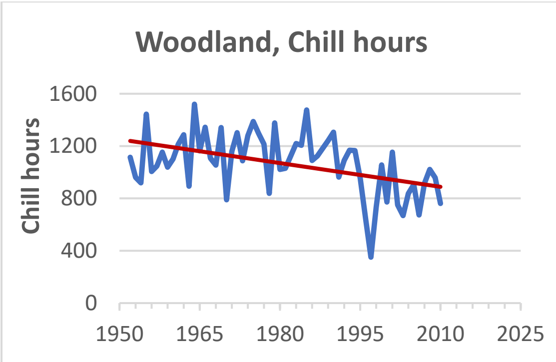

Woodland, Chill hours
Chill hours
1600
1200
800
400
0
1950
1965
1980
1995
2010
2025

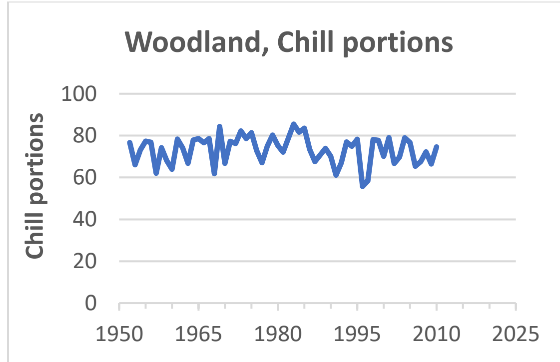

Woodland, Chill portions
Chill portions
100
80
60
40
20
0
1950
1965
1980
1995
2010
2025

COOLING AND HEATING DEGREE DAYS

Cooling degree days and heating degree days are temperature-based metrics used to help estimate cooling and heating needs. Other things being equal, the higher the cooling degree days over a period, the more energy required to cool a building to a given temperature. Similarly, the higher the heating degree days, the less energy it takes. In California, cooling degree days have gradually increased and heating degree days have gradually decreased.

Figure 1. Cooling and Heating Degree Days Statewide

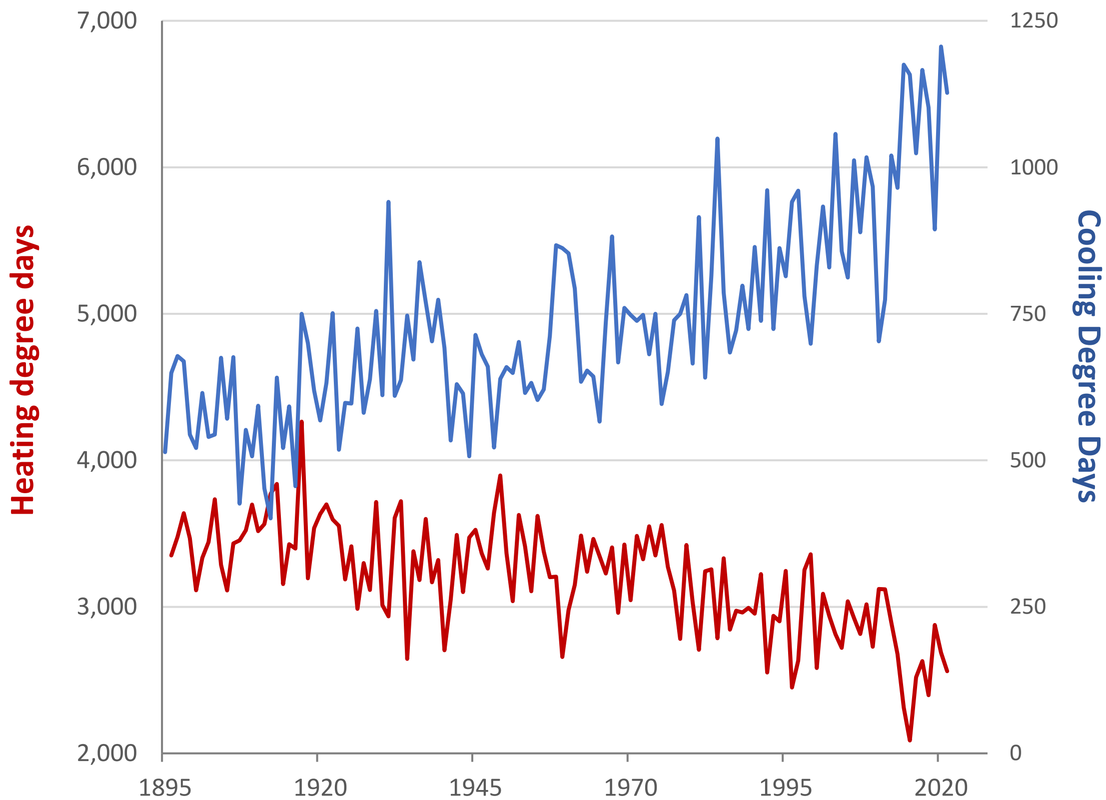

Source: NOAA 2022

Note: Degree days measure the difference between the average daily temperature and a reference temperature, in this case, 65 degrees Fahrenheit (°F). Cooling degree days measure how much the average daily temperature is higher than 65°F; heating degree days, how much it is lower than 65°F. For example, an average statewide temperature of 75°F on one day corresponds to a cooling degree day value of 10. Average is defined as the midpoint of the hourly minimum and maximum temperature for the day. Each value shown in the graph is the sum of degree days for

What does the indicator show?

Annual cooling degree days (CDD) in California increased between 1895 and 2020, while heating degree days (HDD) decreased over the same period (Figure 1). Both trends are consistent with national patterns (NOAA, 2021a) and are especially visible in the past five decades, with the past few years showing some unusually high statewide CDDs and unusually low HDDs.

California's 100 million acres encompass diverse terrains and geographies with various climates. Long-term trends in degree days show regional variations, as shown in Figures 2, 3, and 4 and Table 1 for California's seven NOAA climate divisions.[1] All seven divisions show an increase in CDD and a decrease in HDD over the last century, but to varying extents (see Figures 2-4). Coastal California shows greater percentage increases in CDD over the last century compared to inland areas of the state, partly because they had low CDDs to begin with. The Central Coast and especially the South Coast had the largest percentage declines in HDD.

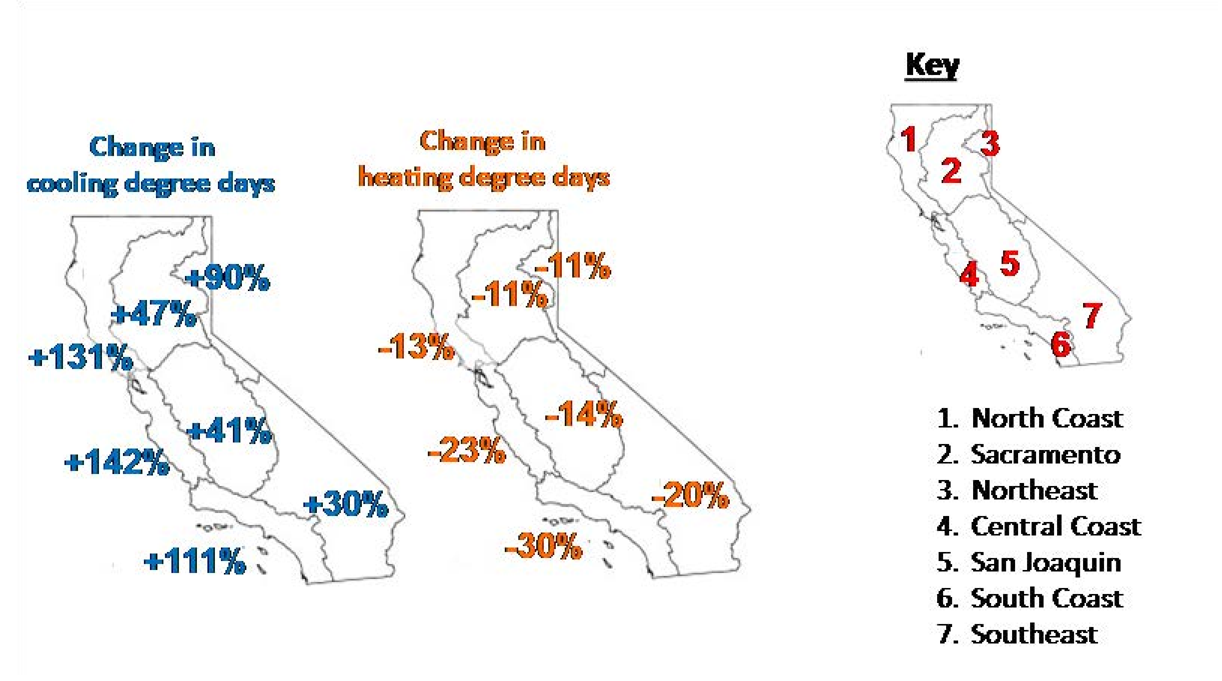

Source: NOAA, 2022a

Table 1 presents these trends in terms of changes in annual cooling and heating degree days (base 65°F) for the seven climate divisions, expressed as a linear rate of change per decade. Trends are reported for two periods: 1895 to 1970, and 1971 to 2020. In each region, cooling degree days increased and heating degree days decreased over both periods. The regional rates of change for the most recent 50 years (1972-2021) are substantially higher than for the previous 77-year period (1895-1971).

---

[1] National Oceanic and Atmospheric Administration (NOAA) climate divisions span the contiguous United States, subdividing each state into ten or fewer climate divisions; other indicators in this report are based on data from the Western Regional Climate Center, which divides California into eleven climate regions.

Table 1. Divisional Trends in Cooling and Heating Degree Days

Trends are presented for each of California's climate divisions. Values presented are the slope of linear trends, representing the rate of change in cooling or heating degree days per year.

Climate Division	Trends, 1895-1971 (Degree Days per Decade)		Trends, 1972-2021 (Degree Days per Decade)	
	Cooling	Heating	Cooling	Heating
North Coast Drainage	+8	-32	+45	-135
Sacramento Drainage	+18	-18	+62	-119
Northeast Interior Basins	+6	-68	+27	-157
Central Coast Drainage	+16	-35	+63	-138
San Joaquin Drainage	+15	-12	+82	-135
South Coast Drainage	+27	-45	+86	-147
Southeast Desert Basins	+38	-24	+111	-98

Source: NOAA, 2021a.

Figure 3. Cooling degree days by Division, 1895-2021*

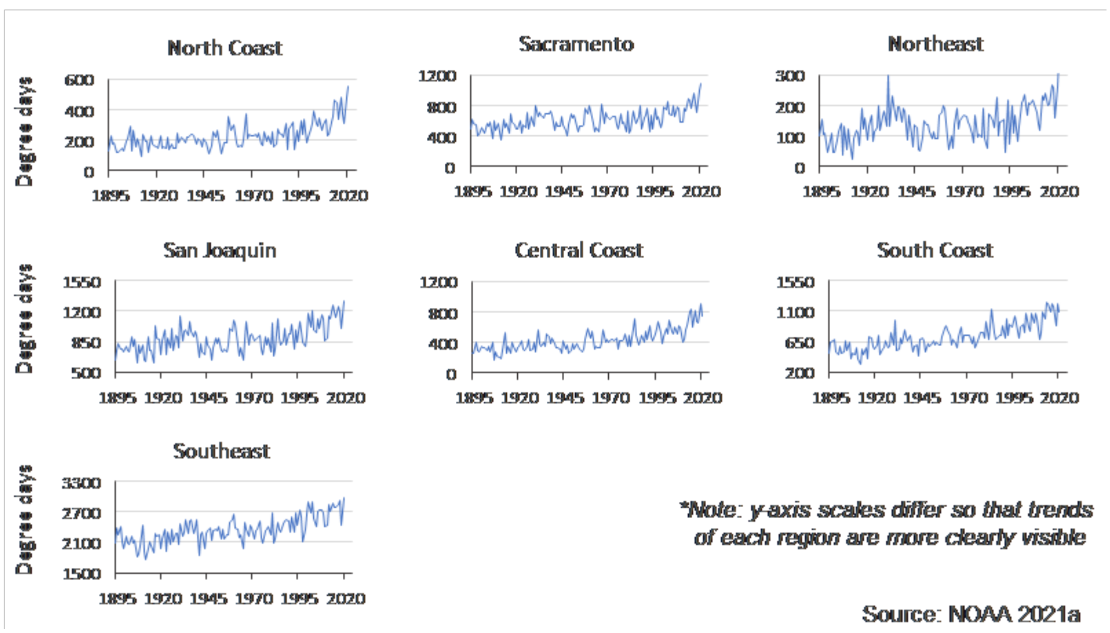

Figure 4. Heating degree days by Division, 1895-2021*

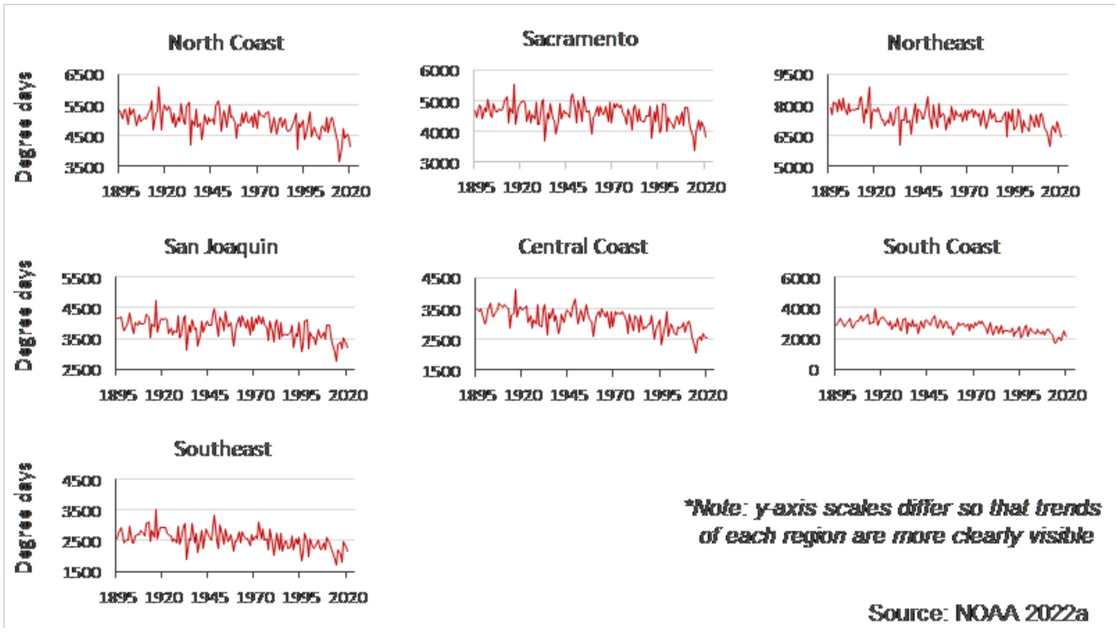

Why is this indicator important?

Since the 1930s, degree days have been used as a proxy for the energy needed to cool or heat homes and buildings, to benchmark building performance, and to inform utility planning and construction decisions (Marston, 1935; Meng and Mourshed, 2017; NOAA, 2005; USGCRP, 2020), as well as in estimating changes in biological systems such as in agriculture. The relationship between degree days and building heating and cooling energy use is approximate and depends on many factors that vary by building and over time. These include building construction and thermal characteristics (such as building size, ventilation, insulation, and number, placement and energy efficiency rating of windows and doors), building type and function (single-family residential, multi-family residential and the myriad of commercial and industrial uses), the type and efficiency of cooling and heating technologies, and cooling and heating practices (for example, based on occupancy, tolerance for heat or cold, and use of heat-generating appliances and equipment) (Meng and Mourshed, 2017; US EPA, 2016). Compressor-based air conditioning was not introduced into U.S. homes until the middle of the 20th century (Cooper, 1998). Prior to that, home cooling did not use much energy; other such changes can be expected as energy use and technology evolve.

As the climate continues to warm, heating needs will likely decline, and energy consumption is expected to shift from cooler months to warmer months (CEC, 2015) due to increased cooling energy use from expanded presence of air conditioning and higher levels of use. In 2019, 58% of California households had central cooling, while in

2003 only 44% did (DNV, 2021).[2] That is, in 2019, California homes were 32% more likely to have central cooling than in 2003. Meeting a growing demand for cooling creates specific challenges for new energy generation and distribution infrastructure, including encouraging higher levels of load flexibility to manage peak demand and system reliability (CEC, 2020; US EPA, 2016). At the same time, warming temperatures, sea level rise, and wildfires can negatively impact the operation or the efficiency of power plants, transmission networks, and natural gas facilities (CEC, 2009, 2012, 2020; Patrick and Fardo, 2009; US EPA, 2016). Climate change can also affect renewable energy, given its dependence on natural resources like water, wind, biomass and available incoming solar radiation, which are all influenced by climate variations (CEC, 2009).

For lower-income households, heating and cooling costs represent a bigger fraction of household income than for higher-income households (CalEPA, 2010). The impact of increased summer heat is disproportionate across households and communities. Lower-income households are less likely to own well-functioning efficient air conditioners or even any air conditioners at all (Chen et al., 2020; Fernandez-Bou et al., 2021), which potentially makes them more vulnerable to health effects of summer heat extremes.

What factors influence this indicator?

Since heating and cooling degree days reflect trends in temperature, factors that influence temperature affect this indicator. These factors are discussed in the *Annual air temperature* indicator.

Technical considerations

Data characteristics

The values for degree days are downloaded from NOAA's Climate at a Glance website (NOAA, 2021c). They are derived by NOAA using daily temperature observations at major weather stations in the United States with NOAA's Climate Divisional Database (nClimDiv). nClimDiv uses a 5 km gridded approach to compute temperature, precipitation, and drought values for United States climate divisions. A mean daily temperature (average of daily maximum and minimum temperatures) of 65˚F serves as the reference temperature for degree day calculations for this data set. Cooling degree days are calculated by summing the positive differences between the mean daily temperature and the 65˚F reference temperature. Heating degree days are calculated by summing the negative differences between the mean daily temperature and 65˚F.

Strengths and limitations of the data

The nClimDiv dataset is an improved version of an older climate dataset from NOAA, benefitting from additional quality assurance reviews and temperature bias adjustments

[2] This comparison pertains only to households served by California's three investor-owned utilities (Pacific Gas & Electric, Southern California Edison, and San Diego Gas & Electric) or LADWP, which are the utilities surveyed in both the 2003 and 2019 Residential Appliance Saturation Surveys.

and providing more robust values than its predecessor. New methodologies include a transition to a grid-based calculation and additional stations from before the 1930s (NOAA, 2021b).

There are important limitations to keep in mind when relating degree days to energy use. First, the thermal comfort of building occupants depends on more than just indoor temperatures (Kwok and Rajkovich, 2010). Heating and cooling energy use for a given set of degree days also depends on a variety of factors beyond the technical characteristics of structures and equipment, such as social practices, occupant preferences, and thermal comfort management regimes (Deumling et al., 2019; McGilligan et al. 2011). Second, degree days cannot fully express the complexity of weather, how and where it changes, or how these changes affect indoor conditions (Azevedo et al., 2015). For example, nighttime low temperatures have increased more than daytime high temperatures in much of California, especially since 2000 (Lindsey, 2018; see the *Annual air temperature indicators*). This can reduce the contribution of nighttime temperatures to natural cooling but is scarcely captured in degree days indicators. Also, though 65˚F is the standard base temperature used for computing degree days in U.S. energy applications, different base temperatures—such as a higher base temperature for CDD (EIA,1983) — could give different results for energy predictions. Overall, since climate patterns, land use, construction, building technologies, social patterns, and modeling methods are changing, legacy computational practices using CDD and HDD might be usefully revamped as well.

OEHHA acknowledges the expert contribution of the following to this report:

MMithra Moezzi
CCalifornia Energy Commission
(((916) 891-8619
Mithra.Moezzi@energy.ca.gov

References:

Azevedo JA, Chapman L and Muller CL (2015). Critique and suggested modifications of the degree days methodology to enable long-term electricity consumption assessments: A case study in Birmingham, UK. *Meterological Applications* **22**(4): 789-796.

CalEPA (2010). *Indicators of Climate Change in California: Environmental Justice Impacts*.

CEC (2009). California Energy Commission. *Potential Impacts of Climate Change on California's Energy Infrastructure and Identification of Adaptation Measures* (CEC-150-2009-001).

CEC (2012). California Energy Commission. *Our Changing Climate 2012: Vulnerability & Adaptation to the Increasing Risks from Climate Change in California* (CEC-500-2012-007).

CEC (2015). California Energy Commission. *2015 Integrated Energy Policy Report* (CEC-100-2015-001-CMF).

CEC (2018). California Energy Commission. *Tracking Progress. Energy Equity Indicators*.

CEC (2020). California Energy Commission. *Final 2019 Integrated Energy Policy Report* (CEC-100-2019-001-CMF).

Chen, M, Ban-Weiss GA and Sanders KT (2020). Utilizing smart-meter data to project impacts of urban warming on residential electricity use for vulnerable populations in southern California. *Environmental Research Letters* **15** (6): 064001.

Cooper G (1998). *Air-Conditioning America: Engineers and the Controlled Environment 1900-1960*. Baltimore, MD: The Johns Hopkins University Press.

Deumling, R, Poskanzer D, and Meier AK (2018). 'Everyone has a peer in the low user tier': The diversity of low residential energy users. *Energy Efficiency* **12**(1): 244-259.

DNV (2021). Det Norske Veritas. California Statewide Residential Appliance Saturation Study Data Server.

Fernandez-Bou SA, Ortiz-Partida JP, Dobbin KB, Flores-Landeros H, et al. (2021). Underrepresented, understudied, underserved: Gaps and opportunities for advancing justice in disadvantaged communities. *Environmental Science & Policy.* **122**: 92–100.

Kwok AG and Rajkovich NB. (2010). Addressing climate change in comfort standards. *Building and Environment* **45**(1): 18-22.

Lindsey R (2018). NOAA News & Features: Extreme Overnight Heat in California and the Great Basin in July 2018.

Marston AD (1935). Degree days for cooling. *Bulletin of the American Meteorological Society* **16**(10): 242-244.

McGilligan C, Natarajan S, and Nikolopoulou M (2011). Adaptive comfort degree-days: A metric to compare adaptive comfort standards and estimate changes in energy consumption for future UK climates. *Energy and Buildings* **43**(10): 2767-2778.

Meng Q and Mourshed M (2017). Degree-day based non-domestic building energy analytics and modelling should use building and type specific base temperatures. *Energy and Buildings* **155**: 260–268.

NOAA (2005). National Oceanic and Atmospheric Administration. NOAA National Weather Service Climate Prediction Center Degree Day Monitoring and Data: Explanation*.* Retrieved October 2016.

NOAA (2021a). National Oceanic and Atmospheric Administration. NOAA Climate at a Glance: U.S. Time Series. Retrieved March 2021.

NOAA (2021b). National Oceanic and Atmospheric Administration. NOAA Monitoring References: U.S. Climate Divisions. Retrieved March 2021.

NOAA (2021c). National Oceanic and Atmospheric Administration. Degree Day Monitoring & Data, National Weather Service Climate Prediction Center. Retrieved April 7, 2021.

Patrick DR and Fardo SW (2009). Ch 7: Power Distribution Equipment. *In: Electrical Distribution Systems* (2nd ed). Lilburn, Georgia: The Fairmont Press, Inc.

US EIA (1983). US Energy Information Administration. *Regression Analysis of Energy Consumption by End Use*.

US EIA (2009). US Energy Information Administration. *Household Energy Use in California*.

US EIA (2013). US Energy Information Administration. *Residential Energy Consumption Survey*.

US EPA (2016). US Environmental Protection Agency. Climate Change Indicators in the United States. Retrieved December 15, 2017.

USGCRP (2020). US Global Change Research Program. National Climate Assessment. Retrieved August 16, 2020.

PRECIPITATION

While the amount of annual precipitation over time shows no statewide trend, year-to-year variability has increased since the 1980s. In recent years, the fraction of precipitation that falls as rain instead of snow has increased in the Sierra Nevada and Southern Cascades, reducing the water stored in the snowpack that provides most of California's water supply.

Figure 1. Statewide annual precipitation (1895-2021)

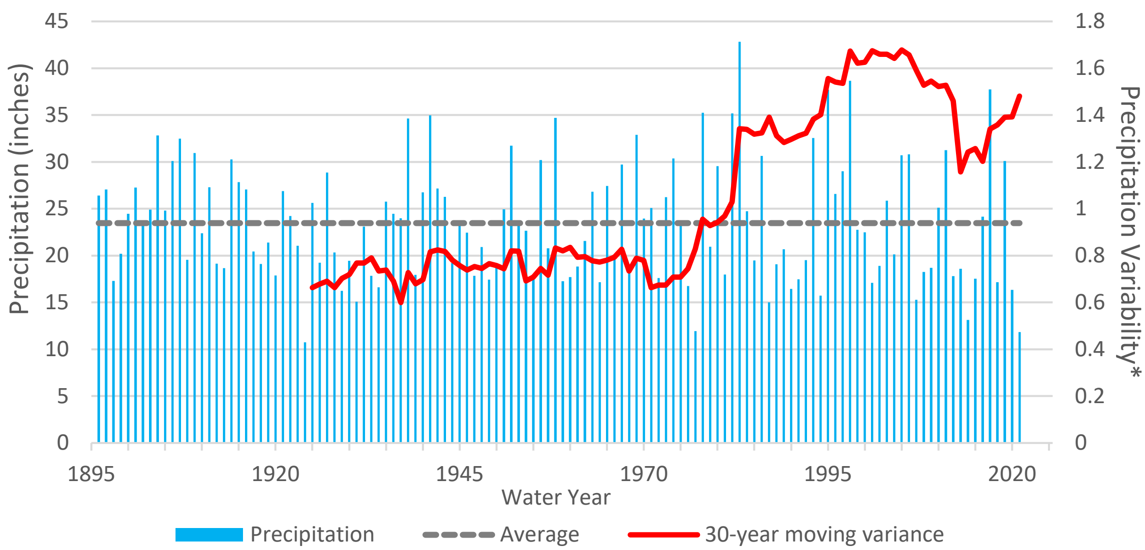

Source: WRCC, 2022

***Precipitation variability**: *the value shown for each year beginning in 1925 is the ratio of the variance for the 30-year period ending in that year to the variance over the entire period (1895-2021). A ratio above 1 means precipitation was more variable; below one, less variable.*

What does the indicator show?

California experiences high year-to-year variability in precipitation: some years are very wet, while others are very dry. Since the early 1980s, precipitation over the state has become more variable (Figure 1, red line). The same is true across the state's climate regions (see appendix; also He and Guatam, 2016). The past decade included the third wettest year on record (2017) and the second driest (2021). In 2017 California emerged from a severe and prolonged drought. From October 2018 to September 2019, California transitioned from a very dry fall into a very wet winter. The water year 2021 was the second driest on record, following 1924.

Precipitation totals are tracked by "water year," from the beginning of the rainy season in October through the following September, the end of the dry season. This is more useful than a calendar year in California due to its typically dry summer and wet winter ("Mediterranean") climate. On average, 75 percent of the state's annual precipitation occurs from November through March, with 50 percent occurring from December through February.

No clear trend is evident in the amount of total annual precipitation (Figure 1, blue bars). Statewide precipitation is the area-weighted average of regional precipitation values. In other words, the regional precipitation values — computed as an area-weighted average of precipitation at the climate stations in the region — are weighted by the area covered by each region, and an average is calculated as the statewide value. Since records began in 1895, statewide annual precipitation has ranged from a low of 10.75 inches in 1924 to a high of 42.82 inches in 1983. The water years spanning 2012 to 2015 set a record for the driest consecutive four-year period of statewide precipitation. The average annual precipitation varies greatly among California's eleven climate regions (as defined by the Western Regional Climate Center): from 4.7 inches in the Sonora Desert to 67.8 inches in the North Coast.

Figure 2. Rain as a percentage of total precipitation* (1949-2020)

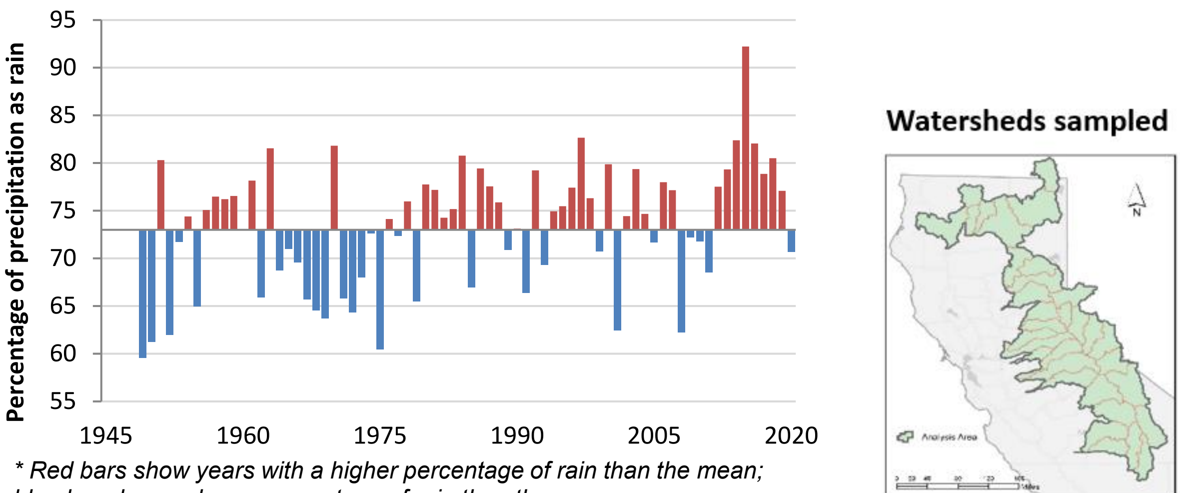

** Red bars show years with a higher percentage of rain than the mean; blue bars have a lower percentage of rain than the mean.*

Source: DWR, 2021a

Figure 2 shows the percentage of yearly precipitation falling as rain over the 33 watersheds that provide most of the state's water supply. Each value shown represents the difference between that year's percentage of rain compared to the average of 73 percent (mean, black line) for the entire period (1949 to 2020). Red bars show years with more rain than average (and thus less snow), and blue bars show years with less rain than average. Despite high year-to-year variability, recent years clearly show a trend toward more precipitation falling as rain. The percentage of precipitation falling as rain for 8 of the last 10 years was higher than average. The 2015 water year, which had the lowest snowpack on record, also had the highest percentage of rain, at about 92 percent.

Why is this indicator important?

Precipitation, in the form of rain and snow, provides most of California's supply of water. The fraction of precipitation falling as rain significantly affects how much water is stored as snow. During warmer months, the state relies on Sierra Nevada snowmelt to meet a large fraction of its water demand (see *Snow-water content* and *Snowmelt runoff* indicators). Tracking changes in the amount and physical state of precipitation, and in the patterns of storm events gives critical information for balancing the multiple water management objectives of reservoir operations, including storage and flood protection. Historical trends help inform short- and long-term water management planning and provide the basis for future projections (Siirila-Woodburn et al. 2021; Sterle et al., 2019).

Changes in the timing of precipitation are also important to track. A comparison of historical and current precipitation (1960–1989 vs 1990–2019) averaged over the entire state shows a change in the monthly distribution of precipitation (Luković et al., 2021). This study found a progressively delayed and shorter, sharper rainy season in California. This is consistent with climate change projections (Oakley et al. 2019; Polade et al. 2014, Swain et al., 2018).

Along with providing water to people in California, precipitation also nourishes the natural environment. Changes to precipitation or water availability can manifest in ecosystems in various ways. During the 2012-2016 drought, five consecutive dry winters resulted in severe ecological impacts, including massive tree mortality, catastrophic wildfires, and steep drops in winter-run Chinook salmon fry survival and in the number of adult Coho salmon returning to spawn (DWR, 2021b).

As dry and wet extremes continue to occur more often, shifts between droughts and floods will become more frequent. Shifts between extreme dry years to extreme wet years are anticipated to happen more often in southern California (Swain et al., 2018). California's recent rapid shift from severe drought (2012-2016) to heavy precipitation and flooding (2016-2017 winter) exemplifies what so-called precipitation "whiplash" looks like and what its impacts can be: hundreds of roads and other infrastructure throughout California were damaged by floods and mass movements such as landslides. Heavy runoff in the Feather River watershed contributed to the failure of the Oroville Dam spillway, forcing the evacuation of almost a quarter of a million people (Swain et al., 2018). A wet-to-dry whiplash promotes the growth of vegetation that later dries and serve as fuel for fires (Williams et al., 2019). Altogether, projections of climate change suggest that California will spend most of the year in a perennial drought, interrupted periodically by large storms that produce heavy precipitation (Allen and Luptowitz, 2017; Gershunov et al., 2019; Huang et al, 2020; Pottinger, 2020).

Floods, landslides, and even avalanches following heavy rainfall threaten human life and property (Collins et al., 2020; Hatchett et al., 2017 and 2020). Fast-moving, highly destructive debris flows triggered by intense rain can happen after a wildfire due to vegetation loss and soil exposure (USGS, 2021). An example of the devastating nature of post-debris flows occurred January 2018, when high intensity rainfall in southern California over an area recently burned by the Thomas Fire triggered landslides that killed 23 people, destroyed over 130 homes, severely damaged infrastructure in Montecito and Carpinteria, and caused the closure of Highway 101 for 13 days (Lukashov et al., 2019). Figure 3 shows shallow landslide and debris flow scars caused by another storm on March 22, 2018, at the Tuolumne River Canyon (near the town of Groveland, in the Sierra Nevada foothills). This storm created a flash flood that caused infrastructure damage in the tens of millions of dollars, led to more than 500 landslides, and moved more sediment in one day than the Tuolumne River would normally transport in a year (Collins et al., 2020).

Figure 3. Heavy rainfall triggered over 500 landslides at the Tuolumne River canyon in 2018

Source: Collins,et al. 2020; Photo credit: Wayne Hadley (used with permission)

The chances of an extreme 200-year flood event, last seen in the extraordinary “Great Flood” of 1861-1862, is more likely than not to occur within the next 40 years, and multiple occurrences are plausible by 2100 on a business-as-usual greenhouse gas emissions trajectory (Swain et al., 2018). During the Great Flood, flood waters remained throughout the state for months, transforming the land and making roads impassable (Jones, 2019). A storm of this magnitude today would probably lead to considerable loss of life and economic damages approaching a trillion dollars (Swain et al., 2018; USGS, 2011).

What factors influence this indicator?

High year-to-year variability in precipitation is a natural part of California’s climate: the western United States has experienced great swings between wet and dry for thousands of years (Ibarra et al., 2018; Sterle et al. 2019). During the summer, California experiences a deep “seasonal drought” as atmospheric moisture gets diverted away from the state by dense blobs of air parked over the north Pacific Ocean (also known as a “high pressure zone”). In the southeastern desert regions, however, some monsoonal activity in the summertime may bring thunderstorm precipitation (Corbosiero et al., 2009; WRCC, 2021). Precipitation deficits during the recent drought have been associated with a prominent region of high pressure nicknamed the “ridiculously resilient ridge” that diverted storm tracks northward during California’s rainy season from 2012 to 2015 (Swain, 2015). During winter, the Pacific high pressure zone retreats southward, and much of California’s annual precipitation falls during a few large “atmospheric river” storms (Lamjiri et al., 2018; WRCC, 2021).

Figure 4. Satellite-derived image of an atmospheric river

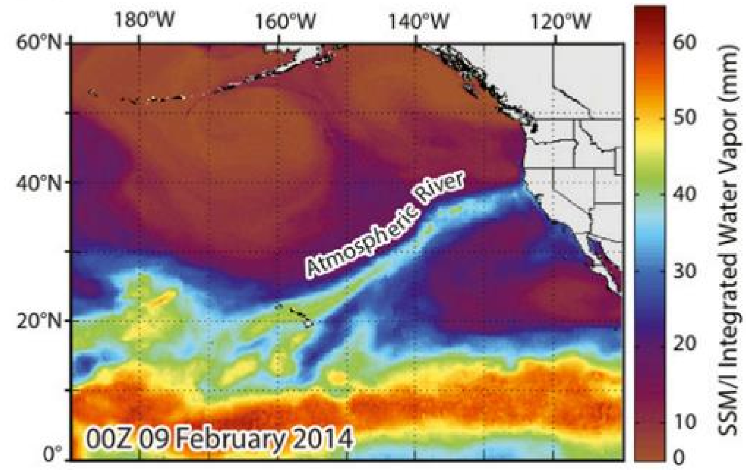

Source: Hatchett et al., 2017

An atmospheric river along the western United States identified using satellite-derived integrated water vapor or the amount of water vapor in the atmosphere (shown according to the color scale on the right).

Atmospheric rivers are long, narrow bands of water vapor, greater than 1,000 miles long and typically about 250 to 370 miles wide (Figure 4). A natural part of the global water cycle, they transport most of the water vapor outside of the tropics. Some atmospheric rivers originate from the Pacific Ocean near Hawaii and make landfall in California, where they can release water vapor in the form of heavy rain or snow (NASA, 2021; NOAA, 2017).

Precipitation from atmospheric rivers supplies 30 to 50 percent of California’s annual precipitation and about 40 percent of the Sierra Nevada snowpack (Dettinger, 2013; Guan et al., 2010). On average, rainfall from atmospheric rivers makes up 79 percent, 76 percent, and 68 percent of all extreme-rainfall accumulations in the North Coast, northern Sierra, and Transverse Ranges of southern California, respectively (Lamjiri et al., 2018). Windward slopes of hills or mountains provide the ideal location for atmospheric rivers to produce heavy precipitation in California through a phenomenon called orographic forcing: when air gets pushed up the slope of a mountain range, the water vapor cools and condenses if the air is moist enough, forming clouds and causing heavy precipitation to fall (Ralph, 2020). Precipitation from atmospheric rivers in western North America will become more frequent, heavy, and extreme (Gershunov et al., 2019; Hagos et al., 2016; Polade et al., 2017). Although climate change will enhance the amount of precipitation delivered by landfalling atmospheric rivers along the West Coast, the overall frequency of precipitation will decrease as fewer storms not caused by atmospheric rivers are projected (Gershunov et al, 2019).

Most of the water vapor that provides the state’s precipitation comes from the Pacific Ocean. Much of the variability in the state’s precipitation is related to El Niño and La Niña in the tropical Pacific, which are the warm and cool phases of a recurring climate pattern called the El Niño-Southern Oscillation, or ENSO. The warm phase of

ENSO, El Niño, happens in years when warm surface waters in the ocean intensify a current of strong, high-altitude winds called the Pacific jet stream and shift it south. This causes wet winters in the southern part of the United States (including southern California) and warmer and drier conditions in the northern United States. During the cool phase of ENSO, La Niña, unusually cool surface water conditions in the ocean displace the jet stream northward, leading to drought in the southern United States and heavy rain in the Pacific Northwest. Climate change may make extreme El Niño and La Niña events become more frequent and stronger by the end of the century (NOAA, 2020).

Regarding physical state, precipitation falls as rain or snow depending on the temperature of the air and the ground, the local geography, and the characteristics of the storm itself. Warming temperatures and their influence on a rising snowline (the altitude above which snow remains on the ground) make winter precipitation more likely to fall as rain instead of snow and run off into the ocean instead of being stored in reservoirs (Gonzales et al, 2019; Hatchett et al, 2017; Huang et al, 2020, Lynn et al, 2020). This higher runoff poses a greater flood risk (Huang et al, 2020).

Modeling simulations show that greenhouse gases including carbon dioxide and methane, as well as solar forcing, can increase California wintertime precipitation. Precipitation also changes in response to aerosols: sulfate aerosol increases California wintertime precipitation, whereas black carbon reduces it. California precipitation is more sensitive to aerosols, especially regional emissions from Europe and Asia, than to greenhouse gases (Allen et al., 2020).

A climate change signal can be found in extreme precipitation events globally over the past several decades (Dong et al., 2020). Observed increases in precipitation extremes in California are consistent with projected impacts of climate change in the state (Swain et al., 2018). At the national level, projections suggest that climate change will increase the size and frequency of very heavy and rare rainfall events across the United States (Swain et al., 2020).

Technical Considerations

Data characteristics

Data for Figure 1 come from the California Climate Tracker, an operational database tracker for weather and climate monitoring information. This indicator tracks precipitation amount in a “water year” defined as October 1 to September 30. This operational product, the California Climate Tracker, is updated periodically online at the Western Regional Climate Center. Data, including historical data, is continuously monitored and updated. The data provided here is the dataset available as of April 7, 2021, from WRCC with the most up-to-date values for modeled historical data.

Precipitation data for nearly 200 climate stations in the NOAA Cooperative Network (COOP) within California were obtained from the Western Regional Climate Center database archive of quality-controlled data from the National Climatic Data Center. For this study, COOP data from 1948-2020 were utilized. Gridded climate data from Parameter-elevation Regressions on Independent Slopes Model (Daly et al., 1997) were acquired from the PRISM group at Oregon State University for the period 1895-2021. PRISM provides complete spatial coverage of the state, where the station data serve to fill in recent data, until PRISM is processed each month. Because climate stations are not evenly spaced, the PRISM data are used to provide even and complete coverage across the state. These are combined to create a time series of annual statewide precipitation dating back to 1895.

Time series datasets prior to 1981 were modeled using climatologically aided interpolation that used the long-term average pattern (i.e., the 30-year normals) as first-guess of the spatial pattern of climatic conditions for a given month or day. Data are based on monthly modeling (PRISM, 2021).

The methodology for determining the rain/snow trends presented in Figure 2 combined fine-scale gridded precipitation data with coarse-scale freezing level and precipitation data from an atmospheric reanalysis. Snowfall was estimated as a fraction of total precipitation at a high spatial resolution, with output from WRCC's North American Freezing Level Tracker (NAFLT). For more information about the methods used, see Lynn et al. (2020).

Strengths and limitations of the data

The datasets used in this work were subjected to their own separate quality control procedures, to account for potentially incorrect data reported by the observer, missing data, and to remove inconsistencies such as station relocation or instrument change. The PRISM data offer complete coverage across the state for every month of the record. Limitations include the bias of station data toward populated areas and the limited ability of quality control processes in remote or high terrain areas. The results cited here offer a hybrid using both gridded and station data, considered more robust than either data set used independently (Abatzoglou et al., 2009).

A major advantage of the rain/snow approach used by Lynn et al. (2020) is that the NAFLT can be periodically updated as higher resolution gridded data products become available. This type of analysis can play an important role in developing and implementing adaptive strategies for water management. However, the methodology used interpolations based on observational data which are sparse in mountainous regions. It also might not fully reflect snow line variability in complex terrains.

OEHHA acknowledges the expert contribution of the following to this report:

Michael Anderson, Ph.D., P.E.
State Climatologist
California Department of Water Resources
(916) 574-2830
Michael.L.Anderson@water.ca.gov

Benjamin Hatchett, Ph.D.
Regional Climatologist
Western Regional Climate Center
(775) 674-7111
Benjamin.Hatchett@dri.edu

References:

Abatzoglou JT, Redmond KT and Edwards LM (2009). Classification of regional climate variability in the state of California. *Journal of Applied Meteorology and Climatology* **48**(8): 1527-1541.

Aguilera R, Gershunov A and Benmarhnia T (2019). Atmospheric rivers impact California's coastal water quality via extreme precipitation. *Science of the Total Environment* **671**: 488-494.

Allen RJ and Luptowitz R (2017). El Niño-like teleconnection increases California precipitation in response to warming. *Nature Communications* **8**(1): 1-5.

Bonfils CJ, Santer BD, Fyfe JC, Marvel K, Phillips TJ and Zimmerman SR (2020). Human influence on joint changes in temperature, rainfall and continental aridity. *Nature Climate Change* **10**(8): 726-731.

Bucciarelli GM, Clark MA, Delaney KS, Riley SP, Shaffer HB, et al. (2020). Amphibian responses in the aftermath of extreme climate events. *Scientific Reports* **10**(1): 1-7.

Collins BD, Oakley NS, Perkins JP, East AE, Corbett SC and Hatchett BJ (2020). Linking mesoscale meteorology with extreme landscape response: effects of narrow cold frontal rainbands (NCFR). *Journal of Geophysical Research: Earth Surface* **125**(10): e2020JF005675.

Corbosiero KL, Dickinson MJ and Bosart LF (2009). The contribution of eastern North Pacific tropical cyclones to the rainfall climatology of the southwest United States. *Monthly Weather Review* **137**(8): 2415-2435.

Daly C, Taylor G and Gibson W (1997). *The PRISM approach to mapping precipitation and temperature. 10th Conference on Applied Climatology*. American Meteorological Society.

Deguines N, Brashares JS and Prugh LR (2017). Precipitation alters interactions in a grassland ecological community. *Journal of Animal Ecology* **86**(2): 262-272.

Dettinger MD (2011). Climate change, atmospheric rivers, and floods in California-A multimodel analysis of storm frequency and magnitude changes. *Journal of the American Water Resources Association* **47**: 514-523.

Dettinger MD (2013). Atmospheric rivers as drought busters on the U.S. west coast. *Journal of Hydrometeorology* **14**: 1721-1732.

Dong S, Sun Y, Li C, Zhang X, Min SK and Kim YH (2021). Attribution of extreme precipitation with updated observations and CMIP6 simulations. *Journal of Climate* **34**(3): 871-881.

DWR (2015). *California's Most Significant Droughts: Comparing Historical and Recent Contributions*, California Department of Water Resources. February 2015.

DWR (2019). *The California Hydroclimate Report, Hydroclimate Report Water Year 2018.* California Department of Water Resources.

DWR (2020). "The California Hydroclimate Report, *Hydroclimate Report Water Year 2019.* California Department of Water Resources.

DWR (2021a). *The California Hydroclimate Report, Hydroclimate Report Water Year 2020.* California Department of Water Resources.

DWR (2021b). *California's Drought of 2012-2016: An Overview.* California Department of Water Resources.

Gershunov A, Shulgina T, Clemesha RES, Guirguis K, Pierce DW, et al. (2019). Precipitation regime change in Western North America: The role of atmospheric rivers. *Scientific Reports* **9**(1): 1-11.

Gonzales KR, Swain DL, Nardi KM, Barnes EA and Diffenbaugh NS (2019). Recent warming of landfalling atmospheric rivers along the west coast of the United States. *Journal of Geophysical Research: Atmospheres* **124**(13): 6810-6826.

Goss M, Swain DL, Abatzoglou JT, Sarhadi A, Kolden CA, et al. (2020). Climate change is increasing the likelihood of extreme autumn wildfire conditions across California. *Environmental Research Letters* **15**(9):094016.

Guan B, Molotch NP, Waliser DE, Fetzer EJ and Neiman PJ (2010). Extreme snowfall events linked to atmospheric rivers and surface air temperature via satellite measurements. *Geophysical Research Letters* **37**(20).

Hagos SM, Leung LR, Yoon JH, Lu J and Gao Y (2016). A projection of changes in landfalling atmospheric river frequency and extreme precipitation over western North America from the Large Ensemble CESM simulations. *Geophysical Research Letters* **43**(3): 1357-1363.

Hatchett BJ, Burak S, Rutz JJ, Oakley NS, Bair EH and Kaplan ML (2017). Avalanche fatalities during atmospheric river events in the western United States. *Journal of Hydrometeorology* **18**(5): 1359-1374.

Hatchett BJ, Cao Q, Dawson PB, Ellis CJ, Hecht CW, et al. (2020). Observations of an extreme atmospheric river storm with a diverse sensor network. *Earth and Space Science* **7(**8): e2020EA001129.

Hatchett BJ, Daudert B, Garner CB, Oakley NS, Putnam AE and White AB (2017). Winter snow level rise in the northern Sierra Nevada from 2008 to 2017. *Water* **9**(11): 899.

He M and Guatam M (2016). Variability and trends in precipitaiton, temperature and drought indices in the state of California. *Hydrology* **3**(2): 14.

Jones L (2019). *The Big Ones: How Natural Disasters Have Shaped Us (and What We Can Do about Them).* Knopf Doubleday Publishing Group. New York, United States.

Kirchmeier-Young MC and Zhang X (2020). Human influence has intensified extreme precipitation in North America. *Proceedings of the National Academy of Sciences* **117**(24): 13308-13313.

Lamjiri MA, Dettinger MD, Ralph FM, Oakley NS and Rutz JJ (2018). Hourly analyses of the large storms and atmospheric rivers that provide most of California's precipitation in only 10 to 100 hours per year. *San Francisco Estuary and Watershed Science* **16**(4).

Lukashov SG, Lancaster JT, Oakley NS and Swanson BJ (2019). Post-fire debris flows of 9 January 2018, Thomas fire, southern California: initiation areas, precipitation and impacts. 7th International Conference on Debris-Flow Hazards Mitigation.

Luković J, Chiang JC, Blagojević D and Sekulić A (2021). A later onset of the rainy season in California. *Geophysical Research Letters* **48**(4): e2020GL090350.

Lynn E, Cuthbertson A, He M, Vasquez JP, Anderson ML, et al. (2020) Precipitation-phase partitioning at landscape scales to regional scales. *Hydrology and Earth System Sciences* **24**(11): 5317-5328.

NASA (2021). Potent Atmospheric Rivers Douse the Pacific Northwest. Retrieved August 2, 2021.

NOAA (2017). National Oceanic and Atmospheric Administration: What Are Atmospheric Rivers?. Retrieved August 2, 2021.

NOAA (2018). National Oceanic and Atmospheric Administration: California Drought 2011-2017 (storymap). Retrieved May 26, 2021.

NOAA (2020). National Oceanic and Atmospheric Administration: How will climate change change El Nino and La Nina? Retrieved May 26, 2021.

Oakley NS, Hatchett BJ, McEvoy D and Rodriguez L (2019). *Projected Changes in Ventura County Climate*. Western Regional Climate Center, Desert Research Institute, Reno, Nevada.

Polade SD, Gershunov A, Cayan DR, Dettinger MD and Pierce DW (2017). Precipitation in a warming world: Assessing projected hydro-climate changes in California and other Mediterranean climate regions. *Scientific Reports* **7**(1): 1-10.

Polade SD, Pierce DW, Cayan DR, Gershunov A and Dettinger MD (2014). The key role of dry days in changing regional climate and precipitation regimes. *Scientific Reports* **4**(1): 1-8.

Porter K, Wein A, Alpers CN, Baez A, Barnard PL, et al. (2011) *Overview of the ARkStorm Scenario*. U.S. Geological Survey Open-File Report 2010-1312.

Pottinger (2020). Public Institute Policy of California: Droughts Aren't Just About Water Anymore. Retrieved June 30, 2022.

PRISM (2021). *Historical Past (1895-1980).* Retrieved June 8, 2021.

Siirila-Woodburn ER, Rhoades AM, Hatchett BJ, Huning LS, Szinai J, et al. (2021). A low-to-no snow future and its impacts on water resources in the western United States. *Nature Reviews Earth & Environment* 1-20.

Sterle K, Hatchett BJ, Singletary L and Pohll G (2019). Hydroclimate variability in snow-fed river systems: local water managers' perspectives on adapting to the new normal. *Bulletin of the American Meteorological Society* **100**(6): 1031-1048.

Swain DL *(*2015*).* A tale of two California droughts: Lessons amidst record warmth and dryness in a region of complex physical and human geography*, Geophysical Research Letters* **42***:* 9999-10,003*.*

Swain DL (2021). “Sharpening seasonality and shifting hydrology: Implications for wildfire and flood risk in a warming California“, presented at UC ANR's Climate Change: What Does it Mean for Southern California webinar April 27, 2021.

Swain DL, Langenbrunner B, Neelin JD and Hall A (2018). Increasing precipitation volatility in twenty-first-century California. *Nature Climate Change* **8**(5): 427-433.

Swain DL, Wing OE, Bates PD, Done JM, Johnson KA and Cameron DR (2020). Increased flood exposure due to climate change and population growth in the United States. *Earth's Future* **8**(11): e2020EF001778.

USGS (2011). *Overview of the ARkStorm scenario*. Open-File Report 2010-1312.

USGS (2021). United States Geological Survey: "Post-fire Flooding and Debris Flow," California Water Science. Retrieved April 7, 2021.

Williams AP, Abatzoglou JT, Gershunov A, Guzman-Morales J, Bishop DA, et al. (2019). Observed impacts of anthropogenic climate change on wildfire in California. *Earth's Future* **7**(8): 892-910.

WRCC (2017). Western Regional Climate Center: California Climate Tracker. Retrieved November 14, 2017.

WRCC (2021). Western Regional Climate Center: Climate of California. Western Regional Climate Center. Retrieved June 7, 2021.

Zappa G, Ceppi P and Shepherd TG (2020). Time-evolving sea-surface warming patterns modulate the climate change response of subtropical precipitation over land. *Proceedings of the National Academy of Sciences* **117**(9): 4539-4545.

APPENDIX. Regional precipitation trends in California's climate regions (as defined by the Western Regional Climate Center)

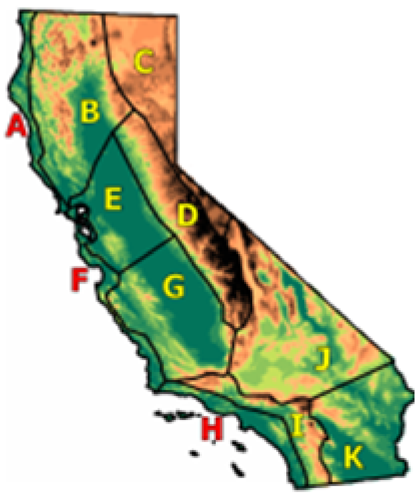

Region	Average precipitation (inches)
A. North Coast	67.9
B. North Central	49.0
C. Northeast	20.5
D. Sierra	44.9
E. Sacramento-Delta	20.3
F. Central Coast	26.4
G. San Joaquin Valley	12.9
H. South Coast	17.2
I. South Interior	19.8
J. Mojave Desert	7.0
K. Sonoran Desert	4.6
Statewide	24.2

Source: WRCC, 2021

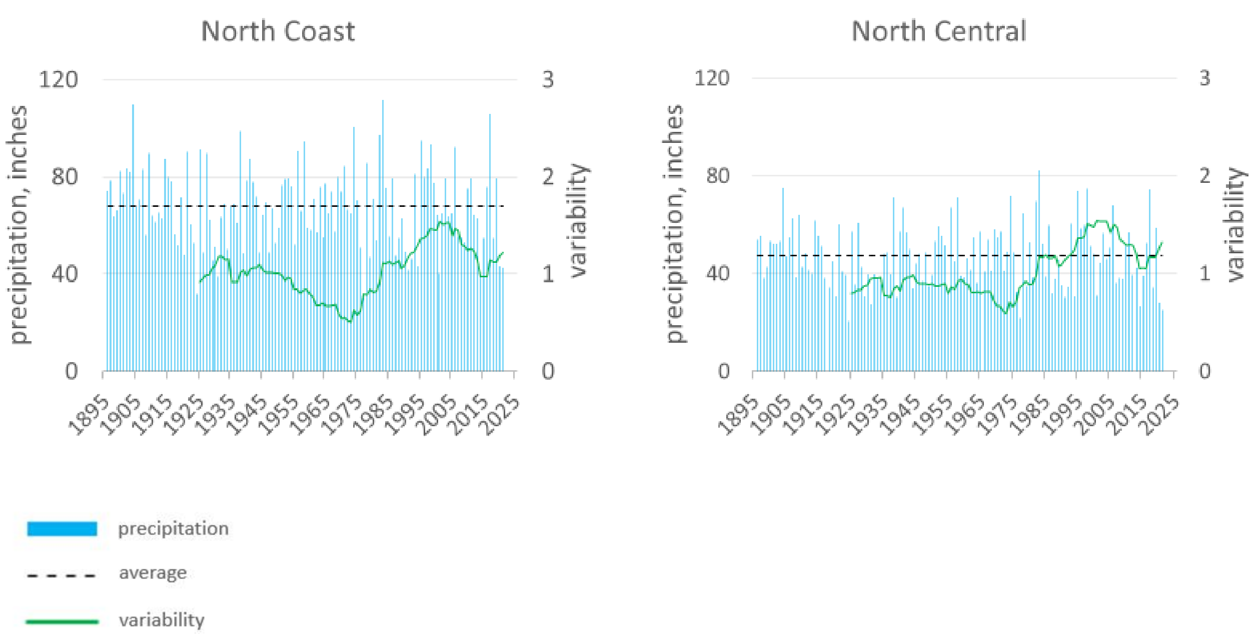

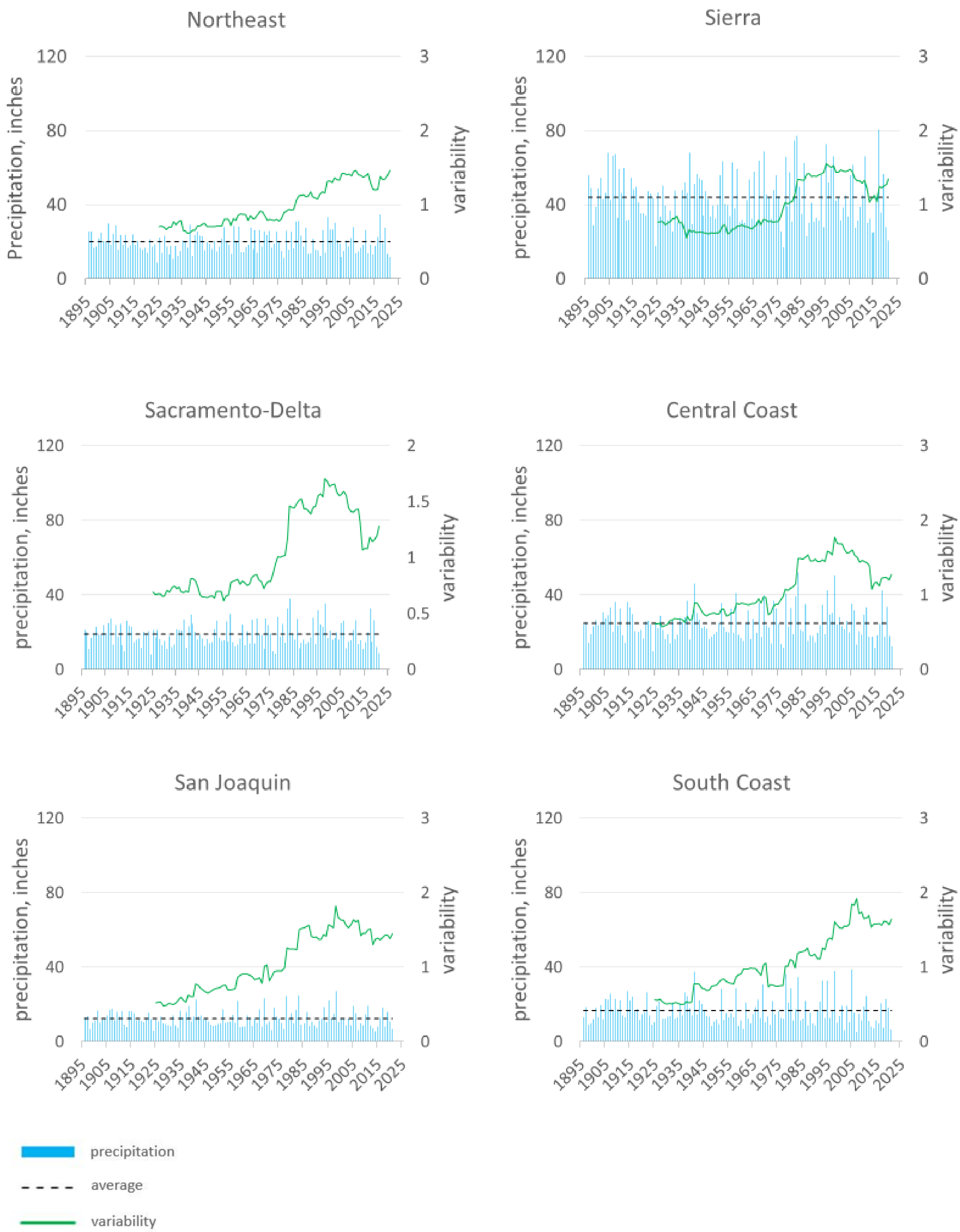
Northeast
Precipitation, inches
variability
Sierra
precipitation, inches
variability
Sacramento-Delta
precipitation, inches
variability
Central Coast
precipitation, inches
variability
San Joaquin
precipitation, inches
variability
South Coast
precipitation, inches
variability
1895 1905 1915 1925 1935 1945 1955 1965 1975 1985 1995 2005 2015 2025
precipitation
average
variability

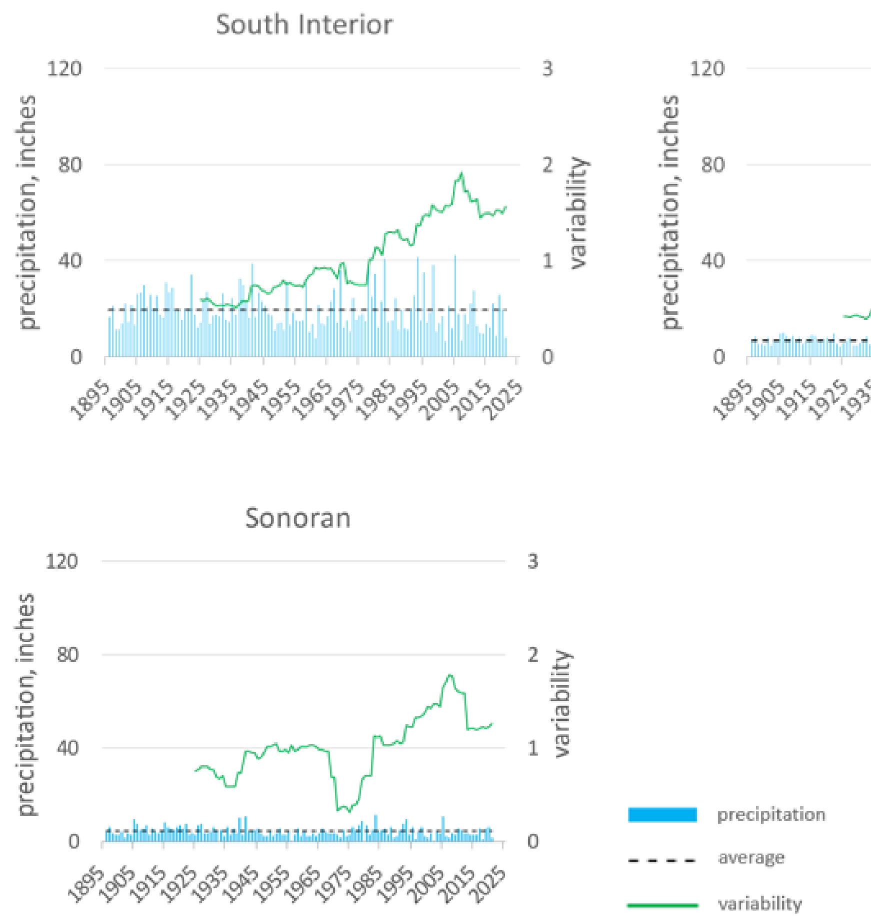
South Interior
Mojave
Sonoran
precipitation, inches
variability
120
80
40
0
3
2
1
0
1895
1905
1915
1925
1935
1945
1955
1965
1975
1985
1995
2005
2015
2025
precipitation
average
variability

DROUGHT

California has become increasingly dry since 1895. Statewide drought conditions by the end of the 2021 water year were comparable to those experienced during 2012 to 2016, the most severe drought since instrumental records began. The area of California land affected by extreme drought during the 2021 water year was larger compared to 2012 to 2016.

Figure 1 California Palmer Drought Severity Index (monthly, January 1895-October 2021)

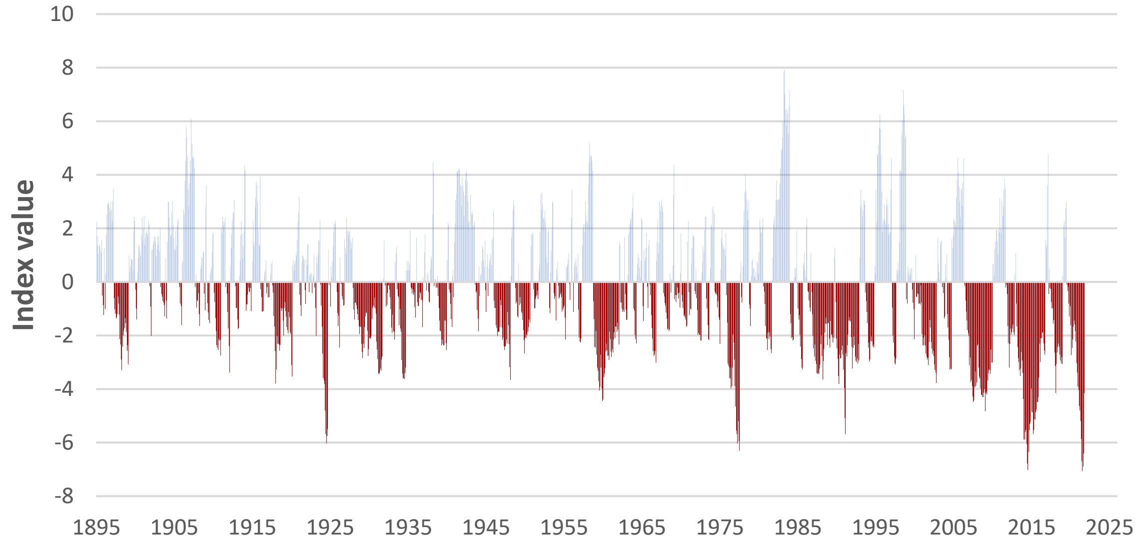

Source: NOAA, 2021

Figure 2. Percentage of California land area in drought (2000 to 2021)*

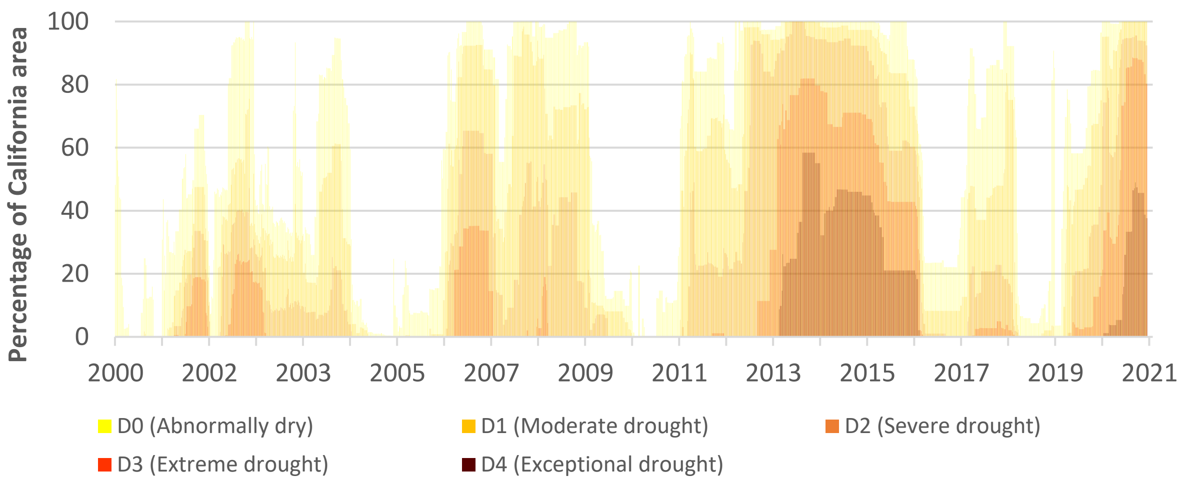

Source: National Drought Mitigation Center (NDMC), 2021a

**Based on weekly assessments of drought intensity published as the U.S. Drought Monitor.*
Note: Category D0 designates abnormally dry conditions, not actual drought.

What does the indicator show?

Droughts refer to periods of unusually dry weather that last long enough to cause a shortage of water (IPCC, 2014). Figures 1 and 2 show values for two metrics of drought: the Palmer Drought Severity Index (PDSI) and the percentage of the land area designated by the U.S. Drought Monitor (USDM) in different drought categories. Developed in the 1960s, the PDSI is universally used and measures the relative dryness of a region by incorporating readily available temperature, precipitation, and soil moisture data (NDMC, 2021b; WMO and GWP, 2016). The newer USDM is a more comprehensive percentile-based drought metric that incorporates soil moisture, streamflow, and precipitation indicators, along with PDSI and local observations and experts' best judgment (NDMC, 2021a). Both the PDSI and the USDM track drought conditions in natural (unmanaged) water systems, and thus directly reflect patterns related to a changing climate. In addition, these indices have direct applicability to activities that rely on unmanaged water supplies, such as dryland farming and livestock grazing.

Figure 1 shows PDSI values since 1895: positive values (blue bars) indicate "wet" years; negative values (red bars) are "dry" years. Values at or below -3 represent severe drought. Values below -6 represent very extreme drought. From 2012 to 2016, California experienced the most severe drought since instrumental records began in 1895 (AghaKouchak et al., 2014; Diffenbaugh et al., 2015; DWR, 2021a; Harootunian, 2018; Griffin and Anchukaitis, 2014; Robeson, 2015; Swain et al., 2014; Williams et al., 2015). It was possibly the most severe for a millennium or more (Griffin and Anchukaitis, 2014; Robeson, 2015). The 2012-2016 drought in California ended with unusually high precipitation in 2017. Drought conditions began developing again in early 2020 and remained through the 2021 water year (October 2020 to September 2021); drought conditions have continued into the 2022 water year. This coincided with a period of anomalously warm temperatures and low precipitation. California's other major droughts occurred from 1929-1934, 1976-1977, and 1987-1992 (DWR, 2015).

Figure 2 shows the percentage of land area in California impacted by different levels of drought severity since 2000 according to the USDM. The index uses five "dryness" categories, from least intense ("D0, abnormally dry" but not considered drought) to most intense ("D4, exceptional drought"). Geographically, the 2012-2016 drought affected the entire state, with more than two-thirds of California experiencing extreme or exceptional drought conditions during that time. During the 2021 water year, at least 90 percent of the state was under severe drought for 22 weeks, during which at least 85 percent was under extreme drought (for 17 consecutive weeks), and at least 45 percent under exceptional drought (for 10 weeks).

The maps in Figure 3 compare the intensity of the drought at the end of the 2021 and the 2015 water years (NDMC, 2021a). In September 2021, the entire state was in drought, with 88 percent experiencing extreme to exceptional drought. In September

2015, 97 percent of the state was experiencing drought, with 71 percent in the "extreme" to "exceptional drought" categories.

Figure 3. Drought intensity in California: Comparison of conditions at the end of the Water Year, 2021 vs. 2015

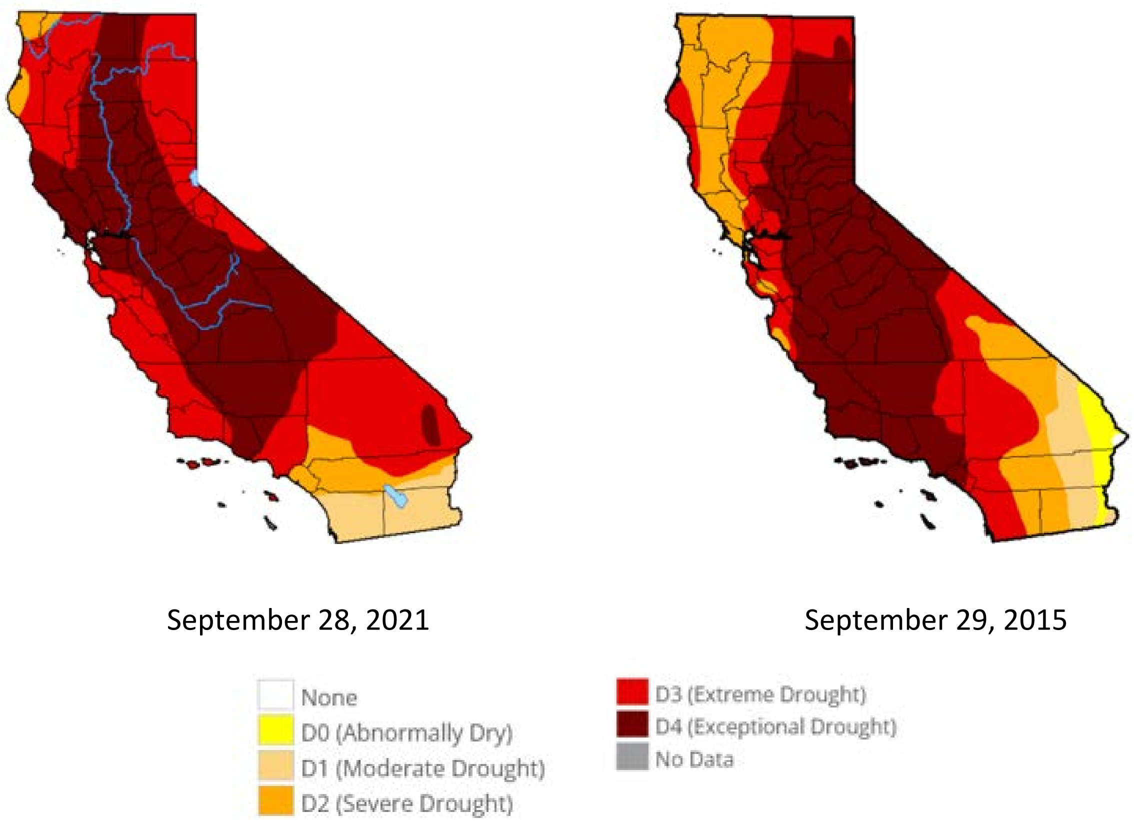

Source: NDMC, 2021a

Why is this indicator important?

Droughts have major environmental, social, and economic repercussions, affecting water availability for human use, such as urban uses (including drinking water supply and industrial uses), agriculture, hydroelectricity generation, and ecosystems (DWR, 2015). The unprecedented drought of 2012-2016 led to significant and widespread impacts across the state, underscoring the need to prepare for drought's broad and devastating effects. These impacts include widespread tree mortality, greater wildfire activity, threatened fish populations, and harmful algal blooms in freshwater bodies. In addition, drought challenges water management systems by exacerbating drinking water shortages, further reducing water deliveries to farmers, and increasing groundwater pumping (CNRA, 2021). The impacts of drought on natural systems, managed water systems, and human health are discussed below.

Natural systems

Forests and aquatic ecosystems are especially vulnerable to the impacts of drought. The record warmth and low stream flows during the 2012-2016 drought put threatened, endangered, and culturally and economically important salmon and steelhead populations, already in decline due to other stressors, at risk (CNRA, 2021; Hanak et al., 2020). Widespread tree mortality, conversion of forests to shrubland and grassland, and changes in habitat range are some ways in which drought has impacted vegetation in California (see the *Changes in forest and woodlands* and *Forest tree mortality* indicators). Dead or dying vegetation increases the risk of wildfires: for example, the unusually high tree mortality seen during the 2012-2016 drought, which was caused by water stress, created a massive fuel load (see *Wildfires* indicator).

Figure 4. Southwestern willow flycatcher

Photo: USGS.
Source: Pala Tribe, 2022

The drying of riparian habitats threatens species dependent on these habitats, including birds such as the southwestern willow flycatcher (*Empidonax trailii extimus;* Figure 4). These songbirds were once abundant in nearly all shrubby riparian areas throughout California but have sharply declined statewide over the past several decades. In the Sierras, for instance, the number and density of willow flycatcher territories declined between 1997 and 2019 at a local watershed (Loffland et al., 2022). In addition, the Pala Band of Mission Indians in Southern California reports that these songbirds have not been seen on their land since 2013, citing drought stress and riparian habitat loss as likely factors of this local extirpation (Pala, 2019), with the latter a primary factor for the decline of this species statewide. Dams, water diversion for agriculture, and groundwater pumping all have altered streamflow, affecting riparian vegetation. Aside from drought, other factors that have impacted riparian habitats include livestock grazing, off-road vehicle use, increased fires, and urban development (NPS, 2016).

Many of the impacts of drought on California’s ecosystems disproportionately affect people who depend on these diverse natural resources. People most reliant on annual rainfall usually feel the impacts of drought first. A single dry year can impair activities like dryland farming or livestock grazing that depend on unmanaged water supplies (DWR, 2015). Drought impacts on local habitats place additional burdens on rural populations that depend on them for food, firewood, or their livelihood (Roos, 2018; SWRCB, 2021a). Furthermore, the loss of culturally significant animals and plants can have profound impacts on Tribes who rely on them for traditional foods, medicine, and cultural practices.

Drought impacts on plant and animal species important to California Tribes include:

- Reduced deer and Bighorn sheep on Tribal lands, hunted for food (Big Pine Paiute and Pala, 2022)
- Loss of Clear Lake hitch, a ceremonial food source (Big Valley Pomo, 2022)
- Declines in shrubs and reeds like tules, used in traditional ceremonies, for weaving and boat building, and as food (Big Valley Pomo, 2022)
- Declining numbers of trees like sugar pines (provide pitch for medicine, and roots for basketry) and coast live oak (source of acorns for food) (Karuk and Pala, 2022)

Managed water systems

Domestic water supply

Although drinking water shortages affected many local and regional water suppliers during the 2012-2016 drought, many large urban water districts with diversified water sources and stored supplies did not suffer major disruptions (Lund et al., 2018). Communities that were highly dependent on supply from a single source and had no connections with other water utilities experienced severe shortages. These included more than 100 small water systems and more than 2,000 domestic wells in some small, poor, rural communities, particularly in the Central Valley and the Sierra Nevada foothills (PPIC, 2016). These small communities – often communities of color – remain vulnerable (PPIC, 2021a).

In addition to water supply, droughts also compromise drinking water quality (Bell et al., 2018). Saltwater intrusion, for instance, can happen because of drought, sea-level rise, and changing water demands (US EPA, 2021). As discussed further below (see "Human health impacts"), pathogens in drinking water are another concern. Compounding this issue, low-income communities and people of color are disproportionately impacted by water quality even during normal (non-drought) years. An analysis of drinking water quality, accessibility, and affordability in California found that water quality is worse in low-income communities and that small drinking water systems face greater affordability challenges compared to larger systems (OEHHA, 2021a). In the San Joaquin Valley, for example, tens of thousands of people living in low-income unincorporated communities often lack access to safe drinking water. Most of the Central Valley's residents who live in low-income unincorporated communities are Hispanic (London et al., 2018).

The rising cost of water services during droughts places an even greater burden on low-income households (Famiglietti, 2014; Feinstein et al., 2017; PPIC, 2021b). Issues of water affordability were exacerbated by the COVID-19 economic recession, when low-income families, women, African Americans, and Latinos were especially impacted by unemployment and underemployment (Bohn et al., 2020). A survey by the California Water Boards (December 2020) found that approximately 1.6 million households in California had water debt at an average amount of $500 per household. A state moratorium on water service shutoffs helped to ensure that homes and small businesses unable to pay their bills continued to have access to water (SWRCB, 2021b).

California's water utilities face fiscal challenges during major droughts and recessions when revenues decline (PPIC, 2021b). Exacerbating this issue, wildfires worsened by droughts can damage water utilities, as seen when the 2018 Camp Fire destroyed the water distribution system at Paradise in northern California (Chow et al., 2021).

Hydroelectric power generation
Drought also impacts the generation of hydroelectricity, a major source of power in California that depends on snowmelt runoff and rainfall. Reductions in hydroelectricity generation during the 2012-2016 drought increased state electricity costs and raised California's carbon footprint until a shift towards different renewable energy sources helped to offset the increased emissions (Gleick, 2016; Hardin et al., 2017; Herrera-Estrada et al., 2018; Szinai et al., 2020; Zohrabian and Sanders, 2018).

Agricultural water supply
As the 2012-2016 drought reduced water deliveries for agricultural use, farmers compensated by fallowing cropland (leaving cropland idle). More than 500,000 acres, or 6 percent of irrigated acreage, were fallowed in 2015. Additional economic impacts on California's agricultural sector from the 2012-2016 drought included abandoned orchards and vineyards and lost jobs; the livelihoods of many people dependent on seasonal farm jobs and agricultural goods and services disappeared (DWR, 2015; Howitt et al., 2014 and 2015; Lund et al., 2018; PPIC, 2016; Roos, 2018).

Along with fallowed land, farmers compensate for water shortages from droughts by pumping groundwater (Lund et al., 2018). Most groundwater in California gets used for agriculture, and to a lesser degree for urban and domestic supply (some communities rely solely on groundwater) and managed wetlands. From 1998 through 2018, groundwater levels decreased in approximately 65 percent of wells statewide (DWR, 2021b).

Overpumping of groundwater in the San Joaquin Valley has depleted the region's groundwater supply. Farmers first started pumping groundwater in the early 1900s. By 1970, about half of San Joaquin Valley experienced land subsidence (i.e., the land surface sinks). Some areas had dropped by as much as 28 feet. Reduced surface water availability during 1976-77, 1986-92, 2007-09, and 2012-2015 caused even more groundwater pumping. Worsening droughts will make it hard to achieve sustainable levels of groundwater by the early 2040s as required by the Sustainable Groundwater

Management Act passed in 2014. People in the San Joaquin Valley may need to permanently fallow 500,000 acres of land (Hanak et al., 2019).

Overpumping of groundwater also results in aquifer compaction, reducing its water-holding capacity, and land subsidence. Some of the most severe recorded land subsidence in history occurred in the western San Joaquin Valley near Mendota, where the land surface has subsided about 30 feet (NASA, 2016; Sneed et al., 2018). The photograph in Figure 5 shows the approximate height of the land surface in 1925 compared to much lower levels in 1955 and 1977 because of excessive groundwater pumping in the San Joaquin Valley. Surface water deliveries from the California Aqueduct replaced reliance on groundwater for irrigation, slowing subsidence showed over a large part of the affected area (Galloway et al., 1999) Land subsidence impacts infrastructure — including water conveyance systems, roads, railways, bridges — aquifer storage capacity, and land topography (USGS, 2017a and 2017b). Moreover, many rivers and wetlands that rely on groundwater for some or most of their flow suffer from groundwater overdraft that worsens during droughts (Hanak et al., 2020; Klausmeyer et al., 2018). Additional impacts of groundwater overuse, exacerbated by droughts, include dying crops, habitat loss, and species extinction (The Nature Conservancy, 2020).

Figure 5. Land subsidence in the San Joaquin Valley

Photo: USGS, 2017c

Land surface in the San Joaquin Valley subsided ~9 m from 1925 to 1977 due to aquifer-system compaction. Signs on the telephone pole indicate the former elevations of the land surface in 1925 and 1955 (Faletti RC, 2022).

Human health

Droughts adversely impact human health in a myriad of ways other than through impacts on drinking water (Bell et al., 2018). For instance, reduced water quantity during periods of drought decreases water flow and promotes the production of pathogens that favor warm, stagnant environments (Paz, 2015; see the *Vector-borne diseases* indicator). Consumption or contact with water containing pathogens, such as *Vibrio* species, may result in ear, eye, wound infections, diarrheal illness, and death (Trtanj et al., 2016). Reduced hand and food washing in response to the drought increased the risk of communicable diseases, such as enteric disease and influenza, and exposure to pesticide residues (CDC, 2016a and 2016b, 2017).

Drought also increases air pollution from wildfires and dust storms (DWR, 2015). Under dry conditions, winds tend to transport inhalable soil particles, leading to air quality concerns. In the Owens Valley, for example, where the soil is alkaline (Big Pine Paiute, 2022), and there has been a rise in the level of PM10 (Bishop Paiute, 2022) the Big Pine Paiute Tribe has reported eye, throat, and lung irritation during dust storms. The Tribe is concerned over the impacts of wind-blown dust on Paiute Tribal elders with lung issues and the growing number of cases of children with asthma and other breathing issues. Drought also stresses peoples' mental and emotional well-being (Barreau et al., 2017; CDC, 2016a and 2016b, 2017; Vins et al., 2015).

A visible surface water quality impact during the 2012-2016 drought came in the form of more frequent harmful algal blooms. These blooms appeared in freshwater bodies throughout the state, from the Klamath River in the north to Lake Elsinore and the Salton Sea in the south (CNRA, 2021). Certain bloom-forming organisms such as cyanobacteria, produce toxins that adversely impact people and their pets. In humans, exposure to these toxins can lead to a wide array of symptoms including skin rashes, blisters, vomiting, and abdominal pain (CWQMC, 2021; OEHHA, 2021b). In pets, exposure can be lethal (CNRA, 2021).

Exposures to the toxins can occur through consuming contaminated water and foods and by direct contact with water. Communities that rely on recreational water use to generate revenue from tourism and those who use freshwater bodies as drinking water sources are disproportionately affected. During periods of bloom, certain Tribes are unable to carry out cultural traditions or practices that involve immersion in, or other contacts with, water bodies. The Karuk's World Renewal Ceremonies in which the medicine man traditionally bathes and drinks Klamath River water overlaps annually with the highest levels of toxin in river water (Karuk, 2022). At Clear Lake, members of the Big Valley Band of Pomo Indians are prevented from spiritual activities, water immersion for ceremonies, using plants for ceremonies and basketry, and the collection and consumption of fish and other aquatic organisms when toxin levels are high (Big Valley, 2022). In addition, the Tribe has reported that clogged drinking water intakes in Clear Lake due to sludge induced by blooms, and that detection of toxins in raw water have led to additional operational and water treatment costs.

What factors influence this indicator?

Droughts are a naturally occurring feature of California's climate (DWR, 2021c). They are naturally influenced by modes of global climate variability such as the El Niño-Southern Oscillation, regional atmospheric pressure anomalies, and the frequency of landfalling "drought-busting" atmospheric rivers (Dettinger, 2013; Griffin and Achukaitis, 2014). Singular wet years composed of frequent landfalling atmospheric rivers can terminate persistent droughts (e.g., Dettinger, 2013; Hatchett et al. 2016). Historically, dry winters in California have been associated with a ridge of high atmospheric pressure off the west coast, and wet winters have been associated with a trough off the west coast and an El Niño event (Seager et al., 2015).

Droughts of the 21st century are hotter, longer lasting, and spatially larger than previous droughts (Crausbay et al., 2017). A growing body of evidence suggests that anthropogenic warming has increased the likelihood of extreme droughts in the state (AghaKouchak et al., 2014; Williams et al., 2015; Diffenbaugh et al., 2015; Shukla et al., 2015; Swain et al., 2014; Griffin and Achukaitis, 2014; Luo et al., 2017; Hatchett et al. 2016; Harootunian, 2018) and worldwide (Chiang et al., 2021). Atmospheric circulation patterns like those observed during California's most extreme dry and hot years have increased during recent decades (Swain et al., 2016). Climate change may be increasing the likelihood of the type of rare atmospheric events associated with the 2012-2016 drought (Swain et al., 2017; Cvijanovic et al., 2017). Notably, this was part of a larger drought across the southwestern United States that has been described as a "megadrought." Using a tree-ring reconstruction to extend summer soil moisture records back to 800 CE, investigators determined 2000-2021 to be the driest 22-year period in the region over this period. About 19 percent and 42 percent of the dryness in 2021 and in 2000-2021, respectively, were attributable to anthropogenic climate change (Williams et al., 2022). Climate change will continue to make dry and warm years happen more often (Diffenbaugh et al., 2015) and drought conditions will worsen (Underwood et al., 2018; Ullrich et al., 2018). Other ways climate change directly contributes to drought conditions include more variable but less frequent precipitation (Gershunov et al., 2019) and widespread snowpack decline (Siirla-Woodburn et al., 2021; see the *Snow-water content* indicator).

As temperatures warm, the atmosphere takes up more water from land through evapotranspiration (McEvoy et al. 2020; Pottinger, 2020). "Evaporative demand," often referred to as the "thirst" of the atmosphere, reflects maximum evapotranspiration assuming unlimited moisture supply and ambient atmospheric conditions. Almost all the western U.S. has seen a rise in the atmosphere's thirstiness since the 1980s when temperatures began to noticeably warm (Pottinger, 2020). During the 2021 summer and water year, the evaporative demand over much of California was higher than it had been over the last 40 years (NIDIS, 2021). A thirstier atmosphere also means California's big storms will get even bigger because more water will go into the atmosphere (see the *Precipitation* indicator for a discussion on atmospheric rivers, which also affect heavy precipitation). Altogether, projections of climate change suggest that California will experience a perennial drought for most of the year, interrupted periodically by large storms that produce heavy to extreme precipitation (Pottinger, 2020).

Regional variations such as geography and local climate patterns also determine the extent and severity of droughts. The 2012-2016 drought was more severe in southern California, which has displayed greater drying trends over the past century than in northern California (Dong et al., 2019).

Technical considerations

Data characteristics

PDSI identifies droughts by incorporating data on temperature, precipitation, and the soil's water-holding capacity. The metric takes into consideration moisture received as precipitation and moisture stored in the soil, while also accounting for potential loss of water due to temperature. It originally functioned to identify drought affecting agriculture but has since been used to identify drought associated with other types of impacts (WMO and GWP, 2016). PDSI is used to assess long-term drought patterns (NOAA, 2017).

The U.S. Drought Monitor provides a big-picture look at drought conditions in the United States. As previously mentioned, along with PDSI, metrics used in the U.S. Drought Monitor include soil moisture data, streamflow conditions, the standardized precipitation index, and blends of various drought indicators.

Strengths and limitations of the data

The PDSI and USDM as used in this report are not intended to gather information about water availability or delivery in California.

PDSI is considered a robust index of drought, universally used, and has been employed since the 1960s. However, PDSI assumes all precipitation comes as rain (Williams et al., 2015) and does not account for frozen precipitation or frozen soils very well (WMO and GWP, 2016). PDSI also does not provide information on human water demand, streamflow and reservoir storage, or groundwater accessibility (Williams et al., 2015). It represents drought conditions in natural (unmanaged) systems only.

The USDM is based on many types of data, including observations from local experts across the country, as well as information about reservoir storage. It can be used to identify likely areas of drought impacts but should not be used to infer specifics about local conditions.

OEHHA acknowledges the expert contribution of the following to this report:

Benjamin Hatchett, Ph.D.
Desert Research Institute
Western Regional Climate Center
Benjamin.Hatchett@dri.edu
(775) 674-7111

Michael L Anderson, Ph.D., P.E.
State Climatologist
California Department of Water Resources
michael.l.anderson@water.ca.gov
(916) 574-2830

Reviewers:
David Simeral
Desert Research Institute
Western Regional Climate Center
David.Simeral@dri.edu

Christopher Hyun and Matthew Holland
California State Water Resources Control Board
Christopher.Hyun@waterboards.ca.gov
Matthew.Holland@waterboards.ca.gov

Amanda Sheffield
National Oceanic and Atmospheric Administration
amanda.sheffield@noaa.gov

References:

AghaKouchak A, Cheng L, Mazdiyasni O and Farahmand A (2014). Global warming and changes in risk of concurrent climate extremes: Insights from the 2014 California drought. *Geophysical Research Letters* **41**: 8847–8852.

Barreau T, Conway D, Haught K, Jackson R, Kreutzer R, et al. (2017). Physical, mental, and financial impacts from drought in two California counties, 2015. *American Journal of Public Health* **107**(5): 783-790.

Bell JE, Brown CL, Conlon K, Herring S, Kunkel KE, et al. (2018). Changes in extreme events and the potential impacts on human health. *Journal of the Air & Waste Management Association* **68**(4): 265-287.

Big Pine Paiute Tribe (2022). *Impacts of Climate Change on the Big Pine Paiute Tribe of the Owens Valley.* In: OEHHA 2022 Indicators of Climate Change in California.

Big Valley Band of Pomo Indians (2022). *Impacts of Climate Change on the Big Valley Band of Pomo Indians.* In: OEHHA 2022 Indicators of Climate Change in California.

Bishop Paiute Tribe (2022). *Impacts of Climate Change on the Bishop Paiute Tribe.* In: OEHHA 2022 Indicators of Climate Change in California.

Bohn S, Bonner D, Lafortune J, and Thorman T (2020). Public Policy Institute of California. Income Inequality and Economic Opportunity in California. Retrieved July 9, 2021.

CDC (2016a). *Community Assessment for Public Health Emergency Response (CASPER) addressing the California drought – Tulare County, California, October, 2015. Final Report, March 25, 2016.*

CDC (2016b). *Community Assessment for Public Health Emergency Response (CASPER) addressing the California drought – Mariposa County, California, November, 2015. Final Report, March 25, 2016.*

CDC (2017). *Community Assessment for Public Health Emergency Response (CASPER) addressing the California drought – Mariposa County, 2016. Mariposa, California. Final Report: January, 2017.*

Chiang F, Mazdiyasni O and AghaKouchak A (2021). Evidence of anthropogenic impacts on global drought frequency, duration, and intensity. *Nature Communications* **12**(1): 1-0.

Chow A T-S, Karanfil T, and Dahlgren RA (2021). Wildfires are Threatening Municipal Water Supplies. EOS, Science News by AGU. Retrieved Nov 18, 2021.

CNRA (2021). *Report to the Legislature on the 2012-2016 Drought. As Required by Chapter 340 of 2016.* March 2021. California Natural Resources Agency.

Crausbay SD, Ramirez AR, Carter SL, Cross MS, Hall KR, et al. (2017). Defining ecological drought for the twenty-first century. *Bulletin of the American Meteorological Society* **98**(12): 2543-2550.

Cvijanovic I, Santer BD, Bonfils C, Lucas DD, Chiang JC and Zimmerman S (2017). Future loss of Arctic sea-ice cover could drive a substantial decrease in California's rainfall. *Nature Communications* **8**(1): 1-0.

CWQMC (2021). California Water Quality Monitoring Council, My Water Quality. *Human Health and HABs.* Retrieved September 17, 2021.

Dettinger MD (2013). Atmospheric rivers as drought busters on the U.S. west coast. *Journal of Hydrometeorology* **14**: 1721-1732.

Diffenbaugh NS, Swain DL and Touma D (2015). Anthropogenic warming has increased drought risk in California. *Proceedings of the National Academy of Sciences* **112**(13): 3931-3936.

Dong C, MacDonald GM, Willis K, Gillespie TW, Okin GS and Williams AP (2019). Vegetation responses to 2012–2016 drought in Northern and Southern California. *Geophysical Research Letters* **46**(7): 3810-3821.

DWR (2015). *California's Most Significant Droughts: Comparing Historical and Recent Conditions.* California Department of Water Resources. Sacramento, CA.

DWR (2017a). California Department of Water Resources: Groundwater Information Center. Retrieved November 15, 2017.

DWR (2017b). California Department of Water Resources: Groundwater Level Change – Fall 2011 to Fall 2016. Retrieved November 15, 2017.

DWR (2021a). *California's Drought of 2012-2016: An Overview.* California Department of Water Resources. Sacramento, CA.

DWR (2021b). *California's Groundwater Update 2020.* California Department of Water Resources. Sacramento, CA.

DWR (2021c). California Department of Water Resources: Drought. Retrieved September 14, 2021.

Faletti RC (2022). The Invisible Sinking Surface. *In: Hydrohumanities Water Discourse and Environmental Futures.* De Wolff K, Faletti RC, and Lopez-Calvo I (Eds). University of California Press.

Famiglietti JS (2014). The global groundwater crisis. *Nature Climate Change* **4**: 945-948.

Feinstein L, Phurisamban R, Ford A, Tyler C and Crawford A (2017). *Drought and Equity in California*. Pacific Institute. Oakland, CA.

Galloway D, Jones DR and Ingebritsen SE (1999). San Joaquin Valley, California. In: Land Subsidence in the United States. Circular 1182, U.S. Department of the Interior, U.S. Geological Survey. Retrieved August 19, 2022.

Gershunov A, Shulgina T, Clemesha RE, Guirguis K, Pierce DW, et al. (2019) Precipitation regime change in Western North America: the role of atmospheric rivers. *Scientific reports* **9**(1): 1-1.

Gleick PH (2016). *Impacts of California's Ongoing Drought: Hydroelectricity Generation – 2015 Update.* Pacific Institute. Oakland, CA.

Griffin D and Anchukaitis KJ (2014). How unusual is the 2012–2014 California drought? *Geophysical Research Letters* **41**: 9017–9023.

Hanak E, Chappelle C, Escriva-Bou A, Gray B, Jezdimirovic J, et al. (2020). *Priorities for California's Water*. Public Policy Institute of California, Water Policy Center. Sacramento, CA.

Hanak E, Escrivu-Bou A, Gray B, Green S, Harter T, et al. (2019). *Water and the Future of the San Joaquin Valley*. Public Policy Institute of California, Water Policy Center. Sacramento, CA.

Hardin E, AghaKouchak A, Qomi MJ, Madani K, Tarroja B, et al. (2017). California drought increases CO2 footprint of energy. *Sustainable Cities and Society* **28**: 450-452.

Harootunian G (2018). *Chapter 10 California: It's Complicated: Drought, Drinking Water, and Drylands.* In: Resilience.

Hatchett BJ, Boyle DP, Garner CB, Kaplan ML, Putnam AE and Bassett SD (2016). Magnitude and frequency of wet years under a megadrought climate in the western Great Basin, USA. *Quaternary Science Reviews* **152**: 197-202.

Herrera-Estrada JE, Diffenbaugh NS, Wagner F, Craft A and Sheffield J (2018). Response of electricity sector air pollution emissions to drought conditions in the western United States. *Environmental Research Letters* **13**(12): 124032.

Howitt R, MacEwan D, Medellín-Azuara J, Lund J and Sumner D (2015). *Economic Analysis of the 2015 Drought for California Agriculture*. UC Davis Center for Watershed Science. Davis, CA.

Howitt R, Medellín-Azuara J, MacEwan D, Lund J, and Sumner D (2014). *Economic Analysis of the 2014 Drought for California Agriculture*. UC Davis Center for Watershed Science. Davis, CA.

IPCC (2014): Annex II: Glossary. Mach KJ, Planton S and von Stechow C (Eds.). In: *Climate Change 2014: Synthesis Report. Contribution of Working Groups I, II and III to the Fifth Assessment Report of the Intergovernmental Panel on Climate Change*. Core Writing Team, Pachauri RK and Meyer LA (Eds.). IPCC, Geneva, Switzerland. pp 117-130.

Karuk Tribe (2022). *Impacts of Climate Change on the Karuk Tribe.* In: OEHHA 2022 Indicators of Climate Change in California.

Klausmeyer K, Howard J, Keeler-Wolf T, Davis-Fadtke K, Hull R and Lyons A (2018). *Mapping Indicators of Groundwater Dependent Ecosystems in California: Methods Report*. San Francisco, California.

Loffland HL, Schofield LN, Siegel RB, and Christman B (2022). Sierra Nevada Willow Flycatcher decline continues but losses abate at two restored meadows. *Western Birds* **53**: 52–69.

London J, Fenci A, Watterson S, Jarin J, Aranda A, et al. (2018). *The Struggle for Water Justice in California's San Joaquin Valley: A Focus on Disadvantaged Unincorporated Communities*. UC Davis Center for Regional Change. Davis, CA.

Lund J, Medelin-Azuara J, Durand J and Stone K (2018). Lessons from California's 2012-2016 drought. *Journal of Water Resources Planning and Management* **144**(10): 04018067.

Luo L, Apps D, Arcand S, Xu H, Pan M and Hoerling M (2017). Contribution of temperature and precipitation anomalies to the California drought during 2012–2015. *Geophysical Research Letters* **44**(7): 3184-3192.

McEvoy DJ, Pierce DW, Kalansky JF, Cayan DR and Abatzoglou JT (2020). Projected changes in reference evapotranspiration in California and Nevada: Implications for drought and wildland fire danger. *Earth's Future* **8**(11): e2020EF001736.

NASA (2016). San Joaquin Valley is Still Sinking. Retrieved March 7, 2022.

NDMC (2021a). National Drought Mitigation Center U.S. Drought Monitor. Retrieved November 18, 2021.

NDMC (2021b). National Drought Mitigation Center: Measuring Drought. Retrieved September 24, 2021.

NIDIS (2021). Drought Status Update for California-Nevada September 22, 2021. Retrieved September 23, 2021.

NOAA (2017). NOAA Historical Palmer Drought Indices. Retrieved December 26, 2017.

NOAA (2021). NOAA National Centers for Environmental information: Climate at a Glance, Time Series. Palmer Drought Severity Index. Retrieved June 23, 2021.

NPS (2016). Southwestern Willow Flycatcher. Retrieved March 7, 2022.

OEHHA (2021a). *Achieving the Human Right to Water in California: An Assessment of the State's Community Water Systems*. Office of the Environmental Health Hazard Assessment, California Environmental Protection Agency.

OEHHA (2021b). Cyanobacteria Harmful Algal Blooms (HABs) and Cyanotoxins in Recreational Waters. Retrieved March 4, 2022.

Pala Tribe (2019). *Climate Change Vulnerability Assessment.* Pala Band of Mission Indians.

Paz S (2015). Climate change impacts on West Nile virus transmission in a global context. *Philosophical Transactions of the Royal Society B: Biological Sciences* **370**(1665): 20130561.

Pottinger L (2020). Droughts Aren't Just About Water Anymore. Public Policy Institute of California, Water Policy Center. Retrieved June 21, 2021.

PPIC (2016). *Managing Droughts.* Public Policy Institute of California, Water Policy Center. Sacramento, CA.

PPIC (2021a). Public Policy Institute of California Just the Facts: Droughts in California. Retrieved June 22, 2021.

PPIC (2021b). Public Policy Institute of California Just the Facts: Paying for California's Water System. Retrieved June 22, 2021.

Robeson SM (2015). Revisiting the recent California drought as an extreme value. *Geophysical Research Letters* **42**(16): 6771-6779.

Roos M (2018). *Climate Justice Summary Report. California's Fourth Climate Change Assessment.* Publication number: SUM-CCCA4-2018-012.

Seager R, Hoerling M, Schubert S, Wang H, Lyon B, et al. (2015). Causes of the 2011-14 California drought. *Journal of Climate* **28**(18): 6997–7024.

Shukla S, Safeeq M, AghaKouchak A, Guan K and Funk C (2015). Temperature impacts on the water year 2014 drought in California. *Geophysical Research Letters* **42**(11): 4384-4393.

Siirila-Woodburn ER, Rhoades AM, Hatchett BJ, Huning LS, Szinai J, et al. (2021) A low-to-no snow future and its impacts on water resources in the western United States. *Nature Reviews Earth & Environment* 1-20.

Sneed M, Brandt JT and Solt M (2018). *Land subsidence along the California aqueduct in West-Central San Joaquin Valley, California, 2003–10.* Scientific Investigations Report 2018-5144. US Geological Survey.

Swain DL (2015). A tale of two California droughts: Lessons amidst record warmth and dryness in a region of complex physical and human geography. *Geophysical Research Letters* **42**(22): 9999-10003.

Swain DL, Horton DE, Singh D and Diffenbaugh NS (2016). Trends in atmospheric patterns conducive to seasonal precipitation and temperature extremes in California. *Science Advances* **2(**4): e1501344.

Swain DL, Singh D, Horton DE, Mankin JS, Ballard TC and Diffenbaugh NS (2017). Remote linkages to anomalous winter atmospheric ridging over the northeastern Pacific. *Journal of Geophysical Research: Atmospheres* **122**(22): 12-94.

Swain DL, Tsiang M, Haugen M, Singh D, Charland A, et al. (2014). The extraordinary California drought of 2013/2014: Character, context, and the role of climate change. *Bulletin of American Meteorological Society* **95**(9): S3-S7.

SWRCB (2021a). *State Water Resources Control Board Resolution No. 2021-0050*.

SWRCB (2021b). Drinking Water COVID-19 Financial Impacts Survey. Retrieved November 30, 2021.

Szinai JK, Deshmukh R, Kammen DM and Jones AD (2020). Evaluating cross-sectoral impacts of climate change and adaptations on the energy-water nexus: a framework and California case study. *Environmental Research Letters*.

The Nature Conservancy (2020). Stories in California: The California Water Program. Retrieved June 23, 2021.

Trtanj J, Jantarasami L, Brunkard J, Collier T, Jacobs J, et al. (2016). Ch. 6: Climate Impacts on Water-Related Illness. In: *The Impacts of Climate Change on Human Health in the United States: A Scientific Assessment*. U.S. Global Change Research Program, Washington, DC, 157–188.

Ullrich PA, Xu Z, Rhoades AM, Dettinger MD, Mount JF, et al. (2018). California's drought of the future: A midcentury recreation of the exceptional conditions of 2012–2017. Earth's Future **6**(11):1568-1587.

Underwood EC, Hollander AD, Flint LE, Flint AL and Safford HD (2018). Climate change impacts on hydrological services in southern California. *Environmental Research Letters* **13**(12): 124019.

US EPA (2021). Climate Adaptation and Saltwater Intrusion. Retrieved December 1, 2021.

USGS (2017a). USGS California Water Science Center: Drought Impacts. Retrieved November 22, 2017.

USGS (2017b). USGS California Water Science Center: Land Subsidence: Cause & Effect. Retrieved December 14, 2017.

USGS (2017c). USGS Groundwater Information: Groundwater Resources for the Future. Retrieved December 14, 2017.

Vins H, Bell J, Saha S, and Hess JJ (2015). The mental health outcomes of drought: A systematic review and causal process diagram. *International Journal of Environmental Research and Public Health* **12**(10): 13251-13275.

Wang S-Y, Hipps L, Gilles RR and Yoon JH (2014). Probable causes of the abnormal ridge accompanying the 2013-2014 California drought: ENSO precursor and anthropogenic warming footprint. *Geophysical Research Letters* **41**(9): 3220-3226.

Wang SY, Yoon JH, Becker E and Gillies R (2017). California from drought to deluge. *Nature Climate Change* **7**(7): 465-468.

Williams AP, Cook BI and Smerdon JE (2022). Rapid intensification of the emerging southwestern North American megadrought in 2020–2021. *Nature Climate Change* **14**: 1-3.

Williams AP, Cook ER, Smerdon JE, Cook BI, Abatzoglou JT, et al. (2020). Large contribution from anthropogenic warming to an emerging North American megadrought. *Science* **368**(6488):314-318.

Williams AP, Seager R, Abatzoglou JT, Cook BI, Smerdon JE, et al. (2015). Contribution of anthropogenic warming to California drought during 2012-2014. *Geophysical Research Letters* **42**(16): 6819-6828.

WMO and GWP (2016). *Handbook of Drought Indicators and Indices.* Integrated Drought Management Programme, World Meteorological Organization and Global Water Partnership. Geneva, Switzerland.

Zohrabian A and Sanders KT (2018). Assessing the impact of drought on the emissions and water intensity of California's transitioning power sector. *Energy Policy* **123**: 461-470.